OPEN ACCESS
IOP Publishing | Songshan Lake Materials Laboratory

MATERIALS FUTURES

Mater. Futures 4 (2025) 042301 (50pp) https://doi.org/10.1088/2752-5724/ae03db

Topical Review

Harnessing the potential of graphene quantum dots in emerging biomedical applications: interaction mechanisms, multifunctional roles, and future perspectives

Aumber Abbas[1,10,*], Jamal Kazmi[2,10], Saleem Abbas[3,10], Taskeen Zahra[1], Faisal Saleem[4], Nur Nasyifa Mohd Maidin[5], Tanveer A Tabish[6], David James Young[7], Maqusood Ahamed[8,*], Tuti Mariana Lim[9,*] and Junfei Ou[1,*]

[1] School of Materials Engineering, Jiangsu University of Technology, Changzhou 213001, People's Republic of China
[2] Institute of Fundamental and Frontier Sciences, University of Electronic Science and Technology of China, Chengdu 610051, People's Republic of China
[3] Department of Physics, Constituent College Depalpur, University of Agriculture, Faisalabad, Pakistan
[4] Department of Chemical and Polymer Engineering, University of Engineering and Technology, Lahore, Faisalabad Campus, Faisalabad, Pakistan
[5] Institute of Microengineering and Nanoelectronics (IMEN), National University of Malaysia (UKM), Bangi 43600, Malaysia
[6] Radcliffe Department of Medicine, University of Oxford, Oxford OX3 7BN, United Kingdom
[7] James Watt School of Engineering, University of Glasgow, University Avenue, Glasgow G12 8QQ, United Kingdom
[8] King Abdullah Institute for Nanotechnology, King Saud University, Riyadh 11451, Saudi Arabia
[9] School of Civil and Environmental Engineering, Nanyang Technological University, 639798, Singapore

E-mail: Aumber.abbas@jsut.edu.cn, mahamed@ksu.edu.sa, tmlim@ntu.edu.sg and oujunfei_1982@163.com

Received 15 April 2025, revised 16 July 2025
Accepted for publication 5 September 2025
Published 9 October 2025

Abstract

Graphene quantum dots (GQDs) have emerged as a transformative technology in biomedicine, driven by their exceptional optical, electronic, physicochemical, and biological properties. Their substantial π-conjugated system, low toxicity, biocompatibility, and tunable surface chemistries enable diverse functionalities, including adjustable fluorescence for biosensing and bioimaging, high drug loading capacity, effective cell membrane penetration for targeted delivery, and

[10] These authors contributed equally to this work.
[*] Authors to whom any correspondence should be addressed.

efficient radiation absorption for cancer therapeutics. Despite significant advancements, the interaction mechanisms of GQDs with biological systems remain inadequately explored, hindering their real-world clinical applications. This review summarizes the recent developments in GQD-based technologies, emphasizing the critical role of their interaction mechanisms in multifunctional applications, ranging from detection to therapy. It highlights innovative design strategies and the pivotal influence of GQD interactions with analytes, nucleic acids, and cellular components in enhancing the sensitivity and specificity of biosensors. Furthermore, it presents an in-depth analysis of their multifunctional roles and mechanisms in emerging applications like drug delivery, triple negative breast cancer treatment, and antimicrobial therapies. Particular attention is given to their synergistic role in combinational breast cancer therapies, where interactions with reactive oxygen species and photothermal agents amplify therapeutic efficacy. Finally, it addresses key challenges and proposes future research directions in this evolving field.

Keywords: graphene quantum dots, interaction mechanisms, biomedical applications, multifunctional nanoplatforms, cancer therapeutics

Contents

1. Introduction

Graphene quantum dots (GQDs) are the youngest members of the graphene family. They are zero-dimensional (0D) derivatives of graphene, typically consisting of one or a few graphene layers, with size ranging from 1 to 10 nm. Compared to their graphene counterpart, GQDs offer unique benefits, including the emergence of bandgap due to quantum confinement, strong fluorescence, exceptional dispersibility, a high density of active sites (such as functional groups, edges, and dopants), long-lived valley states, improved tunability of physical and chemical properties, and a size comparable to that of biomolecules [1–3]. These attributes make GQDs ideal for use in various biomedical fields, including bioimaging, biosensing, drug delivery, and cancer therapy [4, 5].

The most notable features of GQDs for biomedical applications are their tunable fluorescence properties and presence of surface reactive groups which allow their multimodal conjugation with potential targets [6], making them ideal candidates for the development of highly sensitive, label-free biosensors [7]. However, their inherent fluorescence quantum yield tends to be modest, and concerns persist regarding their potential long-term toxicity in organisms [8, 9]. Consequently, GQDs

are typically combined with supplementary agents for effective fluorescent detection. GQDs possess a modifiable structure because of their surface functional groups and extended π–π conjugated system, making them amenable to reaction with diverse organic, inorganic, and biological reagents [10–12]. These alterations can overcome native GQDs' shortcomings and broaden their utility, endowing them with enhanced functionality, such as improved photoluminescence (PL). Consequently, fluorescent sensors employing GQDs can be engineered by physical or chemical modification. Their surface can be easily modified to enhance interactions with biological molecules, making them ideal candidates for biosensors that detect specific biomarkers, pathogens, or cellular signals [13]. Their fluorescence response can be engineered to change upon interaction with target molecules, enabling highly sensitive detection for early disease diagnosis [14]. These GQD-based sensors exhibit superior attributes including high sensitivity, selectivity, water solubility, chemical inertness, and robust photostability, compared to conventional small molecule fluorescent sensors [15, 16]. Recent developments have shown the utilization of GQD-based fluorescent sensors for detecting inorganic ions, biomolecules, cellular microenvironments, and disease diagnosis, underscoring their significance in diverse applications [17].

The tunable fluorescence properties of GQDs offer exceptional advantages as fluorescent probes for both *in vitro* and *in vivo* applications [9]. Their emission spectra can be fine-tuned through modifications in size, surface functional groups, and heteroatom doping, enabling the development of GQDs with specific excitation-emission profiles for multicolor imaging in complex biological systems, taking an edge over conventional practices [18]. Importantly, functionalization and biofunctionalization are distinct yet complementary strategies in GQD design. *Functionalization* refers to the chemical modification of the GQD surface with reactive moieties such as hydroxyl (–OH), carboxyl (–COOH), or amine ($–NH_2$) groups, typically introduced during synthesis through oxidation or self-passivation. These groups enhance the aqueous solubility and chemical reactivity of GQDs, making them well-suited for biological environments [19, 20]. In contrast, *biofunctionalization* involves the subsequent conjugation of GQDs with specific biological molecules—such as peptides, antibodies, nucleic acids, or aptamers—to confer target specificity or therapeutic function. Dopants can be embedded within the carbon lattice or attached to the surface-bound oxygen-rich groups, further expanding the physicochemical tunability of GQDs. The combination of high surface area and abundant reactive sites makes GQDs ideal platforms for biofunctionalization, enabling precise interaction with cellular targets. This targeted capability enhances the precision and sensitivity of imaging modalities, thereby facilitating more accurate diagnostics and therapeutic monitoring [21, 22]. Additionally, the intrinsic photostability and resistance to photobleaching of GQDs offer distinct advantages of long-term imaging applications, positioning them as a superior alternative to traditional organic dyes and cadmium-based quantum dots.

In contrast with other materials like 1D and 2D nanostructures [23–26], 0D GQDs are being explored as versatile nanoplatforms for drug delivery applications, especially for cancer therapeutics. Their high surface area and functional groups enable the easy attachment of beneficial components such as ligands that target tumors or chemotherapeutic agents, which can be used in systems for delivering drugs to treat cancer [27–29]. Many other drug delivery systems use nanoparticles that are stabilized with a polymeric layer [30, 31]. This layer limits the number of accessible sites on the nanoparticle's surface for chemotherapeutic conjugation [32]. By contrast, GQDs possess a high surface area to volume ratio because of their flat structure. As a result, they may accommodate a relatively large proportion of drugs and thereby facilitate more effective administration of chemotherapeutic agents. In addition, the sp^2-hybridized GQD lattice can form π-stacking interactions with chemotherapeutic molecules containing an aromatic ring for drug transport [9, 33, 34]. Moreover, GQDs themselves possess photothermal and photodynamic properties, which can be harnessed for cancer treatment [35]. Under light irradiation, GQDs can generate localized heat or reactive oxygen species (ROS), effectively killing cancer cells and providing a synergistic approach to therapy. The ability to integrate diagnostic and therapeutic functions within a single platform enhances the precision of treatment and monitoring. Recent advancements have demonstrated that GQDs have the capability to significantly contribute to the biomedical field (figure 1) [33, 36–40].

The synthesis, modification and application of GQDs, as well as their integration with 2D materials, have been reviewed from different perspectives [41, 42]. Li *et al* [43] have summarized the development of GQD-based fluorescent sensors for biomedical use. Kalluri *et al* [44] focused on the synthesis, modifications and applications of GQDs in bioimaging, and drug delivery, while Handayani *et al* [45] detailed the developments in graphene and GQDs for biomedical engineering. Tade and More [46] discussed the GQD-based photodynamic and photothermal therapies, and Zhao *et al* [47] covered synthetic techniques, *in vivo* imaging, and *in vitro* biosensing. However, the interaction mechanisms of GQDs within multifunctional platforms—integrating diverse applications from fluorescent detection to therapeutic interventions—remains underexplored. Therefore, it is crucial to summarize how GQDs can be utilized to create multifunctional platforms for biomedical applications. This review aims to bridge that gap by providing a thorough analysis of the interaction mechanism of GQDs as multifunctional nanoplatforms across various biomedical applications. Specifically, we focus on five key areas: biosensing, bioimaging, drug delivery, cancer therapeutics, and antimicrobial therapies (figure 1).

This review begins with a thorough analysis of the unique characteristics of GQDs responsible for their multifunctionality. It then focuses on fluorescence sensing mechanisms, explaining many sensing processes and physical and chemical synthetic methods that are used to develop fluorescent sensors based on GQDs for bio-detection, bioimaging and

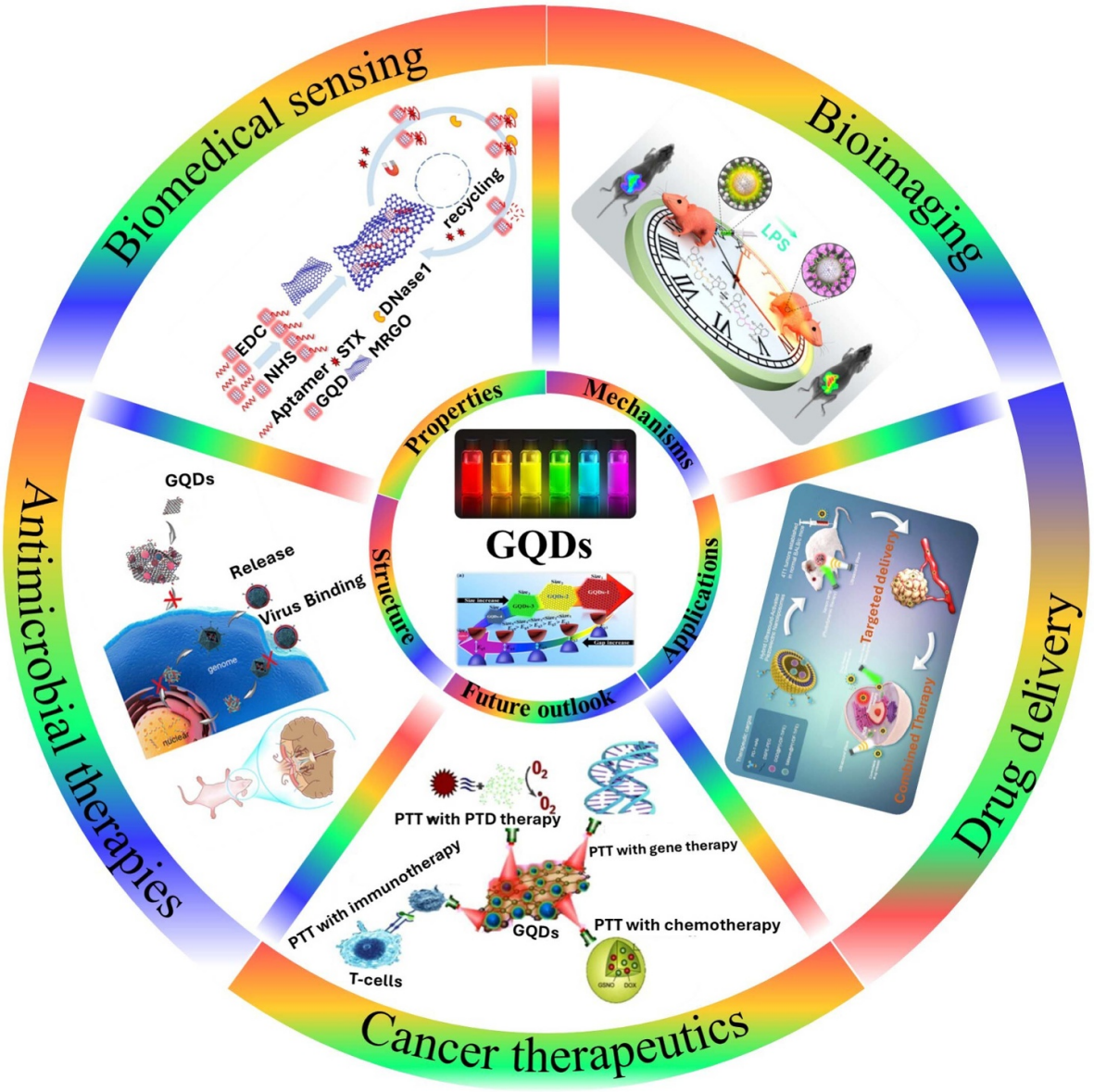

Figure 1. Schematic illustration of the structure, properties, interaction mechanism, and utilization of GQDs in various biomedical applications.

biomedical monitoring. The following sections thoroughly discuss the mechanism and multifunctionality of GQDs for diverse applications including drug delivery, controlled drug release, breast cancer therapies, along with antiviral and antibacterial therapies.

2. Unique properties of GQDs

2.1. Physicochemical properties

GQDs are 0D nanostructures of graphene with lateral dimensions typically ranging from 1 to 10 nm in size [48, 49], which imparts unique quantum effects. They are nanoscale particles made of graphene and graphene oxide (GO) that display quantum confinement in all three spatial dimensions [50, 51]. Both graphene and GO are single layers of hexagonally arranged sp^2-hybridized carbon atoms. However, GO contains point defects distributed in its lattice and along its edges [52]. Amorphous carbon quantum dots (CQDs) are a different form of carbon containing sp^3 hybridized carbon atoms arranged in a non-crystalline manner. The variations in structure among graphene, GO, GQDs, and CQDs result in significant differences in the characteristics of these carbon allotropes (figure 2(a)). The distinguishing feature between GQDs and CQDs is in the crystallinity of the graphene [53]. The GQDs are highly crystalline fragments of graphene, exhibiting quantum confinement due to sp^2 hybridized carbon structure. By comparison, CQDs usually refer to spherical nanoparticles of amorphous carbon that display PL properties as a result of surface passivation [54], and these are altered by surface changes [55, 56]. Although graphitic domains are present

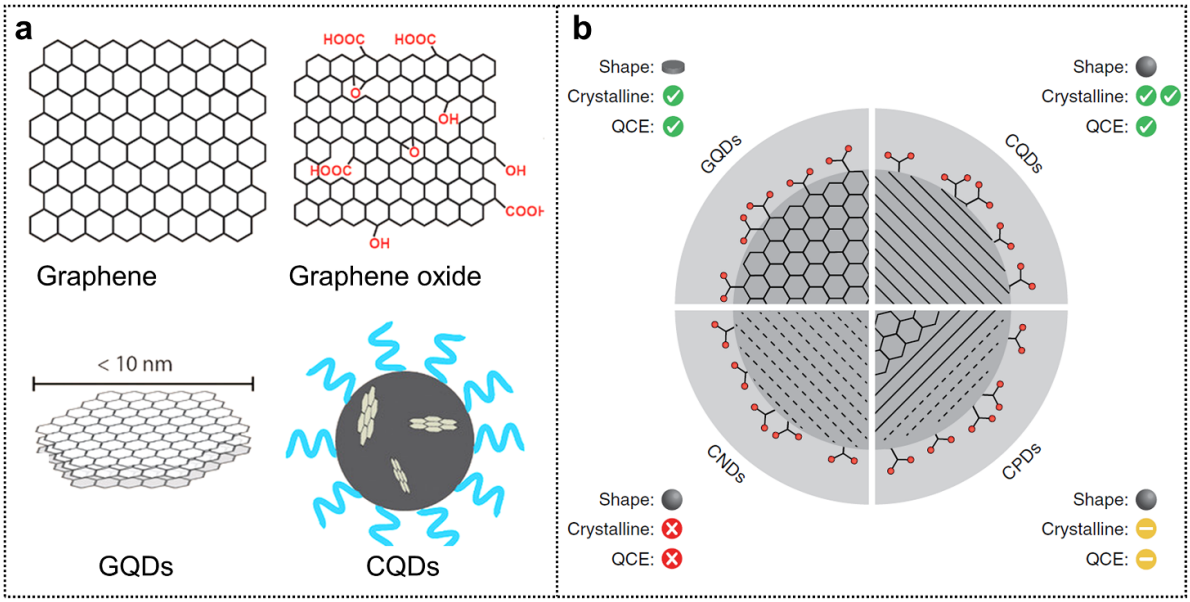

Figure 2. Structural variations among graphene, GO, GQDs and CQDs. [60] John Wiley & Sons. © 2019 WILEY-VCH Verlag GmbH & Co. KGaA, Weinheim. Differences among GQDs, CQDs, CNDs, and CPDs based on their physicochemical properties. Reproduced from [61], with permission from Springer Nature.

throughout the structure, CQDs are significantly less crystalline compared to GQDs [57, 58]. In addition, the GQD structure can be modified by the introduction of defects, dopants, spatial dimension variations or functional groups along the edges [59]. By adjusting their structure, GQD can be tailored for different biological applications.

One of the most fascinating aspects of GQDs is the manifestation of quantum confinement effects at the nanoscale [62]. The quantum confinement found in GQDs is a consequence of the abundant sp^2-hybridized carbon atoms in crystalline graphene. As GQDs shrink in size, charge carriers, such as electrons and holes, become confined within the graphene lattice. This confinement leads to quantized energy levels, and thereby unique electronic and optical properties [62]. These quantum confinement effects are particularly pronounced in GQDs because of their small dimensions, enabling researchers to precisely tune their properties by controlling size, shape, and edge structure. Understanding and exploiting these effects are crucial for harnessing the full potential of GQDs for various applications [63].

The difference between the properties of GQDs and their counterparts such as CQDs, carbonized polymer dots (CPDs), and carbon nanodots (CNDs) are summarized in figure 2(b) and table 1. GQDs are flat, circular sheets made of graphene. They have the same structure as graphene and exhibit quantum confinement effects because of their small size, specifically the size of the emissive π domains. On the other hand, CQDs have a quasi-spherical morphology and possess crystallinity derived from both the interplane stacking and graphene lattice. Additionally, they feature surface functional groups and demonstrate quantum confinement effects to some extent. CNDs have a nearly spherical form and a carbonized amorphous structure with surface functional groups. CPDs are distinguished by their quasi-spherical shape and a hybrid structure, comprising a carbon-based core and surface functional groups and/or polymers [61]. The desired characteristics of GQDs can be acquired by modifying their chemical composition, size, shape, and edge structure [64], thereby positioning GQDs as a promising platform for various biological applications.

2.2. *Optical and electronic properties*

GQDs exhibit intriguing optical properties that stem from their nanoscale dimensions and unique electronic structure [65, 66]. One of the most prominent optical phenomena observed in GQDs is strong PL, where they emit light upon excitation by an external energy source, such as photons [62]. The emission of light from a GQD is affected by its size, dopants, surface functionalization, defects, and the surrounding environment [67]. The PL emission of GQDs can cover a broad spectrum of wavelengths, ranging from ultraviolet (UV) to near-infrared (NIR), depending on factors such as size, surface functionalization, and defect density. Size-dependent PL peak shifts and intensity variations are the result of quantum confinement effects and surface chemistry modification. Additionally, graphene and carbon dots (CDs) have recently demonstrated long phosphorescence emission enabling optical security, anticounterfeiting and information encryption applications [68–71]. Moreover, GQDs demonstrate broadband absorption across the UV–visible–NIR spectrum, rendering them potentially suitable for sensing and biomedical applications.

To enhance the versatility of GQDs, their structure is tailored for specific applications. Modifications can be accomplished by doping with heteroatoms, surface functionalization, compositing, and regulating the size and shape of the GQDs (figure 3) [72]. The GQDs' bandgap defines the specific wavelength of PL emission. Graphene with a zero-bandgap

Table 1. Comparative overview of GQDs, CQDs, CNDs, and CPDs.

Feature	GQDs	CQDs	CNDs	CPDs
Core structure	Graphene fragments (sp^2)	Amorphous or partially crystalline carbon core	Nearly spherical amorphous carbon nanoparticles	Hybrid core-shell of carbon core and polymers
Crystallinity	High (graphitic lattice)	Low to moderate	Low	Low
Synthesis methods	Top–down (oxidative cutting, electrochemical) or bottom–up	Hydrothermal, microwave, or laser ablation	Carbonization of organic precursors	Polymerization/ carbonization of polymer precursors
Fluorescence mechanism	Quantum confinement and edge effects	Surface states and defect-related emission	Surface state-dominated	Molecular fluorophore and cross-linking structures
Optical properties	Tunable PL, high stability, narrow emission	Broad emission, lower stability	Broad spectrum PL	Often dual or multiple emissions
Biomedical applications	Imaging, sensing, drug delivery, cancer therapy	Imaging, bio-labeling, sensors	Bioimaging, antioxidant therapy	Drug delivery, tissue engineering, multicolor imaging

does not display PL, but GQDs can display PL if their structures are varied, such as by modifying their physical dimensions, adding surface groups, or adjusting dopant concentration, in order to achieve a nonzero bandgap. The primary mechanisms governing the PL in GQDs are: (1) quantum confinement, which is determined by the size of the GQDs, and (2) the bandgap of the GQDs, which is influenced by variations in energy levels associated with edge states, dopants, and surface functional groups [62, 73]. The modification of these parameters has been documented to result in GQDs emitting light at various wavelengths, including deep UV, blue, green, orange, red, and NIR [74, 75]. The electronic properties of GQDs are determined by their band structure. GQDs exhibit size-dependent electronic band structures, which are influenced by factors such as size, shape, and edge termination [76]. For smaller GQDs, strong quantum confinement effects result in a significant bandgap, making them behave more like semiconductors. Larger GQDs, on the other hand, may exhibit band structures resembling bulk graphene, with overlapping energy bands and enhanced metallic behavior. Additionally, the presence of edge states in GQDs further modifies their electronic properties, affecting phenomenon such as charge transport [76, 77].

GQDs possess good optical and electronic properties, however, to enhance their versatility in many domains, GQDs can be modified through various techniques to tailor their characteristics for specific purposes (figure 3). The observed changes in the electrical characteristics of graphene and GQDs are mostly due to many-body phenomena, specifically the interactions between electrons and between electrons and holes. These activities have been examined through both experimental and theoretical investigations [82–85]. Edge functionalization can modify electronic characteristics. The effect of chemical functionalization on the energy bandgap was examined using theoretical modeling and the energy bandgap was found to be highly influenced by the conformation of GQDs, with a value of 3.269 eV in the armchair configuration and 0.273 eV in the zigzag configuration. Functionalization had little impact on the bandgap. Nevertheless, substituting the hydrogen atoms with highly electronegative atoms such as oxygen or fluorine resulted in a substantial reduction in bandgap [86]. Although these theoretical investigations contribute to our understanding of the electronic structure of a single GQD with precise dimensions and structure, it is important to note that many GQDs described in the literature have different sizes and variations in functional groups. Although theoretical bandgaps are determined using GQD models with specified structures, experimental evidence demonstrates that GQDs frequently display PL emission spectra that vary depending on the excitation wavelength [60].

2.3. *Functionalization techniques of GQDs*

GQDs can be functionally tailored using a variety of strategies to improve their solubility, stability, and compatibility with targeted applications. These functionalization techniques influence their physicochemical properties, enabling a broader spectrum of biomedical, sensing, and optoelectronic uses. The primary methods include covalent and non-covalent functionalization, surface doping, polymer grafting, ligand exchange, and biomolecular conjugation.

2.3.1. Covalent functionalization. Covalent functionalization introduces specific functional groups onto the GQD surface via stable covalent bonds. This process typically involves chemical reactions such as amidation, esterification, diazonium coupling, and click chemistry to incorporate groups like hydroxyl (–OH), carboxyl (–COOH), and amine ($–NH_2$).

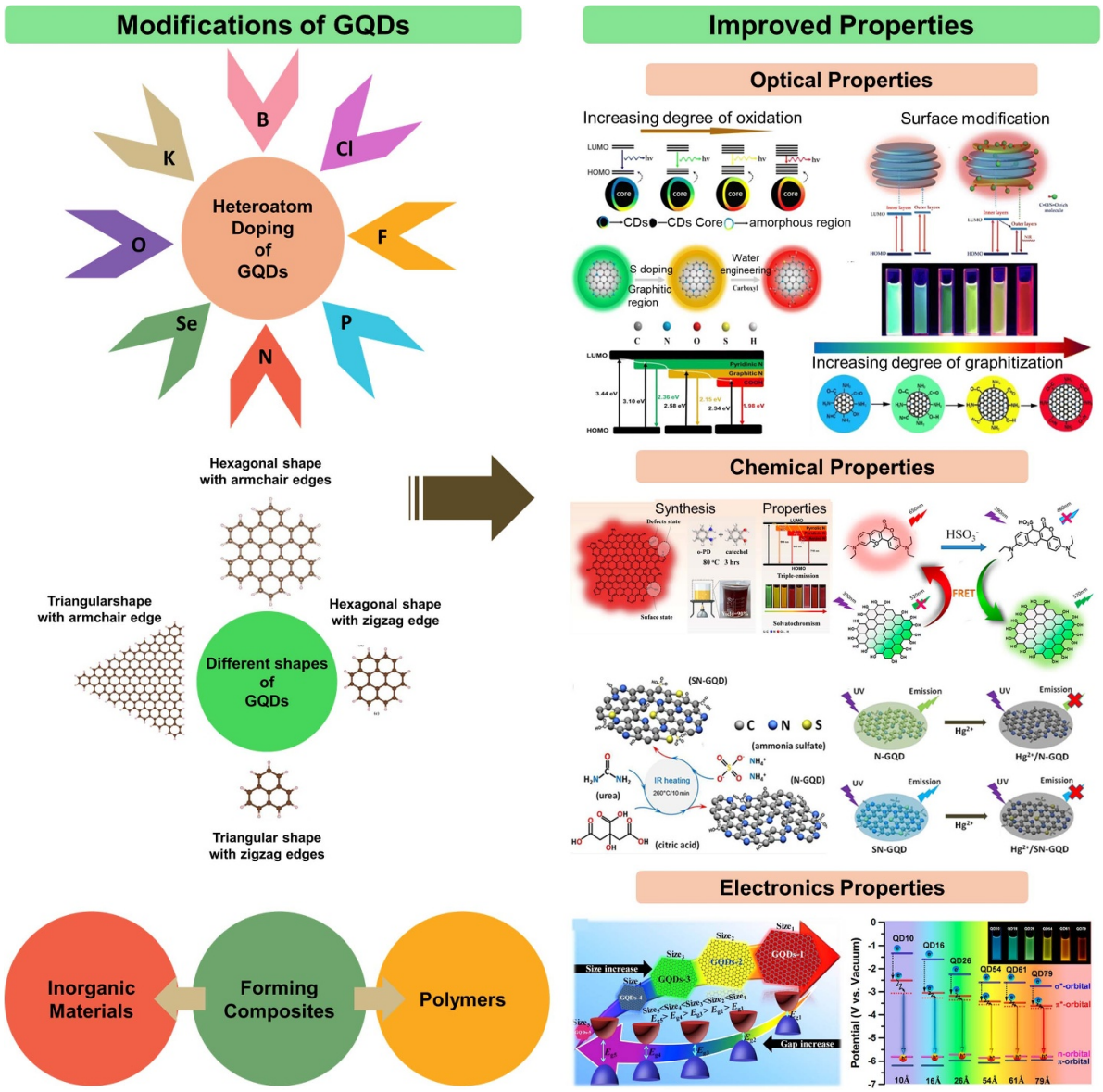

Figure 3. The left panel shows the schematic illustrations of the modifications of GQDs by heteroatom doping, size and shape variation, and composite formation, while the right panel shows the improvement in optical, chemical and electronics properties. (Right panel) Reprinted from [74], Copyright (2022), with permission from Elsevier. Reproduced from [78] with permission from the Royal Society of Chemistry. Reprinted with permission from [79]. Copyright (2019) American Chemical Society. Reprinted with permission from [80]. Copyright (2019) American Chemical Society. Reproduced from [81]. CC BY 4.0.

These modifications provide robust, tunable interfaces suitable for advanced hybrid materials and polymer integration. For instance, linking sulfonated and amine-terminated moieties through covalent interactions has been shown to enhance membrane performance in water purification by improving salt rejection and water flux [87]. Similarly, functionalizing GQDs with bovine serum albumin (BSA) via amidation has enabled selective chiral sensing platforms, leveraging exposed chiral sites and hydrogen-bonding interactions to distinguish between enantiomers [88].

2.3.2. Non-covalent functionalization. This approach utilizes weak physical interactions—such as π–π stacking, van der Waals forces, hydrophobic forces, and electrostatic attraction—to associate functional molecules with GQD surfaces. Unlike covalent bonding, these interactions preserve the intrinsic electronic and structural properties of GQDs. Non-covalent strategies are reversible and particularly useful for temporary or switchable functionalization, often employed in drug delivery systems or supramolecular assemblies [89, 90].

2.3.3. Surface doping. Surface doping involves the incorporation of heteroatoms or foreign elements (e.g. nitrogen, sulfur, boron, or phosphorus) into the GQD structure, which can modulate its bandgap, charge carrier dynamics, and chemical reactivity. These dopants are typically introduced during synthesis or through post-synthetic treatments. Doped GQDs have

shown improved electrical conductivity and tunable luminescent properties, which are advantageous in catalysis, imaging, and optoelectronic applications [91].

2.3.4. Surface polymerization. In this technique, monomers are polymerized directly on the surface of GQDs to form protective or functional polymeric coatings. Methods such as surface-initiated polymerization or *in situ* polymerization allow precise control over shell thickness and chemical functionality [92]. Polymer-grafted GQDs often exhibit enhanced solubility, mechanical stability, and processability, making them suitable for integration into composite materials or biological media.

2.3.5. Ligand exchange. Ligand exchange enables the replacement of original surface-bound ligands on GQDs with new functional molecules that better suit the target application. This transformation is typically achieved through solvent-assisted processes, displacement reactions, or phase-transfer techniques. By customizing the surface ligands, researchers can tailor GQD dispersibility, solubility in non-aqueous media, and interaction with other components in a hybrid system [93].

2.3.6. Biomolecular functionalization. Biomolecular functionalization of GQDs involves the attachment of biological macromolecules—such as proteins, peptides, DNA, RNA, or antibodies—to their surface [94]. This functionalization enhances the biocompatibility, targeting ability, and specificity of GQDs, making them highly suitable for a range of biomedical applications, including biosensing, bioimaging, drug delivery, and diagnostics. The modification can be achieved through covalent bonding, where functional groups such as –COOH on the GQD surface react with $–NH_2$ groups on biomolecules via amide bond formation, or through non-covalent interactions like hydrogen bonding, electrostatic attraction, or π–π stacking. These strategies enable the retention of both the optical properties of GQDs and the biological activity of the attached biomolecules [1, 95].

Recent advances highlight the integration of GQDs with biopolymers and smart ligands to achieve highly specific biofunctionalization. For instance, the conjugation of GQDs with folate-linked polyethylene glycol (PEG) enables targeted imaging of folate receptor-overexpressing tumors [35]. Covalent functionalization via ethyl-3-3-(dimethylaminopropyl) carbodiimide (EDC)/NHS chemistry facilitates stable antibody attachment, enhancing biosensor selectivity. Moreover, machine learning algorithms have been applied to predict optimal functionalization parameters for desired biological outcomes. A particularly insightful example of this functionalization is the conjugation of GQDs with BSA for the development of a chiral sensing platform [88]. This was accomplished through an amidation reaction, which not only anchored BSA onto the GQD surface but also altered its three-dimensional (3D) structure. As a result, additional chiral sites on BSA were exposed, enhancing the system's enantioselectivity. This GQD-BSA hybrid exhibited a strong preferential interaction with L-tryptophan over D-tryptophan, which was attributed to hydrogen bonding between the amino acid residues on BSA and the tryptophan molecules. Theoretical calculations using density functional theory (DFT) further confirmed that the enhanced chiral recognition was due to the favorable binding energies and orientation of L-tryptophan within the modified protein environment.

Another advanced approach to biomolecular functionalization involves nitrogen-doping of GQDs using nitrogen-rich molecules [96]. This modification allows precise tuning of the electronic properties, such as HOMO–lowest unoccupied molecular orbital (LUMO) energy levels and PL behavior. The incorporation of different nitrogen-containing groups—such as primary amines, tertiary amines, or aromatic diamines—alters the orbital interactions within the GQD structure. As a result, significant shifts in energy levels and emission spectra are observed. These nitrogen-functionalized GQDs (NGQDs) not only exhibit strong multicolor PL under UV excitation but also demonstrate enhanced performance in optoelectronic devices. For example, in perovskite solar cells, NGQDs improve charge separation and transport, resulting in higher photoconductive gain and responsivity. This dual functionality emphasizes the versatility of biomolecular and nitrogen-based functionalization in bridging biological systems with electronic and photonic technologies.

2.4. Biological properties

The biomedical applications of GQDs rely on their low toxicity, stability, hydrophilicity, and biocompatibility [61]. The extent to which a material is biocompatible depends on its capacity to fulfill its intended purpose without causing undesired biological responses [97, 98]. While toxicity resulting from aggregation is observed in various carbon-based nanoparticles [99], GQDs exhibit remarkable water solubility and serve as a non-toxic substitute for metal-based nanoparticles. A common method for evaluating biocompatibility involves measuring *in vitro* cytotoxicity. GQDs functionalized with $–NH_2$, –COOH, and $–CHO–N–(CH_3)_2$ exhibited minimal *in vitro* cytotoxicity up to 200 μg ml^{-1} concentrations. Conversely, GQDs modified with hydroxyl group (–OH) displayed some cytotoxic effects at concentrations beyond 100 μg ml^{-1} [100]. The cytotoxicity mechanism of hydroxylated GQDs was previously believed to be caused by the generation of cellular senescence and intracellular ROS (ROS). However, a closer investigation revealed that the increase in ROS was observed only after a significant decline in cell viability. Additionally, the biocompatibility of GQDs with different functionalization, as calculated by cellular uptake, did not show correlation with their corresponding cytotoxicity [101]. Studying the cytotoxicity of nanoparticles is more valuable than making broad generalizations when evaluating the biocompatibility of GQDs, as cellular interactions with nanoparticles can be intricate.

The cytotoxicity and biodistribution of carboxylated GQDs have been studied using intravenous administration in animal models [102–104]. *In vivo* bioimaging of the mice and *ex vivo*

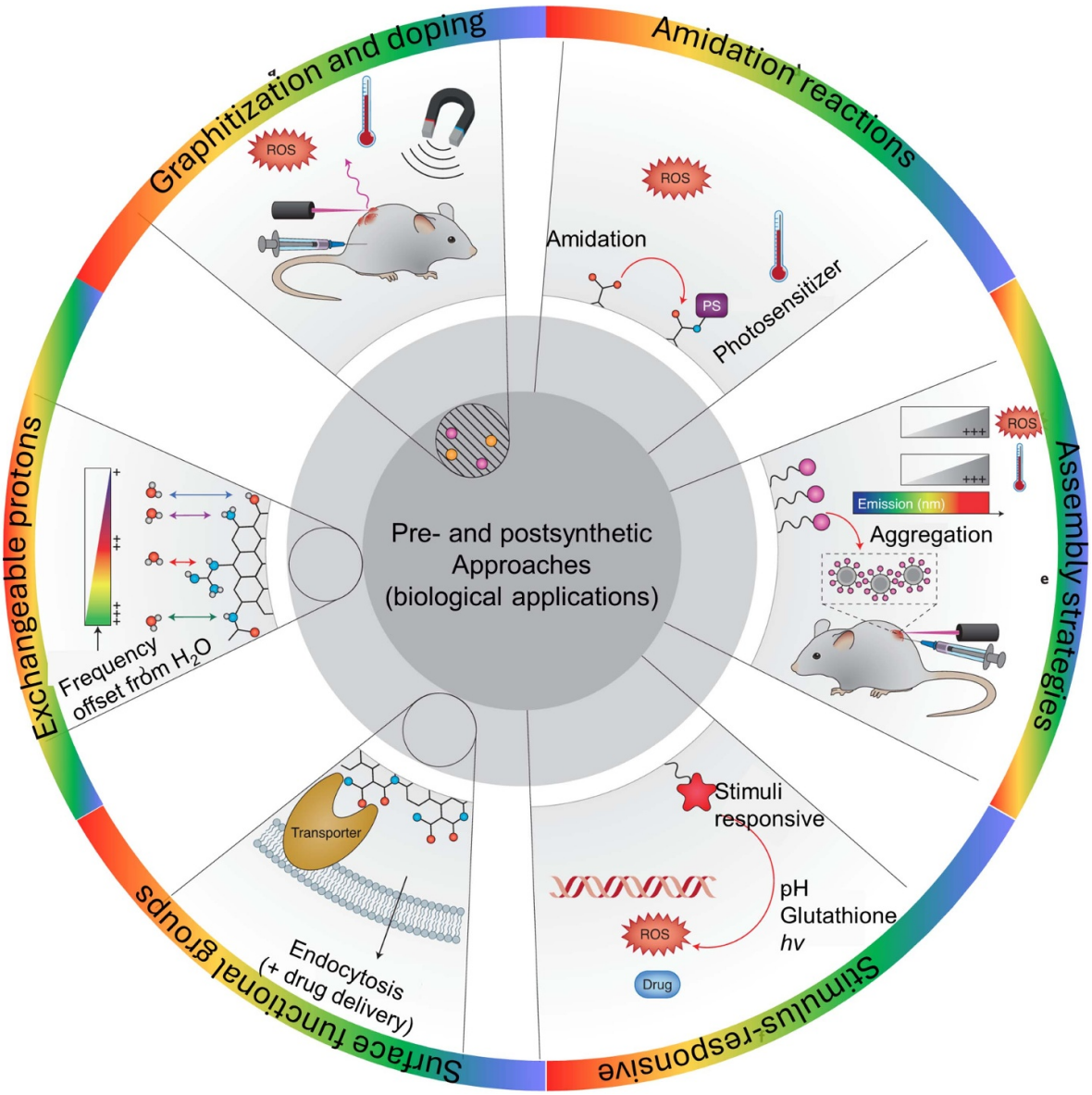

Figure 4. A survey of methods to improve the usability of GQDs in biomedical applications. These methods include graphitization and doping, exchanging protons, surface functional groups, amidation, assembly strategies, and stimulus-responsive design of GQDs based materials. Reproduced from [61], with permission from Springer Nature.

study of their organs revealed that the GQDs started to eliminate from their bodies after 12 h. The whole blood count and histological analysis of mice treated with GQDs and saline, did not indicate any noteworthy changes between the experimental and control groups [105]. This finding is consistent with another recent study [97]. Both investigations observed slight alterations in the histological assessment of kidney and the liver at high doses of GQDs after 30 d. The lack of acute toxicity observed in these *in vivo* experiments provides promising evidence for the biocompatibility of GQDs [14]. Aside from conducting toxicity tests, researchers have also investigated the immunological response to GQDs and explored their degradation mechanism [106]. Emerging studies suggest that surface-functionalized GQDs can interact with immune cells, influencing cytokine expression and macrophage activation. In particular, nitrogen-doped and hydroxyl-rich GQDs have been shown to modulate immune responses by triggering the release of IL-6 and TNF-α in macrophages, indicating mild immune activation [98, 107]. Furthermore, surface charge and size have been found to influence complement activation and dendritic cell maturation, hinting at the potential of GQDs to engage the humoral immune system [108, 109]. However, these findings are preliminary, and further *in vivo* immunotoxicological assessments are needed to establish safety profiles and immunological compatibility.

One of the biological effects of GQDs is their ability to generate photoinduced ROS, which leads to cytotoxicity [61, 97]. A number of methods, including amidation reactions, graphitization and doping, assembly strategies, and stimulus-responsive design, have been introduced to generate ROS in GQDs (figure 4). The impact of functional groups, particularly the oxygen-containing ketones, carboxyl,

and hydroxyl groups, on the capability of GQDs to produce ROS has also been studied [72]. These findings suggested that all oxygen-containing functional groups promote the production of ROS, with the ketones having the biggest effect. The elevated levels of ROS production strongly affected cell viability on prolonged exposure to radiation. However, cell viability remained unaffected after storing in the dark [110, 111]. Subsequent studies verified that the absence of irradiation resulted in an absence of harmful effects on cells treated with GQDs [112]. These investigations indicated that the irradiation of GQDs led to the generation of ROS, which in turn caused cytotoxicity. While GQDs are commonly used in biological research to take advantage of their PL capabilities, which necessitates exposure to light, no harmful effects on cells have been observed in these investigations [38, 113].

Recent studies have examined the use of longer wavelengths to understand the PL characteristics of GQDs. Efficient phototherapy and *in vivo* bioimaging necessitates high absorption and robust PL in the red to NIR range. In recent years, significant efforts have focused on enhancing the optical characteristics within this therapeutic range (figure 4) [61]. Expanding the conjugation of sp^2 domains enhances the effectiveness of GQDs in photothermal treatment and adds imaging capability, as does controlling heteroatom doping, core graphitization, and surface oxidation. Composite materials can be designed to customize GQD characteristics for effective light absorption for therapeutic benefits that are not present in the separate components. However, additional research is needed to fully comprehend the ROS production mechanism.

Beyond general surface interactions, the interaction mechanisms of GQDs with biomolecules (e.g. DNA, proteins, ROS generation) at the molecular level is also important. GQDs interact with DNA primarily through π–π stacking between the graphene basal plane and nucleobases, as well as electrostatic interactions with the negatively charged phosphate backbone [114, 115]. This can lead to structural changes or stabilization of DNA conformation, depending on the GQD surface chemistry. In the case of proteins, surface-functionalized GQDs may form hydrogen bonds or electrostatic interactions with side chains (e.g. lysine, arginine), which can modulate protein folding, enzymatic activity, or induce conformational shifts. These interactions are particularly critical in biosensing and drug delivery systems where GQD–protein conjugation is used for targeting or controlled release.

2.5. Anticancer and drug delivery properties

GQDs have gained considerable attention in the field of nanomedicine due to their remarkable potential for various theranostic applications, particularly in cancer treatment. They possess distinctive physicochemical characteristics, such as exceptional biocompatibility and natural biodegradability, making them highly suitable for *in vitro* and *in vivo* biomedical applications. One of the most notable features of GQDs is their superior optical and photoluminescent properties, which allow for precise imaging and detection of harmful tissues, even in advanced preclinical models like 3D tumor cultures. The efficacy of GQDs is further improved by surface functionalization, which improves their interaction with cellular membranes. This functionalization facilitates better cellular uptake and increases the mobility of GQDs across cell membranes, crucial when they are used in combination with anticancer drugs at sub-therapeutic concentrations. This synergistic approach enhances therapeutic efficacy, especially in various experimental models. In addition, GQDs possess a large surface area, enabling significant adoption of targeting molecules or therapeutic agents, which improves their efficacy in targeted treatments. This modification not only boosts the selectivity of GQDs for cancer cells but also increases their therapeutic potential in tumor targeting. Their size can also be finely tuned to optimize cellular uptake and distribution within the body, a feature that is particularly advantageous when used in 3D tumor models. By customizing the size, GQDs can be tailored for more effective use in clinical applications. Another key attribute of GQDs is their impressive stability against photodegradation under light exposure, which ensures long-lasting imaging capabilities and reliable cancer progression tracking. In conclusion, the diverse set of properties of GQDs include their excellent biocompatibility, functionalization flexibility, and extraordinary optical features, making them highly attractive for use in cancer therapeutics and imaging [116–118].

GQDs present a variety of innovative strategies for monitoring, imaging, diagnosing, and delivering chemotherapy drugs directly to cancerous tissues, thereby making a substantial contribution to cancer nanomedicine. GQDs improve the efficiency of drug delivery by enhancing the therapeutic effectiveness while minimizing systemic toxicity, overpowering biological obstacles, and improving the success rate of cancer treatment. Nanomedicine brings together fields like materials science, pharmacology, molecular biology, medicine, and artificial intelligence to offer a more in-depth knowledge of biological processes and disease mechanisms. As nanocarriers, GQDs can penetrate cellular membranes, facilitating better drug penetration and transport beyond these constraints (figure 5(a)) [4]. Nanomedicine applications utilizing GQDs provide significant clinical benefits, such as enhanced stability, extended circulation duration, and excellent biocompatibility [21, 35]. Moreover, GQDs can be integrated into drug-loaded carriers like liposomes and micelles, which improves their ability to cross biological membranes and deliver drugs directly to targeted cells (figure 5(b)). The cellular uptake, distribution, and elimination of GQDs depend on factors such as their size, shape, and surface characteristics, all of which play a crucial role in optimizing therapeutic outcomes [119].

Numerous nanoparticle-based drug delivery systems, including those using GQDs, are currently undergoing clinical trials for treating different subtypes of breast cancer. New advancements suggest that GQDs can selectively target specific breast cancer subtypes for drug delivery, thereby safeguarding healthy tissues and cells from the toxic side effects commonly seen with chemotherapy. The GQD-based multimodal platform improves therapeutic outcomes by integrating various treatment strategies. This platform can carry a combination of drugs and genetic materials, while also

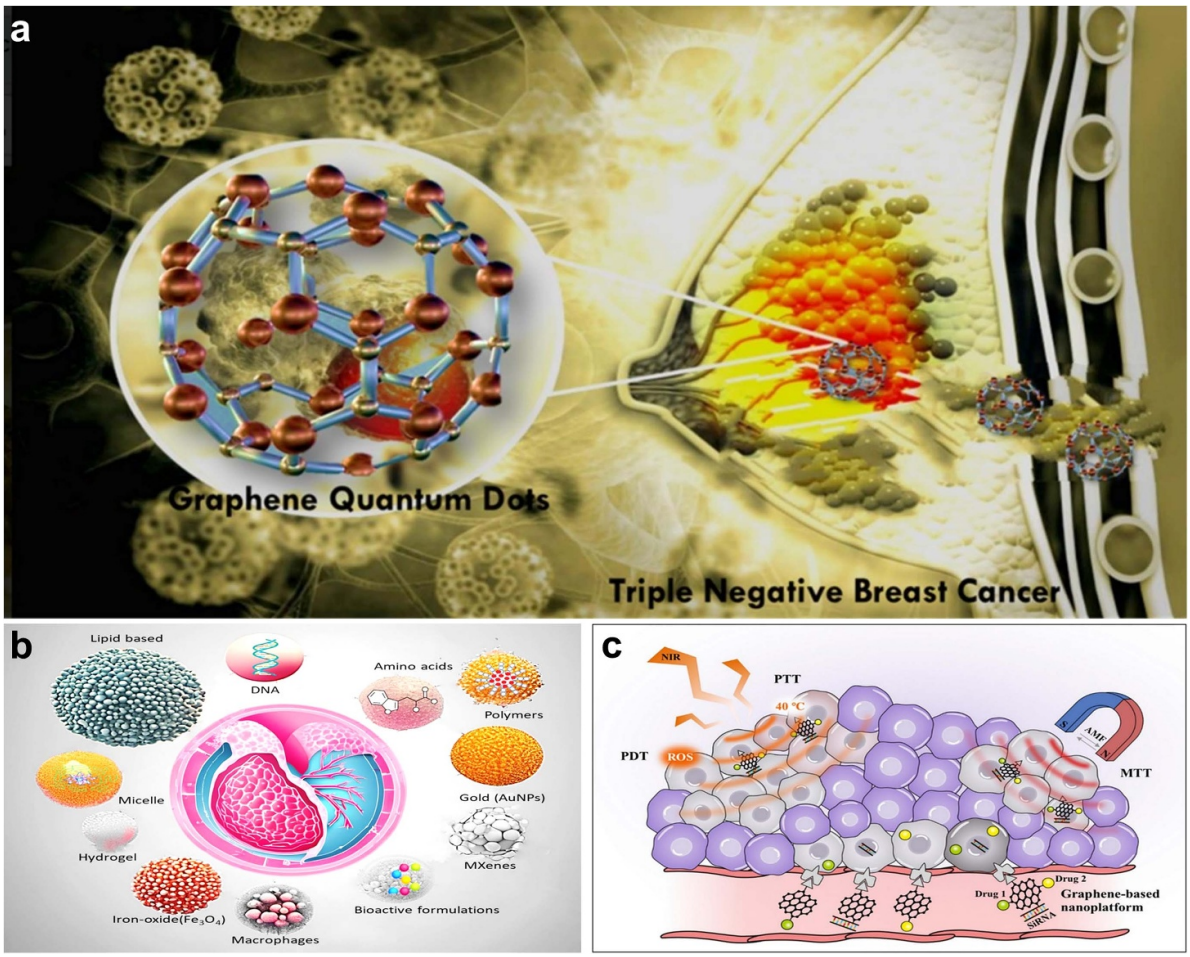

Figure 5. (a) Schematic representation of the use of GQDs in breast cancer therapy, and (b) integration of GQDs with various other nanomedicine for breast cancer treatment. Reprinted from [4], Copyright (2025), with permission from Elsevier. (c) The use of GQDs with other combinational therapies (such as PTT, PDT, and MTT) for simultaneous therapeutic benefits. Reproduced from [120]. CC BY 4.0.

being utilized in combination with phototherapy and magnetothermal therapy (figure 5(c)) [120]. GQDs offer several advantages, including reduced toxicity, excellent biocompatibility, ease of synthesis, and superior encapsulation efficiency. These properties help protect the therapeutic agents from environmental degradation, minimize interaction with healthy cells, and enhance the targeted action of the treatment while reducing adverse side effects. The diverse capabilities of GQDs underscore their potential to greatly improve the precision and efficacy of cancer treatments [121].

2.6. Antimicrobial properties of GQDs

GQDs have recently gained significant attention for their impressive antimicrobial properties, including their ability to produce ROS and their surface charges, which contribute to their antibacterial effectiveness [122]. There are three main mechanisms to exert their antimicrobial effects: (1) the generation of ROS that induces cellular damage and death, (2) the disruption of bacterial cell membranes, and (3) the binding of GQDs to bacterial DNA and RNA, which hinders cellular replication and growth (figure 6(a)) [123]. To determine which of these mechanisms plays a dominant role in a particular application, advanced techniques such as tunneling atomic force microscopy (TUNA) can be employed to quantitatively assess the nanoelectrical and nanomechanical properties of GQDs [124]. In addition, other complementary methods, including SEM, TEM, molecular dynamics simulations and real-time polymerase chain reaction, are useful for gaining a comprehensive understanding of how GQDs interact with bacterial cells and contribute to their antimicrobial effects.

Bacteria possess innate antioxidant defense mechanisms to shield themselves from ROS, such as singlet oxygen ($^1O_2$), superoxide anions ($\bullet O_2^-$), hydrogen peroxide (H_2O_2), and hydroxyl radicals ($\bullet$OH), whether these are produced internally or introduced from external sources. However, when ROS levels surpass the capacity of these protective systems, oxidative stress occurs, leading to damage to cellular structures, including membranes, nucleotides, lipids, and proteins. This oxidative damage can ultimately result in bacterial cell death [126]. GQDs have gained significant attention for their

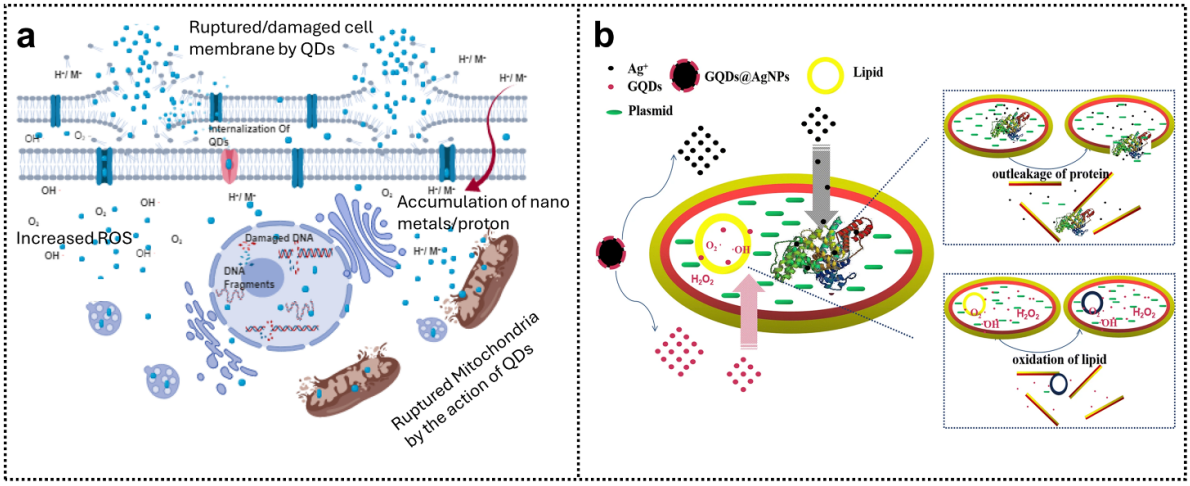

Figure 6. (a) Schematic representation of the mechanism for antimicrobial activity of GQDs. Reproduced from [123]. CC BY 4.0. (b) Schematic of the mechanism for antibacterial activity of functionalized GQDs. Reproduced from [125], with permission from Springer Nature.

ability to generate ROS, which contributes to their antimicrobial properties [127]. Functionalized GQDs exhibit enhanced antibacterial activity through the synergistic effects of surface moieties and the GQDs themselves. For instance, AgNPs disrupt the bacterial cell wall, while GQDs enhance ROS production [125]. This results in the leakage of protein and the generation of ROS, which damage vital bacterial macromolecules, including DNA, lipids, etc. (Figure 6(b)). GQDs can also serve as photosensitizers (PSs), capable of absorbing specific wavelengths of light to produce ROS in a controlled way, targeting pathogens with minimal unintended effects.

The mechanism of ROS generation by GQDs typically involves photoexcitation under UV or visible light, where electron–hole pairs are generated. The excited electrons can transfer to molecular oxygen, forming superoxide radicals ($\bullet O_2^-$), while holes can oxidize water to produce hydroxyl radicals ($\bullet$OH). Surface oxygen-containing functional groups (e.g. carbonyls, hydroxyls) facilitate these reactions by lowering activation energy and stabilizing radical intermediates. Additionally, dopants such as N or S can promote intersystem crossing, enhancing the formation of singlet oxygen ($^1O_2$) via energy transfer.

2.6.1. Strategies to enhance antibacterial activity of GQDs.

Several strategies have been explored to improve the photoexcited antibacterial activity of GQDs. Structural modifications of these GQDs can improve their interaction with bacterial membranes and increase their ability to induce oxidative damage. Additionally, GQDs exhibit greater antibacterial efficacy with extended irradiation times and higher concentrations [127]. Moreover, it has been observed that the ROS-generating capability of GQDs can be further enhanced through heteroatoms doping that improves electron delocalization and reduces the bandgap, thereby boosting the ROS production potential of GQDs [128]. The development of novel strategies to combat the growing threat of antimicrobial resistance has gained significant attention in recent years. While conventional antibiotics target and inhibit crucial bacterial metabolic pathways, GQDs offer an alternative mechanism by disrupting bacterial membranes. This disorder results in the leakage of cellular contents and the generation of ROS, which damage vital bacterial macromolecules, including DNA, lipids, carbohydrates, enzymes, and proteins, ultimately resulting in cell death (figure 7) [5].

Moreover, GQDs offer a significant edge over traditional antibiotics, not only due to their antibacterial efficacy but also in their capability to minimize the development of multidrug-resistant infections [131]. For instance, Wang and his team [132] showed that nitrogen-doped GQDs (N-GQDs) possess strong antibacterial properties against ampicillin-resistant *E. coli* and methicillin-resistant *S. aureus* (MRSA), surpassing the effectiveness of traditional antibiotics such as vancomycin and gentamicin. The antibacterial effect of GQDs could also promote the infected wound healing. For example, chitosan functionalized GQDs induced a synergistic interaction in combination with photodynamic therapy (PDT) and photothermal therapy (PTT), leading to irreversible membrane damage, cytoplasmic leakage, and subsequent bacterial cell death (figures 7(a) and (b)) [129]. GQDs also promote ROS production in suspension and, under light irradiation, exhibit significant phototoxicity against bacterial cells. Their tunable band gap enables absorption of visible and broad UV radiation, allowing them to function as PSs for generating cytotoxic singlet oxygen $^1O_2$, which leads to direct bacterial destruction (figure 7(c)) [130].

Bacterial infections often involve the formation of biofilms, in which bacteria aggregate and secrete an extracellular polymeric substance (EPS) that protects them from both the immune system and antibiotic treatments [133]. These

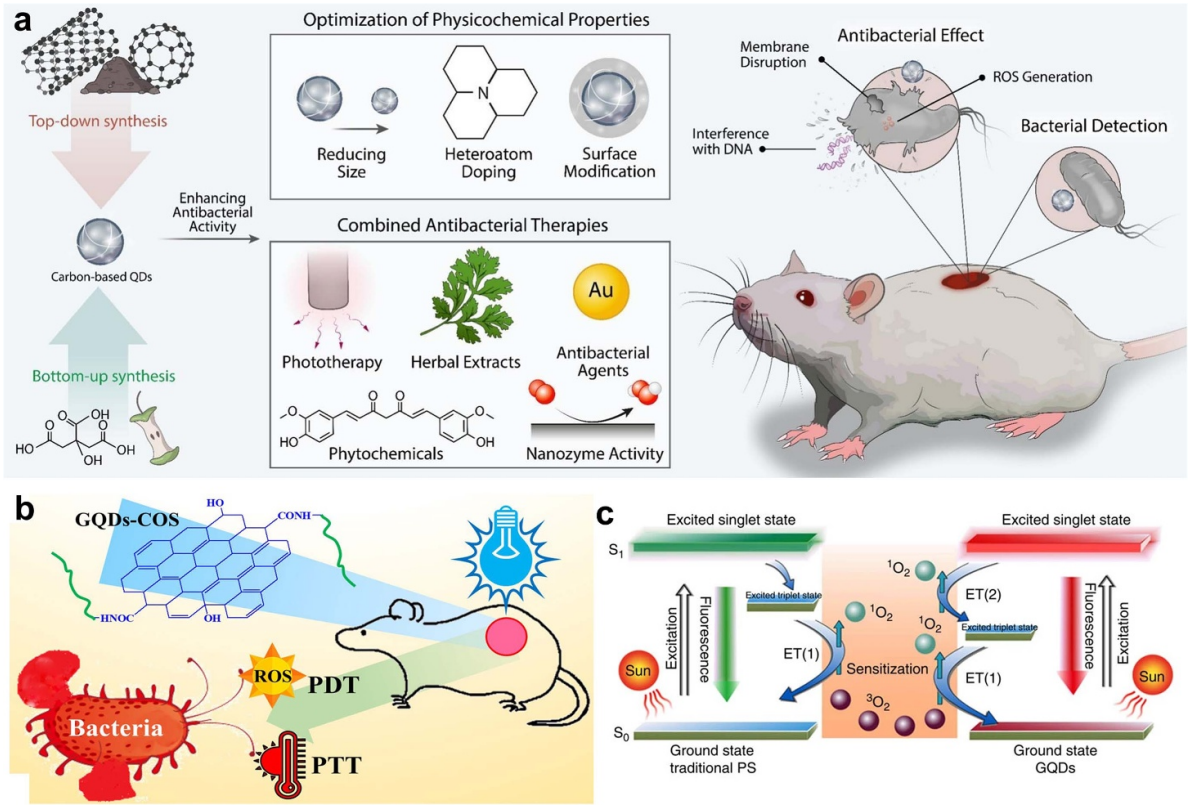

Figure 7. (a) Schematic illustration of the GQDs development and modification for antibacterial therapies. Reprinted from [5], Copyright (2025), with permission from Elsevier. (b) Combination of GQDs with PTT and PDT for antibacterial therapies. Reprinted with permission from [129]. Copyright (2020) American Chemical Society. (c) The mechanism of photo-induced $^1O_2$ production for ROS generation for antibacterial phototoxicity. Reproduced from [130], with permission from Springer Nature.

biofilms can form on a variety of surfaces, both biological and synthetic, presenting a significant challenge in clinical and industrial systems due to their contribution to persistent infections and antibiotic resistance [134]. GQDs offer a novel approach to combating biofilm formation by generating ROS. These ROS are capable of attacking and destabilizing the EPS, which is composed of various components such as polysaccharides (including succinic acid, alginate, and other sugars that facilitate bacterial adhesion), proteins, and extracellular DNA. The oxidative action of ROS interferes with the integrity of the biofilm, weakening its ability to maintain a stable structure and impeding bacterial attachment, thereby mitigating the bacteria's ability to protect themselves from external threats [5, 135, 136].

3. Fluorescent biosensing applications

GQDs exhibit remarkable fluorescent characteristics, with their emission wavelengths being tunable depending on their size and edge defects [137]. Furthermore, the extended π–π conjugated system of GQDs can physically adsorb aromatic molecules. In this section we present a general overview of fluorescence sensors based on GQDs, with a specific emphasis on the diverse detecting mechanisms that have been employed.

3.1. Detection mechanisms of fluorescent biosensors

We classify GQDs based fluorescent sensors into different categories according to their diverse detection mechanisms for biomedical applications:

3.1.1. ON–OFF fluorescent sensors. GQDs are frequently integrated into fluorescent sensors but may be quenched by specific analytes via physical or chemical interactions. In the design of these sensors, GQDs serve as fluorophores, and their specificity for the analyte will determine their usefulness [138–140].

In the presence of certain target molecules capable of undergoing redox reactions with the fluorescent quencher, the quenched fluorescence is returned [141]. Leveraging this approach, composite systems comprising GQDs and fluorescent quenchers have been devised [142, 143]. For example, Shi *et al* [144] created a fluorescence sensor for ascorbic acid (AA) using a composite system that included GQDs, layered double hydroxides (LDHs), and Fe^{3+} (figure 8(a)). LDH was utilized as a carrier in this sensor to inhibit the aggregation of GQDs. The PL emission of the GQDs was suppressed by Fe^{3+} through both electron transfer and dynamic quenching mechanisms. When AA was present, it caused the reduction of

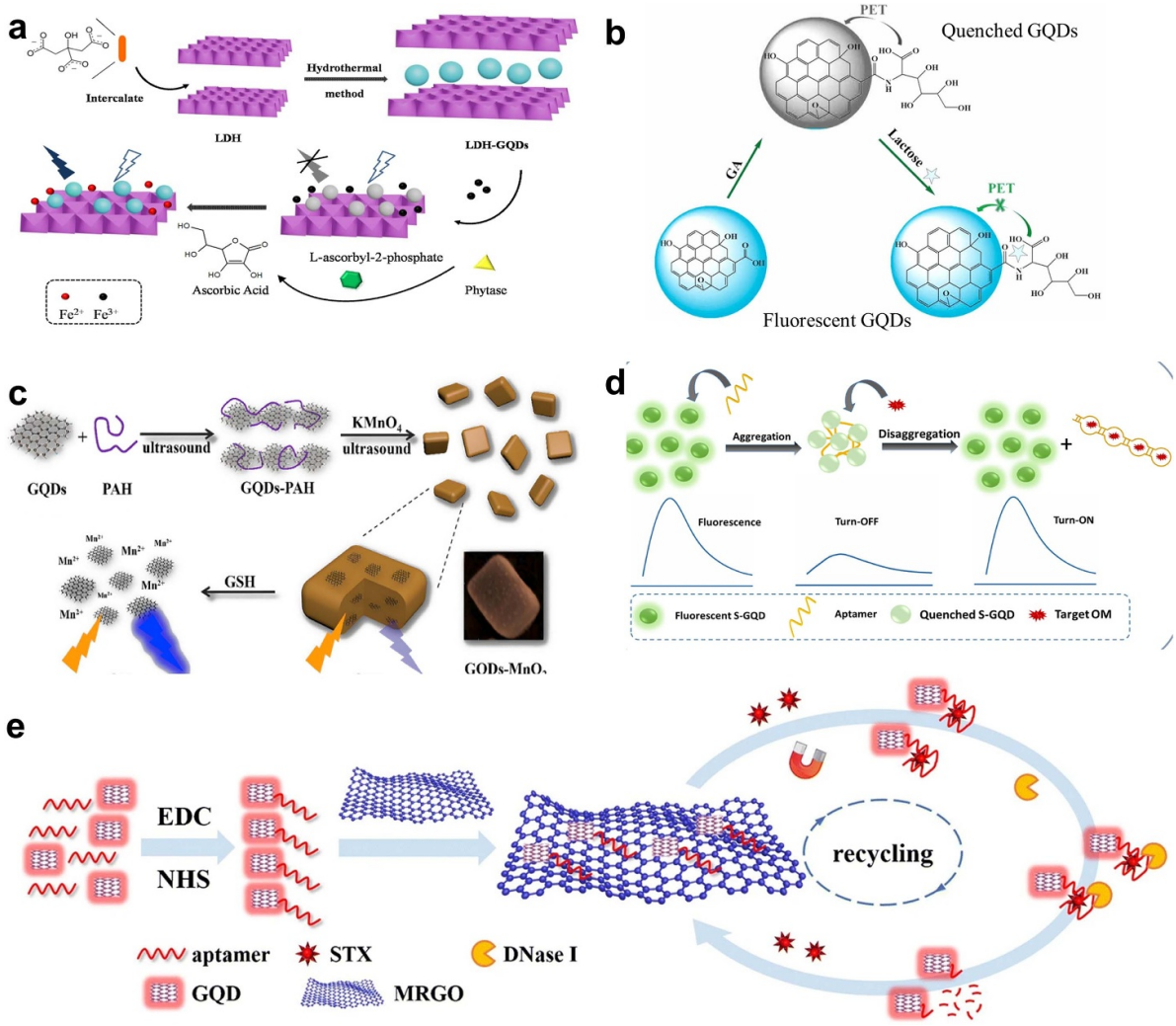

Figure 8. (a) Schematic representation of LDH-GQDs based sensor and sensing mechanism for ascorbic acid and phytase. Reprinted from [144], Copyright (2021), with permission from Elsevier. (b) Schematic of the sensing mechanism of GQDs-GA for lactose sensing. Reprinted from [145], Copyright (2023), with permission from Elsevier. (c) Development technique for GQDs-MnO_2 nanocomposite fluorescence probe for GSH sensing. Reprinted from [146], Copyright (2020), with permission from Elsevier. (d) Sensing mechanism of S-GQD-Apt fluorescence 'switch-on' aptasensor for omethoate detection. Reprinted from [147], Copyright (2021), with permission from Elsevier. (e) Schematic representation of the GQDs-aptamer based fluorescent sensor for marine biotoxins. Reproduced from [148], with permission from Springer Nature.

Fe^{3+} to Fe^{2+}, which resulted in the restoration of GQD emission. The AA was generated from the reaction of phytase and l-ascorbyl-2-phosphate and so the LDH-GQD detection system could also measure the concentration of the enzyme phytase.

In a recent study, Zhou *et al* integrated glucosaminic acid-functionalized GQDs (GQDs-GA) as a fluorescent sensor for lactose in food samples and living cells (figure 8(b)) [145]. GA functions as a receptor for lactose, while the GQDs serve as a transducer for fluorescence signals.

The addition of lactose resulted in a considerable enhancement of fluorescence peaks at 315 and 429 nm due to the inhibition of photoinduced electron transport. This design could be used to trace lactose in living cells. Wang *et al* produced a GQDs-MnO_2 composite based fluorescent sensor for glutathione (GSH) (figure 8(c)) using a similar approach [146]. The combination of poly(allylamine hydrochloride) with GQDs and MnO_2 formed a unique nanocomposite material with a square-plate-like structure. The fluorescence of the GQDs was suppressed by MnO_2 by a combination of energy transfer and the inner filter effect between MnO_2 and GQDs. The addition of GSH initiated a reduction in MnO_2, resulting in the restoration of the GQDs' fluorescence intensity.

Metal ion quenchers that rely on redox reactions can suffer from a lack of selectivity [149]. These substances are susceptible to disruption by other oxidants and reductants. By contrast, the interaction between ligands and aptamers demonstrates exceptional selectivity [150]. Fluorescent sensors involving the competitive interaction between GQDs, target analytes, and aptamers can demonstrate enhanced sensitivity and selectivity, and can be utilized in a biomedical platform [151–156].

Nair *et al* have reported a fluorescence sensor using GQDs and aptamers (figure 8(d)) [147]. In this study, sulfur-doped GQDs (S-GQDs) were used as fluorophores with the

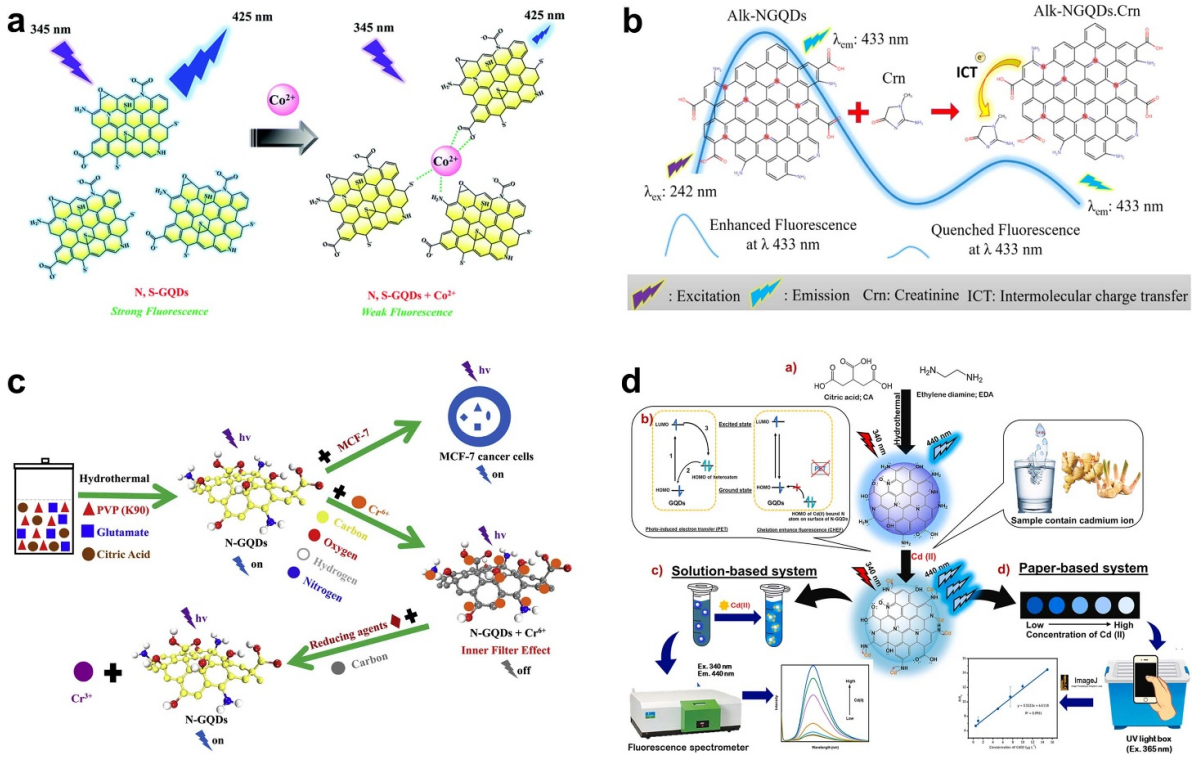

Figure 9. (a) Detection of Co^{2+} by N, S-GQDs complex formation. Reproduced from [166] with permission from the Royal Society of Chemistry. (b) Detection mechanism of Alk-N-GQDs for creatinine sensing. Reproduced from [167]. © IOP Publishing Ltd. All rights reserved. (c) Sensing of Cr^{6+} by N-GQDs. Reprinted from [168], Copyright (2020), with permission from Elsevier. (d) Preparation and sensing mechanism using enhanced fluorescence intensities in solution and paper-based systems. Reprinted from [169], Copyright (2022), with permission from Elsevier.

omethoate aptamer. The fluorescence of S-GQDs was diminished as a result of aggregation induced by the binding of aptamers to S-GQDs. Upon the introduction of omethoate, there was a distinct and highly responsive binding to the aptamer. This binding caused a change in the shape of the aptamer, which disrupted the clustering of the sensor molecules by binding to the same site. The fluorescence of the S-GQDs was thereby restored. In a similar study, Gu *et al* presented the advancement of a GQD-aptamer based fluorescent sensor for the shellfish toxin saxitoxin (STX) (figure 8(e)) [148]. The fluorescence quenching system involved the aptamer STX-41 coupled with GQDs on magnetic reduced GO. The interaction between STX and this aptamer caused the detachment of GQD-aptamer from the GO, resulting in the restoration of fluorescence and therefore the detection of STX. This sensing technology involves magnetic separation and signal amplification to selectively detect STX in seafood. This aptamer strategy can be extended to additional targets of interest.

3.1.2. Detection units based on GQDs. GQDs possess surface groups that are easily modifiable, and large π-conjugated systems, rendering them susceptible to chemical or physical binding by various analytes [157–159]. The PL of GQDs can be suppressed by target analytes through phenomena including the inner filter effect [160], aggregation-caused quenching (ACQ) [161], and other quenching mechanisms [162] that turn the fluorescent signal from 'on' to 'off' [163–165]. Boonta *et al* designed a fluorescent sensor based on N, S co-doped GQDs (N, S-GQDs) to detect Co^{2+} ions (figure 9(a)) [166]. The N, S-GQDs possess surface groups that can coordinate to Co^{2+} ions resulting in static fluorescence quenching. Transmission electron microscope observations revealed aggregation of the N, S-GQDs upon complexation with Co^{2+}. Ravi *et al* have reported an alkaline fluorescence probe made of N-GQDs for the sensitive detection of creatinine (figure 9(b)) [167]. Alk-NGQDs are stable in an alkaline environment of pH 9.5. They form a strong and enduring complex with creatinine by intermolecular charge transfer. The fluorescence titration approach was used for the detection of creatinine in both commercial creatinine samples and human blood samples. Li group have reported a sensor using N-GQDs produced by a hydrothermal approach [168] involving glutamic and citric acids as precursors. The fluorescence of this system was selectively quenched by Cr^{6}. Fluorescence lifetime measurements indicated a dynamic quenching process. The absorption spectrum of Cr^{6+} overlaps with the excitation wavelength of N-GQDs which is indicative of an inner filter fluorescence quenching mechanism (figure 9(c)).

The attachment of GQDs to an analyte might also result in increased fluorescence [170]. Naksen *et al* developed a fluorescence sensor using N-GQDs to detect Cd^{2+} ions [169]. The nitrogen-containing groups of N-GQDs chelate Cd^{2+} resulting

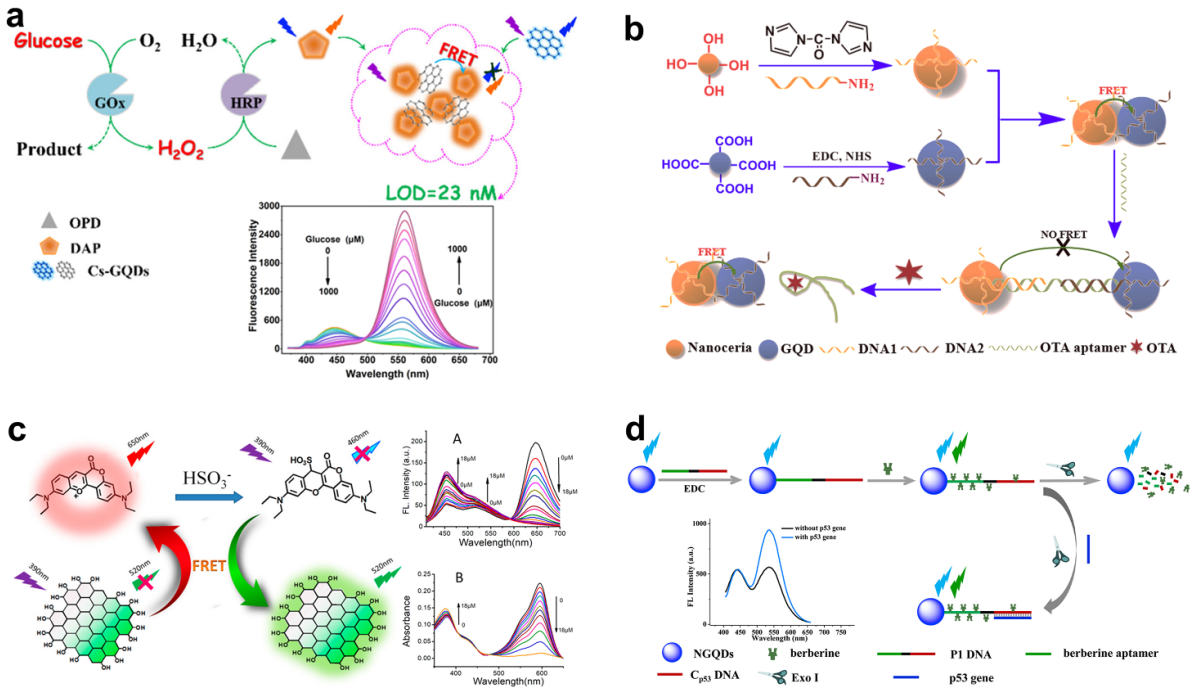

Figure 10. (a) Cs-GQDs based ratiometric sensors for glucose sensing. Reprinted with permission from [172]. Copyright (2021) American Chemical Society. (b) DNA2@GQD and DNA1@nanoceria based FRET aptasensor for OTA detection. Reprinted from [173], Copyright (2018), with permission from Elsevier. (c) CP@GQDs-OH based ratiometric fluorescent sensor for SO_2 sensing, insets show the fluorescence and adsorption spectra. Reprinted with permission from [79]. Copyright (2019) American Chemical Society. (d) NGQDs/P1 and DNA/berberine-based sensor for p53 gene activity analysis. Reprinted from [174], Copyright (2019), with permission from Elsevier.

in fluorescence enhancement (figure 9(d)). The disparity in energy levels between the LUMO of the N-GQDs and the LUMO of Cd^{2+} results in both binding and hindering of light-induced excitation of electrons and subsequent fluorescence.

3.1.3. Ratiometric sensors based on GQDs. Ratiometric fluorescent probes, unlike single-signal 'ON–OFF' probes, minimize interference by evaluating the ratio of fluorescence signals at two different wavelengths. This method overcomes limitations in sensitivity, selectivity, and precision associated with fluorescent sensing, allowing for more reliable identification of particular targets [171].

Wen *et al* have prepared cesium-doped GQDs (Cs-GQDs) as fluorophores for the sensitive sensing of glucose and H_2O_2 [172]. In the presence of horseradish peroxidase, o-phenylenediamine is oxidized by H_2O_2 to produce the yellow, fluorescent 2,3-diaminophenazine (DAP). The fluorescence of Cs-GQDs is quenched by DAP by Förster resonance energy transfer (FRET). A ratiometric fluorescent sensor was developed for detecting H_2O_2 and glucose utilizing this FRET mechanism involving Cs-GQDs and DAP (figure 10(a)). This sensing protocol exhibited a remarkable level of sensitivity for detecting H_2O_2 and glucose, with limits of detection down to 25 and 23 nM, respectively. This approach could sensitively and selectively detect glucose in human serum.

GQDs can function as either energy donors or acceptors in ratiometric fluorescence sensors. A sensing platform can be created by utilizing energy transfer (e.g. FRET) between GQDs and target analytes or other fluorescents [139, 175–177]. Compared to the sensors that use GQDs as a reference signal, the ratiometric fluorescence sensors that use GQDs as donors or acceptors have greater sensitivity and improved resistance to interference. For example, Tian *et al* connected two complementary sequences (DNA1 and DNA2) of ochratoxin A (OTA) aptamer to cerium oxide nanoparticles (nanoceria) and GQDs respectively, resulting in two *viz* DNA1@nanoceria and DNA2@GQD (figure 10(b)) [173].

The fluorescence emission spectra of nanoceria and the absorption spectrum of GQDs overlap, resulting in FRET when DNA1@nanoceria was combined with DNA2@GQD, primarily due to their electrostatic attraction. Upon the addition of OTA aptamer to the mixture, a specific affinity between DNA1 and DNA2 caused the aptamer to hybridize with both DNA strands, resulting in the formation of a rod-like double helix. The greater separation between DNA2@GQD and DNA1@nanoceria resulted in the disruption of the FRET mechanism. The composite exhibited a fluorescence emission at a wavelength of 360 nm. After the introduction of OTA into this system, the aptamer specifically bound OTA, causing the detachment of the OTA aptamer from the composite, and resulting in the recombination of nanoceria with GQDs. In the presence of OTA, the FRET between DNA1 attached to nanoceria and DNA2 attached to GQD was restored. Simultaneously, the fluorescence emission of this composite system progressively suppressed at 360 nm while the fluorescence intensity at 450 nm increased.

This ratiometric sensor demonstrated a low detection limit of 2.5 pg ml^{-1}.

In another study, Lin and coworkers designed a multi-ratiometric fluorescence probe with enhanced precision for sulfur dioxide [79]. This was achieved by employing GQDs with a fluorescent, electron rich aromatic molecule that interacted by π–π stacking (figure 10(c)). The ratiometric fluorescent sensor based on CP@GQDs-OH composite could detect the sulfur dioxide (SO_2) molecular probe CP. This composite relied on green (530 nm) fluorescence emission of GQDs-OH, overlapping with the absorption spectrum of the CP. This overlap enabled a FRET process in which the CP functioned as the energy acceptor, and the GQDs-OH the energy donor. The CP@GQDs-OH could detect SO_2 in both laboratory systems and living organisms, demonstrating three distinct linear ratio changes [79].

GQDs have the potential to be utilized as a reference signal in ratiometric fluorescence sensors, where their fluorescence properties can be used as a benchmark. In these sensors, the ratio of the emitted fluorescence intensities at two different wavelengths can be measured, providing a more accurate and reliable detection method [178, 179]. For example, Su *et al* presented a dual-emission system *viz* N-GQDs@AuNCs/Cu^{2+} for the ratiometric sensing of bleomycin (BLM) [180]. Likewise, they reported an N-GQDs-P1 DNA (figure 10(d)) to detect the p53 gene [174]. This sensor utilizes a ratiometric methodology. P1 DNA comprised a single-stranded DNA that included a berberine aptamer and the complementary sequence of the p53 gene. Blue fluorescence was generated by the N-GQDs and P1 DNA. When berberine was added and bound by the berberine aptamer sequence, the platform showed two types of light emission at wavelengths of 440 nm and 537 nm. Without the presence of the p53 gene, Exonuclease I (Exo I) could break down the P1 DNA, causing the fluorescence emission at 537 nm to be suppressed. When the p53 gene was present, it interacted with P1 DNA to create a double-stranded DNA structure, which effectively inhibited hydrolysis by Exo I. During this process, the fluorescence of N-GQDs acted as the reference signal, ensuring a consistent intensity.

3.2. Development strategies for fluorescent biosensors

GQD can be utilized directly for the direct construction of fluorescent sensors or by physical or chemical modification. The GQDs based fluorescent sensors are categorized below according to the specific interaction focused synthesis methods.

3.2.1. Fluorescent sensors based on edge/surface functionalized GQDs. A significant number of GQDs contain a high concentration of oxygenated groups on their edges and surfaces as a result of oxidation during synthesis [181–183]. Alternatively, the desired functional groups can be incorporated through post-synthesis techniques.

Large surface area is vital to attachment of foreign analytes [184, 185]. The large surface area and modifiable chemical groups present on the surface and edges of GQDs include amino, carboxyl, or hydroxyl groups and can be used for the fabrication of fluorescence sensors [186–189]. For example, Li *et al* developed a fluorescent sensor based on GQDs modified with (2,4-dinitro phenoxy) tyrosine [190]. This sensor was designed for detecting hydrogen sulfide (H_2S). The fluorescence of the sensor was suppressed as a result of photo-induced electron transfer between (2,4-dinitro phenoxy) tyrosine and the GQDs. Tang *et al* designed a ratiometric sensor based on F, N-doped GQDs (FNGQDs)-RhB to detect doxycycline. This was achieved by attaching rhodamine B onto FNGQDs (figure 11(a)) [191]. FNGQDs were prepared by a conventional hydrothermal synthesis approach with levofloxacin as the precursor. Subsequently, rhodamine B was attached to FNGQDs hydrothermally. The newly created sensor displayed two distinct light emissions centered at 466 nm and 592 nm. When doxycycline is added to this system, competitive energy transfer takes place between doxycycline and FNGQDs. The fluorescence of FNGQDs-RhB at 466 nm is suppressed, with a small reduction observed at 592 nm. FNGQDs-RhB demonstrated a strong linear correlation over the concentration range 0.04–100 μM, with a minimal detection limit of 40 nM.

Wang *et al* have similarly created a very sensitive method for detecting multiple DNA targets using GQDs and carbon nanoparticles (CNPs) [192]. They achieved this by a combination of dual-color GQDs with ssDNA probes and a non-fluorescent CNP quencher, using the enzyme EXO III to recycle the target molecules and amplify the detection signal (figure 11(b)). The combination of dual-color GQDs-ssDNA probe and CNPs, together with the Exo III signal amplifying approach, provided a highly effective system for detecting individual targets (THBV and THIV) as well as the concurrent detection of various targets. This system had an impressive detection limit of 6.6 pM and 9.5 pM, respectively, and demonstrated excellent discrimination between DNA targets differing in only a single nucleotide [192]. In another study, Tian *et al* produced a highly efficient 2,4,6-trinitrotoluene (TNT) sensor by including an accumulation layer between the detecting materials and TNT of the optimal distance for FRET [188]. This hy-GQDs-APTES sensor successfully recognized and quantified the presence of TNT with an extremely low limit of detection and exceptional selectivity (figure 11(c)).

In a simpler and more cost-effective approach, Masteri-Farahani *et al* created a turn-on fluorescence nanosensor for measuring glucose levels, using boric acid modified S and N co-doped GQDs [193]. These S, N-GQDs modified with boric acid showed an increase in fluorescence at 455 nm when glucose was added. The interaction between the two cis-diol units in glucose and two boric acid groups on the (B)/S, N-GQDs surface gave structurally stable (B)/S, N-GQDs-glucose aggregates, which increased the PL intensity (figure 11(d)). More recently, Khan and Patil fabricated a sensor using poly-L-lysine-functionalized GQDs to specifically detect cysteine and homocysteine (figure 11(e)) [186]. These studies highlight the potential of surface/edge functionalized GQDs for selective and sensitive sensing of multiple biologically important analytes.

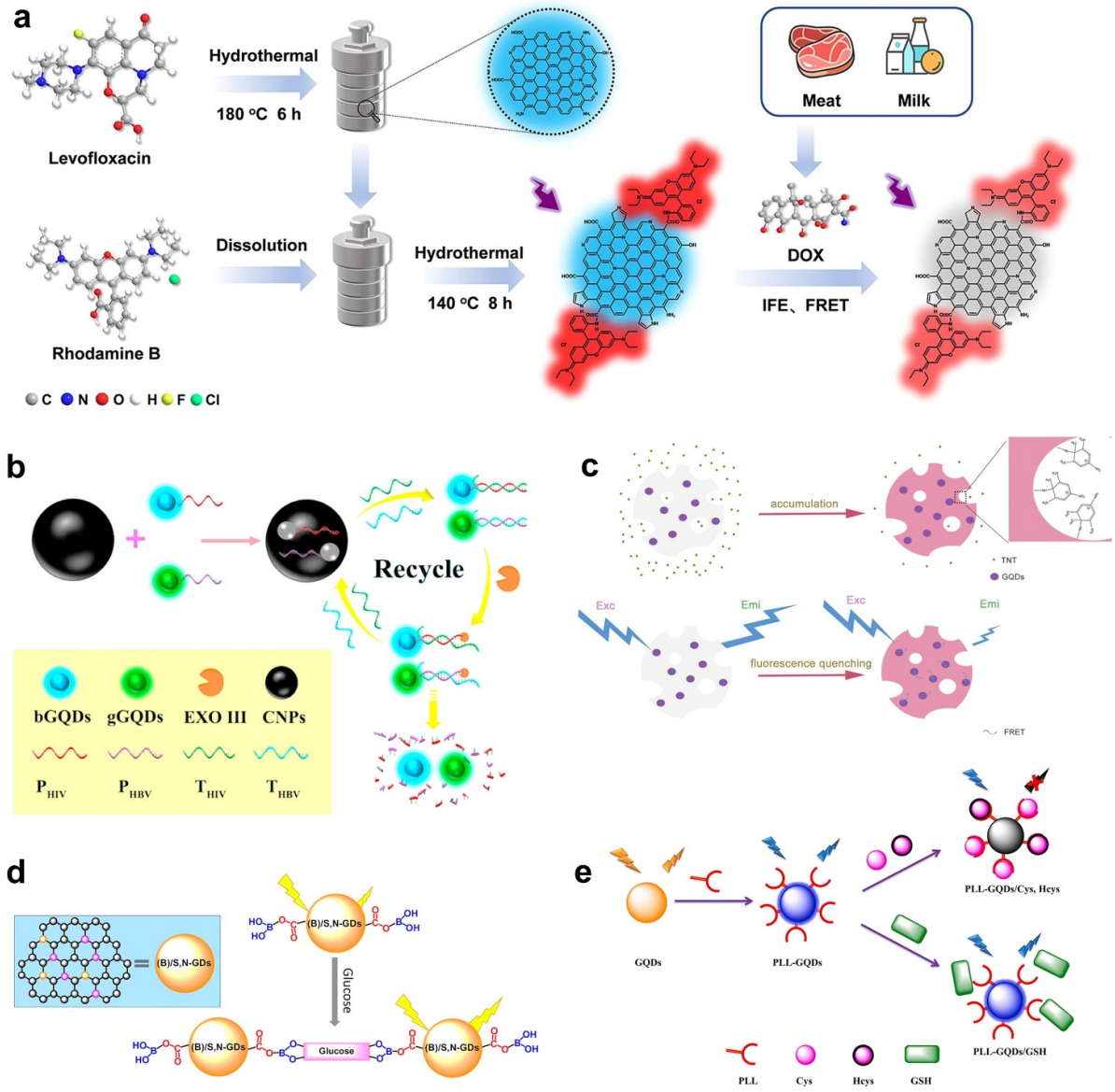

Figure 11. (a) Synthesis of preparing dual-emission FNGQDs-RhB and the sensing mechanism for DOX detection. Reprinted from [191], Copyright (2022), with permission from Elsevier. (b) Dual-color GQDs-DNA probes and CNPs used in the simultaneous detection of THIV and THBV. Reprinted from [192], Copyright (2021), with permission from Elsevier. (c) Sensing mechanism of hy-GQDs-APTES for TNT detection. Reprinted from [188], Copyright (2021), with permission from Elsevier. (d) (B)/S, N-GQDs nanosensor for glucose detection. Reprinted from [193], Copyright (2021), with permission from Elsevier. (e) Poly-L-lysine-functionalized GQDs for cysteine and homocysteine detection. Reprinted from [186], Copyright (2022), with permission from Elsevier.

3.2.2. Element-doped GQDs. Introducing other elements into GQDs can create structural imperfections, enhancing the fluorescence quantum yields, and generating distinct surface functional groups. Oxygen doping can be achieved by oxidation during synthesis [194, 195]. Doping with other elements can be achieved by introducing additional element sources along with oxygen during the fabrication process [196]. These doped GQDs can function as fluorescence sensors without the need for additional processing [197–199]. A variety of nitrogen-containing molecules can serve as a source of nitrogen for synthesizing stable N-GQDs. Nitrogen-containing functional groups on the surface of these N-GQDs can interact with certain target analytes, resulting in modification of their fluorescence emission.

N-GQDs can be synthesized by bottom–up hydrothermal or thermal cracking methods in the presence of N-containing additives [107, 200, 201]. Tang *et al* created a water sensor employing N-GQDs that emit red light [74]. This was achieved by spontaneous oxidation/polymerization and Schiff reactions (figure 12(a)). The chemical precursors used were o-phenylenediamine and catechol. The red PL of N-GQDs is caused by the high concentration of oxygenated surface functional groups and graphitic N structural elements and could be altered by adjusting the proportion of added

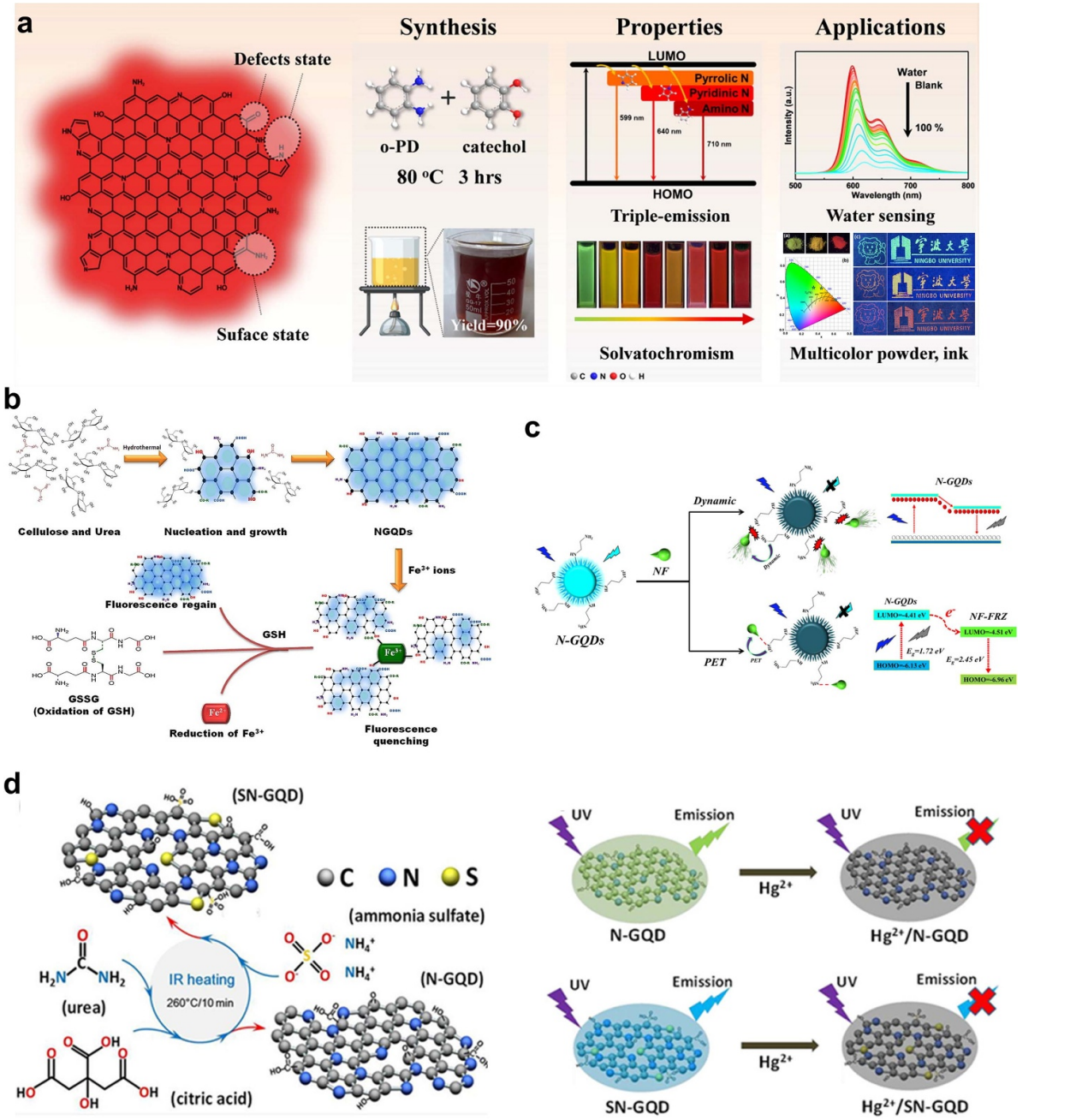

Figure 12. (a) Synthesis, properties and application of N-GQDs as water sensor, multicolor powder, and ink. Reprinted from [74], Copyright (2022), with permission from Elsevier. (b) N-GQDs based GSH and Fe^{3+} sensor. Reprinted from [202], Copyright (2024), with permission from Elsevier. (c) N-GQDs based sensing mechanism of nitrofuran antibiotics and the corresponding energy level diagram. Reprinted with permission from [203]. Copyright (2023) American Chemical Society. (d) N-GQDs and SN-GQDs based fluorescent sensor for Hg^{2+} sensing. Reprinted from [80], Copyright (2019), with permission from Elsevier.

o-phenylenediamine or catechol. The presence of surface amino groups (pyrrolic N, pyridinic N, and amino N) led to unique triple-peak PL emission of the N-GQDs.

N-GQDs can also be produced via top–down processing. In a recent study, Khan *et al* fabricated N-GQDs to detect Fe^{3+} ions and glutathione (GSH) [202]. They synthesized N-GQDs using bamboo fiber in a hydrothermal process (figure 12(b)). These NGQDs displayed intense blue PL that was selectively quenched by Fe^{3+}. The addition of GSH into this NGQDs/Fe^{3+} system led to restoration of PL due to a redox reaction, reducing Fe^{3+} to Fe^{2+} and oxidizing GSH into GSSG (figure 12(b)).

In a similar approach, Sun *et al* prepared N-GQDs for nitrofuran antibiotics detection using sugar cane molasses and ethylenediamine as a carbon and nitrogen source, respectively (figure 12(c)) [203]. The functional groups nitro, furan, C=N, aldehydes, and ethers on the analytes formed transient H-bonds with functional groups on the N-GQDs, resulting in fluorescent quenching by a combination of dynamic quenching and photoinduced electron transfer (figure 12(c)).

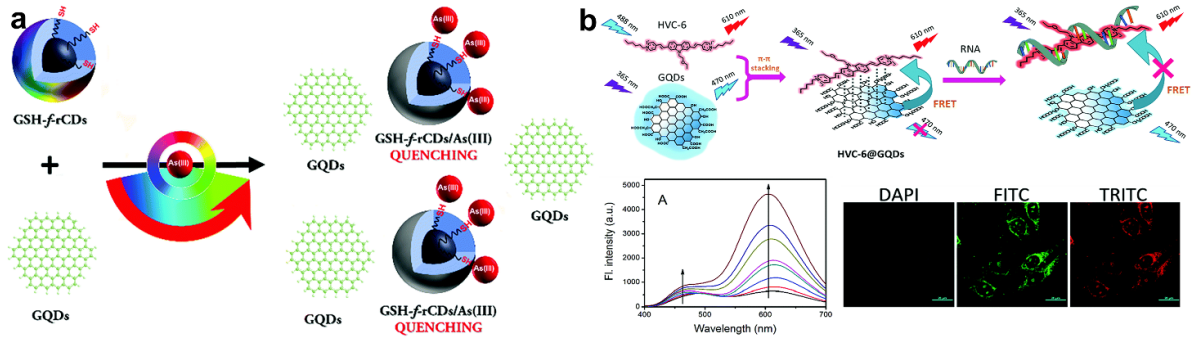

Figure 13. (a) GSH-f-rCD/GQD for detection of As^{3+}. Reproduced from [215] with permission from the Royal Society of Chemistry. (b) Schematic of sensing mechanism of HVC-6@GQDs for RNA detection, fluorescence emission spectra RNA (0–250 μM), and confocal microscopy images of living HeLa cells. Reproduced from [216] with permission from the Royal Society of Chemistry.

In another study, Fu *et al* prepared N-GQDs to detect Fe^{3+} ions in a top–down approach [204]. The Fe^{3+} ions bind to the –OH and $–NH_2$ groups on the surface of N-GQDs, resulting in the formation of aggregates. This interaction leads to quenching of fluorescence by electron transfer.

Sulfur (S), chlorine (Cl), boron (B), and fluorine (F) are also employed as doping elements [205–207]. Fluorescence in GQDs-based sensors can also be controlled by the introduction of multiple elements through co-doping [208–211]. Gu *et al* [80] produced S, N co-doped GQDs (SN-GQDs) using an ionizing radiation (IR)-assisted production technique. They added citric acid, urea, and ammonia sulphate as the source of carbon, nitrogen, and sulfur, respectively (figure 12(d)). These SN-GQDs could detect Hg^{2+} ions with superior sensitivity to N-GQDs due to the presence of sulfur functional groups.

3.2.3. Composite GQDs based fluorescent probes. GQDs have been incorporated into fluorescent composite nanomaterials [212–214] including materials that do not emit light. The fluorescence signal can be altered by the transfer of energy within the sensor, resulting in a change before or after detecting the target analyte. The process of synthesizing GQD composite fluorescent materials is straightforward. Additionally, they can be integrated with other functional materials to meet the specific biological needs of particular application. For example, Gogoi *et al* reported a GQD-based nanohybrid probe that utilized glutathione functionalized reduced CDs (GSH-f-rCDs) and GQDs (figure 13(a)) [215]. This GSH-f-rCDs nanohybrid was synthesized by modifying rCDs using the carbodiimide coupling technique and combining GSH-f-rCDs (which emit in the UV region) with GQDs (which exhibit green fluorescence). The two emissions in this composite system are independent of each other. As^{3+} is complexed by GSH. The presence of As^{3+} on the surface of GSH-f-rCDs led to the reduction in fluorescence intensity. The presence of As^{3+} in aqueous solutions was quantified over the concentration range 0.5–100 ppb. This composite system could be incorporated into a test strip for visual recognition of the presence of As^{3+} ions.

Electrostatic interactions can be used for the combination of GQDs with other luminescent materials [217, 218]. For example, Liu *et al* created a ratiometric sensor for sensing clenbuterol (CLB) using GQDs and $[Ru(bpy)_3]^{2+}$ [219]. Pi-stacking interactions with GQDs have been similarly exploited [220]. Lin group used GQDs and HVC-6 molecular probe to create a composite material HVC-6@GQDs for ratiometric fluorescent detection of RNA based on this π–π stacking approach (figure 13(b)) [216]. HVC-6@GQDs could sense and visually image the localization of endogenous RNA.

4. Biomedical applications

GQDs possess low toxicity, nanoscale dimensions, remarkable optical properties, an extended π-conjugated system, and versatile edge groups, making them suitable materials for numerous biomedical applications [37, 43, 44, 61, 221, 222]. GQDs can be customized to selectively sense analytes in living organisms. In addition, the interaction of GQDs can be controlled by loading pharmaceuticals for dynamic monitoring, targeted drug delivery, and drug release.

4.1. Bioimaging

Fluorescent sensors based on GQDs can provide real-time observation of *in vivo* targets in living organisms [223–225]. Lu *et al* developed a novel sensor that could detect alkaline phosphatase (ALP) by combining colorimetric and fluorescence methods [226]. This sensor utilized ascorbic acid-phosphate (AAP), GQDs, and silver ions (Ag^+). Electrostatic interactions facilitated the attraction of Ag^+ on to the surface of GQDs. AAP was converted to ascorbic acid (AA) by the ALP, and the AA reduced the Ag^+ ions to produce AgNPs on the GQD surface. The FRET process between the GQDs and AgNPs led to the suppression of GQDs' fluorescence. This sensor could measure changes in ALP concentration *in vitro* using both fluorescence and colorimetric dual modes. It was employed to monitor inherent changes in ALP levels in L-02 cell lysates initiated by alcohol-induced damage.

Similarly, Liu *et al* designed a ratiometric sensor based on GQD-hydroIR783 [227]. This probe was developed by integration of GQDs with IR783 (figure 14(a)). GQDs were attached to hydro IR783 using poly(ethylene glycol), which led to the creation of the ratiometric ROS probe. In the absence

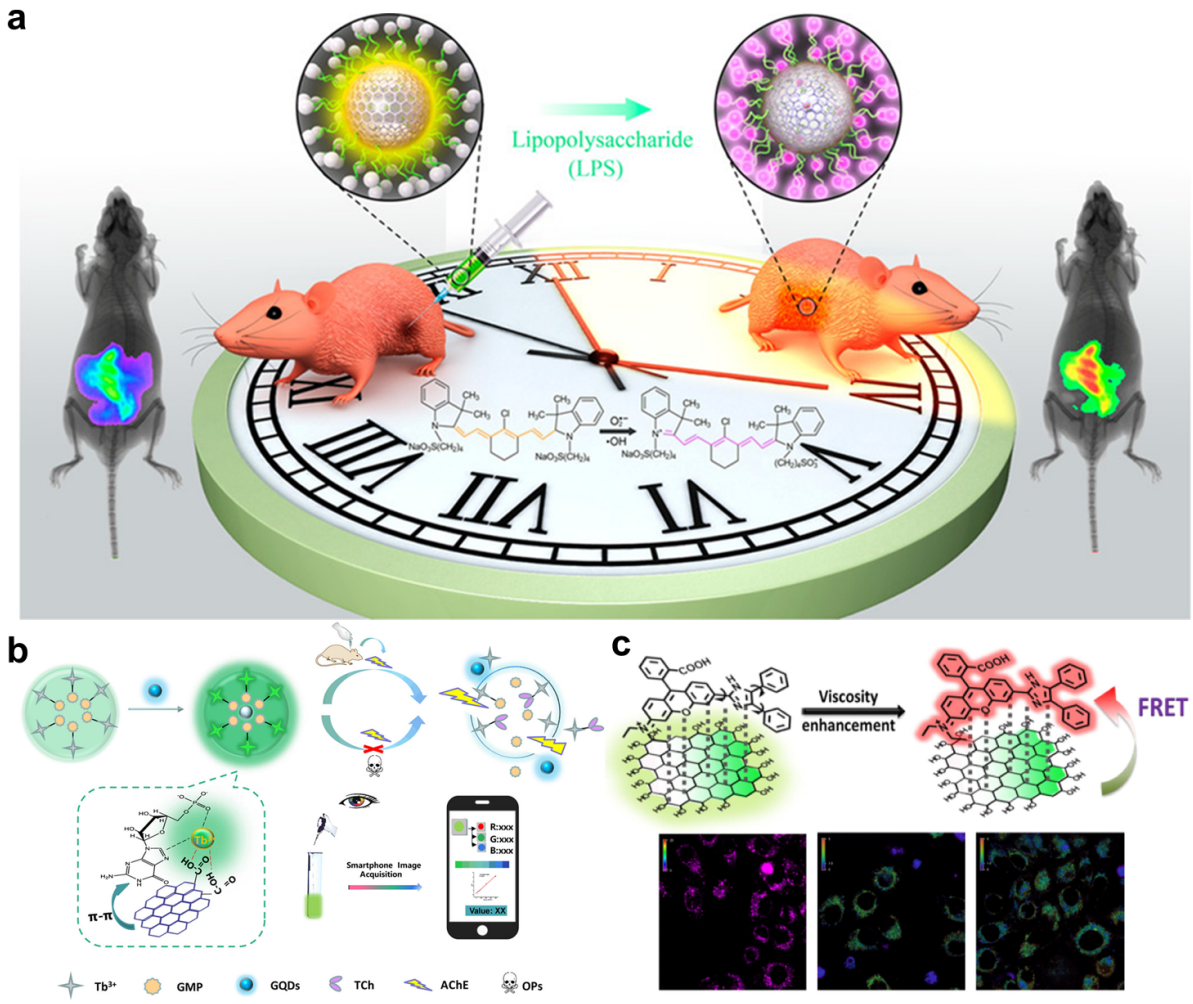

Figure 14. (a) Construction and application of the GQD-hydroIR783 platform. Reprinted with permission from [227]. Copyright (2018) American Chemical Society. (b) GQD-Tb/GMP ICP with dual-detection ratiometric fluorescence. Reprinted with permission from [228]. Copyright (2020) American Chemical Society. (c) RV-1@GQDs-OH system for detection of viscosity changes and imaging in living cells. Reproduced from [229] with permission from the Royal Society of Chemistry.

of ROS, GQD-HydroIR783 fluoresced at 520 nm. In the presence of ROS, the hydroIR783 was converted to IR783, causing a reduction in the fluorescence intensity of the GQDs. This decrease was attributed to the FRET between GQDs and IR783. The fluorescence intensity ratio (I800/I520) showed a direct correlation with the concentration of ROS in the range of 0–20 μM. The use of GQD-HydroIR783 allowed for the continuous monitoring of ROS production, showing excellent resistance to degradation by light and a good signal to background noise ratio. In addition, GQD-HydroIR783 was able to detect ROS both *in vivo* and *in vitro*. Ma *et al* [228] created a new type of fluorescent sensor, *viz* GQD@Tb/GMP to detect organophosphorus pesticides (OPs) and their receptor enzyme acetylcholinesterase (AChE) (figure 14(b)) [228].

A polymer aggregate was formed by coordinating terbium/guanine monophosphate (Tb/GMP) on the GQDs surface. ACQ resulted in suppression of the blue PL of the GQDs in the composite GQD@Tb/GMP and only green PL was emitted from the Tb/GMP. When acetylcholinesterase (AChE) and acetylthiocholine (ATCh) were added simultaneously, thiocholine (TCh) and terbium ions (Tb^{3+}) were released, disrupting the aggregate network with the release of the encapsulated GQDs. As a result, the sensor emitted blue PL. OPs bind AChE, thereby preventing this increase in blue fluorescence. Therefore, GQD@Tb/GMP could detect both Ops and AChE.

A smartphone-based colorimetric device was built to visually detect AChE and OPs using the GQD@Tb/GMP sensing system, making use of its dual-responsive ratiometric fluorescence. This system allowed for the monitoring of CSF acetylcholinesterase (AChE) as a biomarker for organophosphate poisoning and treatment. The fluorescence color in cerebrospinal fluid samples from rats poisoned with sulfur remained consistently green. However, in the samples of cerebrospinal fluid obtained from normal rats and rats treated with an antidote, the fluorescence emission color transitioned to blue green from bright green. This GQD@Tb/GMP sensor showed promise for the early detection and treatment of organophosphate poisoning. In another effort, Lin group developed a fluorescence sensor RV-1@GQDs-OH to detect changes in viscosity. This sensor used GQDs-OH and an NIR cellular

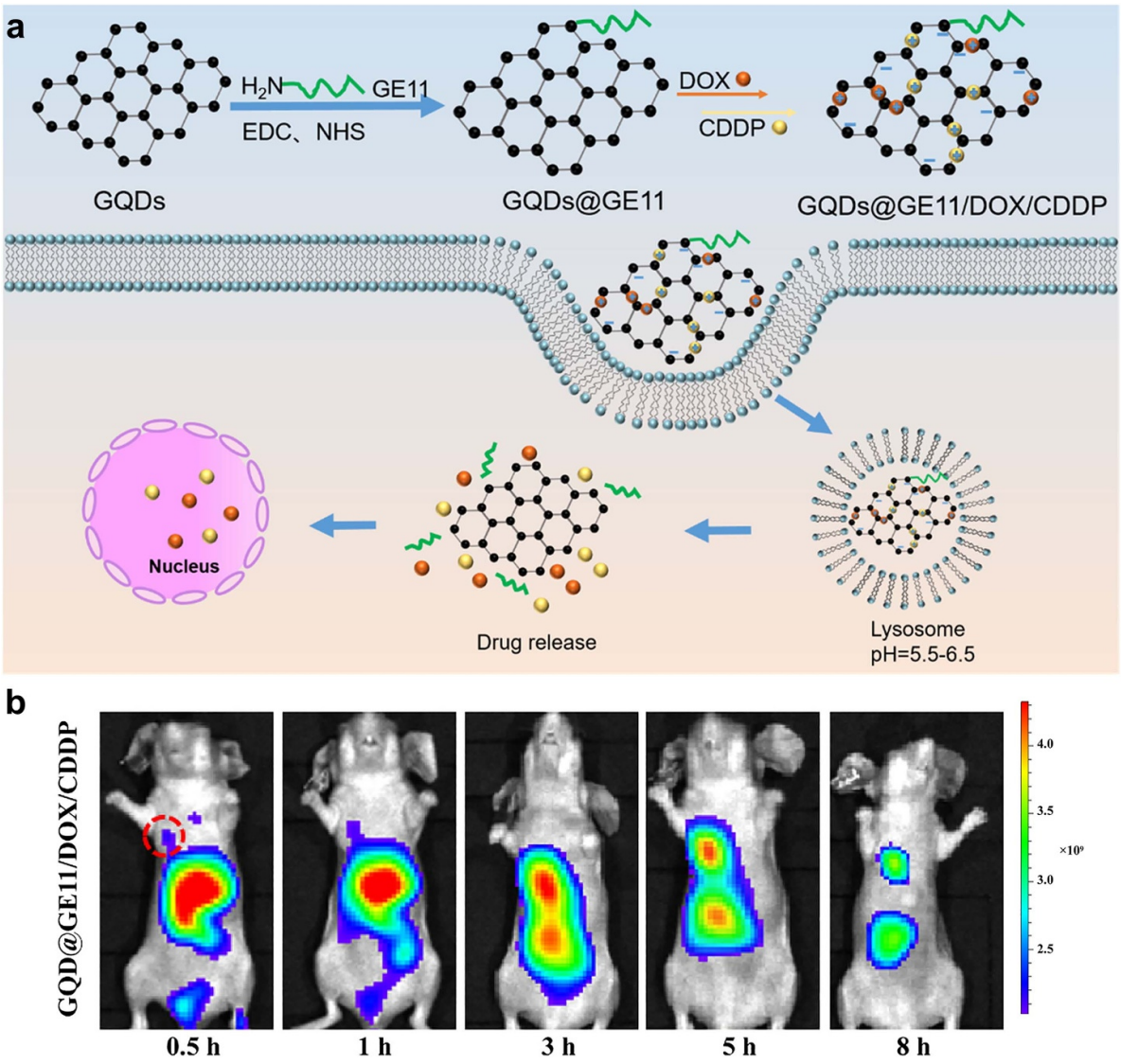

Figure 15. (a) The synthesis of GQDs@GE11/DOX/CDDP, and (b) application of GQDs@GE11/DOX/CDDP for the tumor site imaging and for monitoring of medication release. Reproduced from [121]. CC BY 4.0.

viscosity probe RV-1, which interacted by π–π stacking (figure 14(c)) [229]. At high viscosity, RV-1 emitted in the NIR range with the highest absorption band occurring at 580 nm. At low viscosity, the NIR emission from RV-1 was weakened leading to the recovery of GQDs-OH fluorescence.

Yu *et al* developed a combined composite sensor and drug delivery system (figure 15(a)) [121]. GQDs@GE11 was devised as a pharmaceutical transporter for precise targeting of nasopharyngeal cancer cells. The GE11 peptide, which acts as an antagonist to the EGFR, was attached to the GQD surface by an amidation reaction. The effectiveness of GQDs@GE11 in targeting the EGFR receptor in CNE-2 nasopharyngeal cancer cells was verified by flow cytometry. GQDs@GE11 was loaded with doxorubicin (DOX) and cisplatin (CDDP) in a water-based solution. The excitation range of DOX partially overlapped with the emission range of GQDs within the composites, resulting in a FRET process between the two. Prior to the release of DOX, GQDs@GE11/DOX/CDDP produced red fluorescence from the DOX. As the DOX molecules were slowly released, the blue fluorescence of the GQDs gradually became visible. This blue fluorescence could be used to measure the release kinetics of DOX and CDDP. The assessments conducted both *in vivo* and *in vitro* showed that GQDs@GE11/DOX/CDDP could be used to visualize the tumor site and for monitoring of medication release (figure 15(b)).

Recently, advances in tumor imaging platforms have been made possible by the relatively new approach of conjugating antibodies with nanoparticles. Antibody-decorated nanoparticles can serve as efficient agents for nuclear imaging [230, 231]. A recent study [232] detailed a breast cancer imaging probe consisting of GQDs combined with pembrolizumab (figure 16(a)). A human monoclonal antibody (mAb) targeting the immune checkpoint proteins programmed death receptor-1 (PD-1) and its ligand (PD-L1) was studied. The toxicity of a GQD nanoconjugate was assessed using an MTT

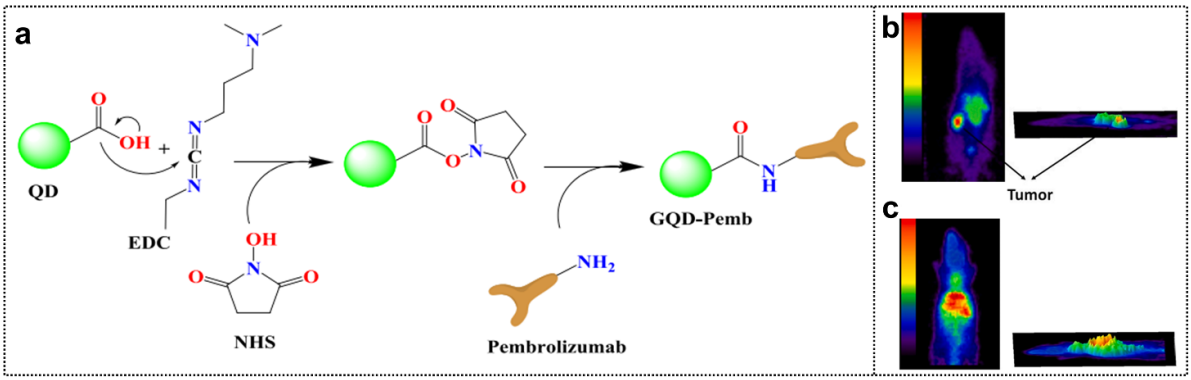

Figure 16. (a) The conjugation mechanism between GQDs and the pembrolizumab antibody involves chemical functionalization, enabling the formation of a stable nanocomplex. SPECT imaging was conducted one-hour post-injection of 7.4 MBq of ^{99m}Tc-GQDs-pembrolizumab via the tail vein in BALB/c mice, including those with 4T1 tumors (b) and healthy controls (c). Reproduced with permission from [232]. © 2023 The Authors. Published by Elsevier B.V. on behalf of King Saud University. CC BY-NC-ND 4.0.

assay on HEK-293 and 4T1 cell lines. This nanoconjugate was radiolabeled with Technetium-99m (^{99m}Tc), resulting in the formulation of ^{99m}Tc-GQDs-pembrolizumab. To analyze its pharmacokinetics and targeting capabilities, biodistribution studies and single-photon emission computed tomography (SPECT) imaging were conducted in a BALB/c mouse model with 4T1 tumors.

Figures 16(b) and (c) illustrates SPECT imaging performed one hour after administering 7.4 MBq of ^{99m}Tc-GQDs-pembrolizumab via the tail vein in BALB/c mice, including those bearing 4T1 tumors and healthy controls. High radiochemical purity (RCP $>$ 95%) indicates GQDs-pembrolizumab's ability to form complexes with ^{99m}Tc [232]. This nanocomposite is an example of a radiopharmaceutical-based mAb therapy that could be tailored to treat a variety of malignancies.

Magnetic resonance imaging (MRI) is a widely used non-invasive imaging method for which GQD-based contrast agents have been developed. MRI contrast is generated by variations in the magnetic relaxivity of hydrogen nuclei in water molecules across different tissues [233, 234]. Contrast agents enhance these variations, either by brightening tissues (T1 contrast agents) or darkening them (T2 contrast agents). Clinically, gadolinium (Gd)-based chelates are commonly employed as T1 contrast agents due to the strong paramagnetic properties of Gd(III) ions. However, concerns about the safety of these agents have grown because of the potential release of toxic heavy metal ions during *in vivo* applications. Despite significant advancements in MRI contrast agent development, the magnetic properties of Gd diethylene penta-acetic acid (Gd-DTPA), the clinical gold standard, remain unmatched by any metal-free alternatives.

A novel single-layer boron-doped GQDs (SL-BGQDs) exhibited superior T1 contrast enhancement compared to Gd-DTPA [235]. The study assessed the performance of SL-BGQDs as an *in vivo* T1 contrast agent by conducting cranial MR imaging of mouse neurovasculature. Imaging was performed before and after the administration of 200 μl of a 5 mg ml^{-1} solution of either SL-BGQDs or Gd-DTPA. Maximum intensity projections of representative pre- and post-injection images illustrate the enhanced imaging capabilities of SL-BGQDs (figures 17(a) and (b)) or Gd-DTPA (figures 17(a) and (c)). In pre-injection photos, cerebral blood vessels were hardly visible for either group. The vascular structures, on the other hand, were evident following the administration of SL-BGQD. Evaluation of the blood–brain barrier (BBB) permeability of SL-BGQDs revealed that they are capable of crossing the BBB, with an extended imaging duration of approximately 60 min, compared to just 10 min for Gd-DTP (figures 17(d)–(k)). The promising ability of GQDs to pass the BBB makes them potential candidates for combating various neurodegenerative diseases [236].

4.2. Drug delivery

Nanoscale multifunctional drug delivery systems have attracted significant attention in the field of cancer therapy. GQDs have numerous desirable characteristics that make them suitable for drug delivery platforms [118, 237]. These include their ability to bind other molecules through π–π interactions and easy functionalization. Moreover, their negligible toxicity to living cells, enhanced catalytic activity for sizes smaller than 10 nm, and well-defined edges facilitate cellular nucleus infiltration [238, 239]. However, smaller GQDs, when present in high concentrations, can induce the production of intracellular ROS, causing significant harm to cellular structures [240]. To address this, Chandra *et al* utilized polymers such as PEG to encapsulate GQDs, resulting in improved biocompatibility and decreased ROS production [30]. GQDs, with their favorable surface area to volume ratios and impressive drug loading capabilities, are suitable for both therapeutic and diagnostic purposes [241, 242]. Simultaneous administration of a chemotherapeutic agent and a diagnostic imaging agent to target cells enables the monitoring of dosage, delivery, and effectiveness. GQDs possess significant potential in this respect.

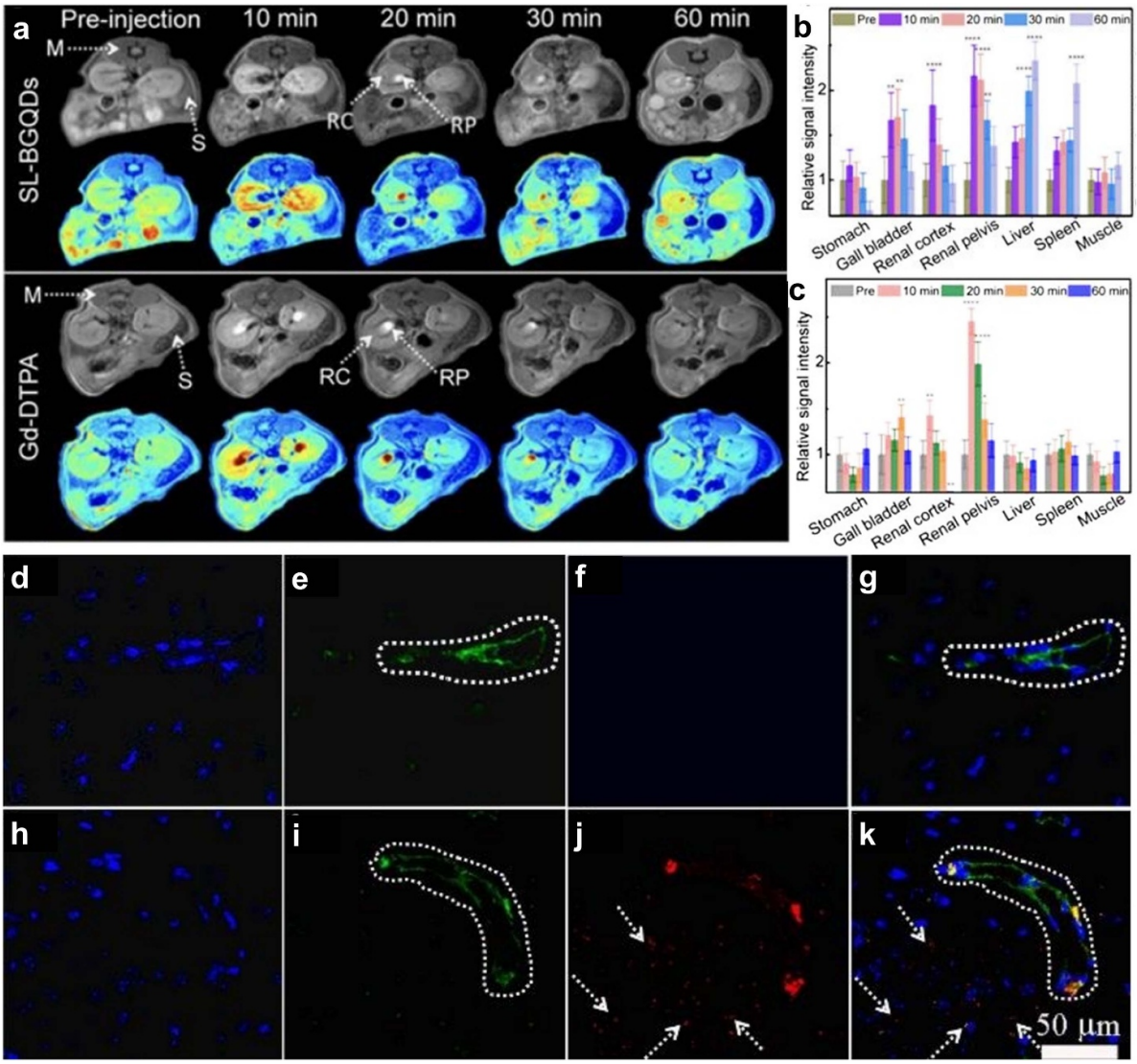

Figure 17. *In vivo* abdominal MR imaging conducted on mice intravenously injected with either SL-BGQDs (upper panel) or Gd-DTPA (lower panel) obtained at various time points post-injection. (b) and (c) The relative T1-weighted signal intensity was measured in mice injected with (b) SL-BGQDs or (c) Gd-DTPA. Confocal microscopic images of mouse brain tissue sections obtained one hour after the injection of PBS (d)–(g) and SL-BGQDs (h)–(k). Reproduced from [235] with permission from the Royal Society of Chemistry.

Mn, N, and S doped carbon based QDs exhibited promising targeted drug delivery with apparent cell toxicity up to 90% toward B16F1 cancer cells [241]. Gharepapagh *et al* investigated the potential toxicity and distribution of GQDs intravenously administered to mice [243]. Su *et al* have described, what they call a size changeable nanoaircraft (SCNA) based on GQDs (figure 18(a)) [237]. RG2 cells and a rat glioma cell line were exposed to both GQDs and SCNAs at different doses for 24 h. Confocal laser scanning microscopy images confirmed the presence of SCNAs in the cytoplasm of RG2 cells after 0.5 h of incubation. At 4 h, most of the particles were observed surround the cell nucleus and the fluorescence of both DOX and of the GQDs was observed (figure 18(b)) [237]. Under NIR irradiation, DOX-loaded SCNAs (DOX/SCNAs) exhibited a synergistic photothermal-chemotherapeutic effect, resulting in approximately 75% cytotoxicity against RG2 cells.

In a recent study, Teng *et al* created a multipurpose nanoplatform using cobalt ferrite, silicon dioxide, and GQDs (figure 19) [244]. Doxorubicin and folic acid (FA) were added to the nanoplatform to HeLa tumor cells. The GQD-CFO/SiO_2/FA nanocomposite exhibited a loading capacity of 65.4 wt% for anticancer drug DOX. An MTT assay demonstrated considerable *in vitro* cytotoxicity. GQDs produce singlet oxygen in the presence of light and so can potentially be used for PDT. Nanometer-scale GQDs were enclosed within hollow mesoporous silica nanoparticles (hMSNs), which had a diameter of approximately 100 nm [245]. These nanocarriers were filled with DOX and irradiated with a laser. The DOX loading capacity in GQDs/hMSN conjugates reached 76%. The cumulative release of DOX from GQDs/hMSN-PEG was pH-dependent, with highest value reaching 61.15% released at pH 5. The result was a notable decrease in

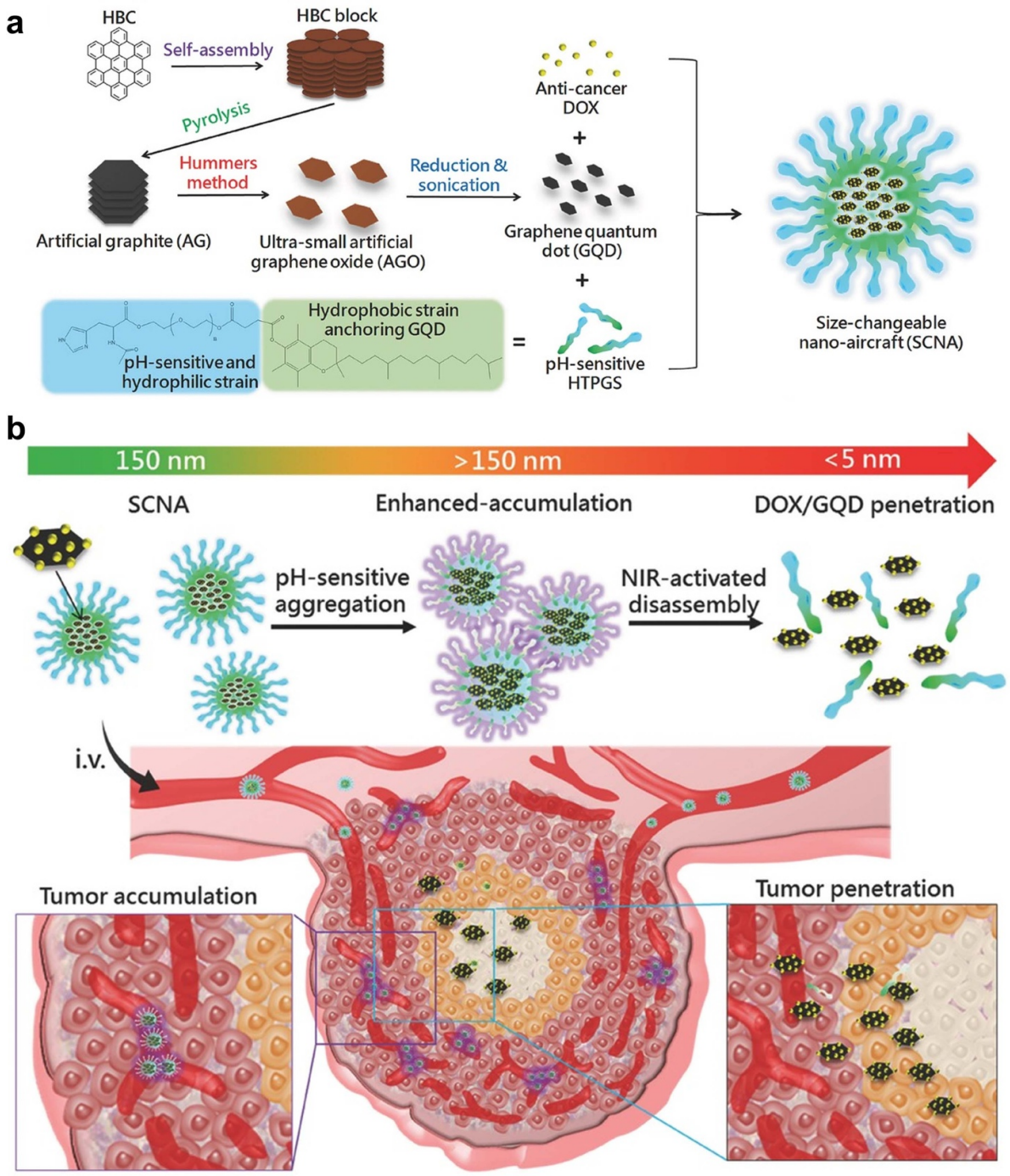

Figure 18. (a) Schematic diagram depicting the essential stages involved in the synthesis of size-changeable nanoaircraft (SCNA). (b) The SCNAs for photopenetrating drug/GQD delivery and hierarchical tumor targeting via an aggregation transition in the weakly acidic tumor environment. [237] John Wiley & Sons. © 2017 WILEY-VCH Verlag GmbH & Co. KGaA, Weinheim.

tumor size compared to when there was no light or no DOX present [246].

4.3. Cancer therapeutics

4.3.1. GQDs in breast cancer. GQDs have gained substantial attention in cancer research due to their unique properties and have been incorporated into a range of treatment strategies, including PTT, PDT, stem cell therapy, gene therapy, immunotherapy, and drug delivery. The integration of GQDs into these medical therapies has shown promising results, particularly in treating triple-negative breast cancer (TNBC), an extremely destructive and treatment-resistant form of the disease.

Breast cancer diagnosis generally follows a two-step procedure: first, immunohistochemistry is used to assess the absence of hormone receptors, followed by different imaging strategies, for example mammography, ultrasonography, and

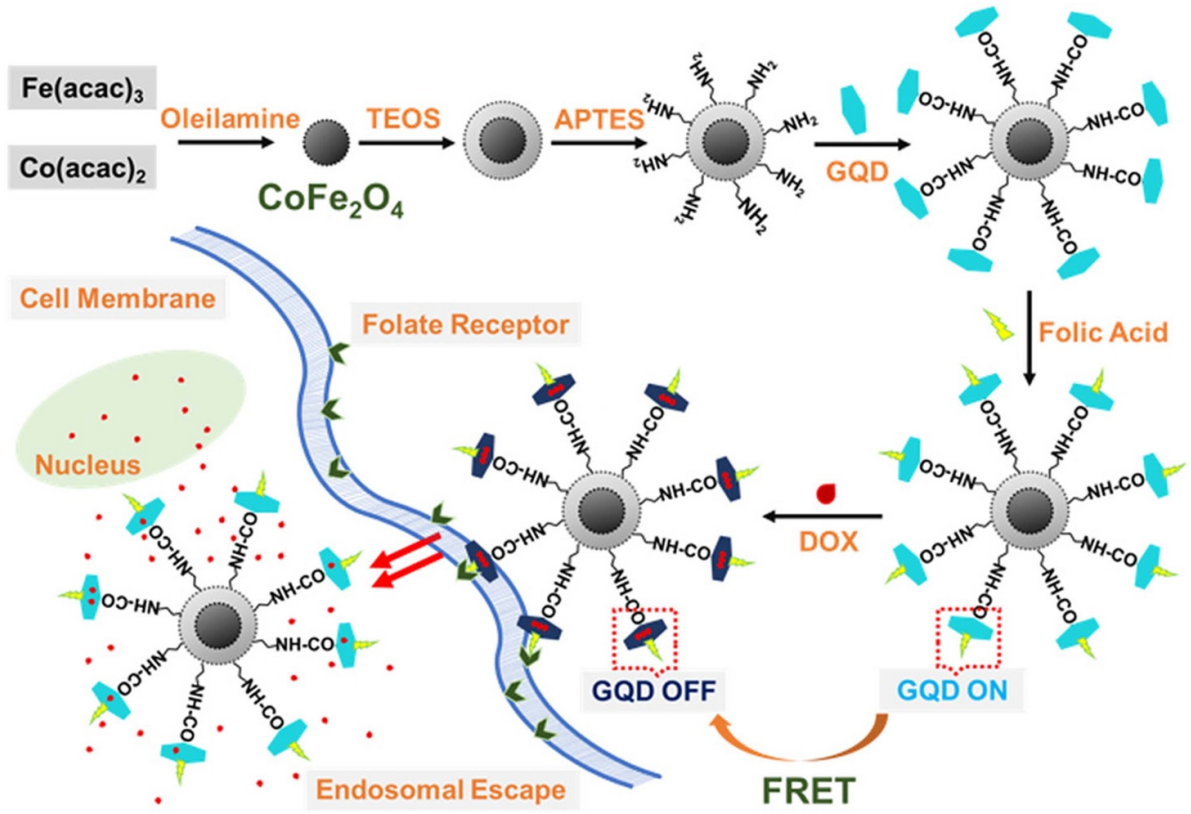

Figure 19. Multifunctional platform GQD-CFO@SiO_2/FA and FRET based drug delivery. Reproduced from [244]. CC BY 4.0.

MRI [4]. Among these, mammography is the most commonly used radiological technique, though its diagnostic accuracy can be limited in breast cancer cases because of the lack of definite abnormal characteristics, which may lead to incorrect diagnosis [247]. Ultrasonography proves particularly helpful when swelling or a lump is detectable by touch but not obvious on a mammogram. When performed accurately, it plays a crucial role in differentiating solid tumors from fluid-filled cysts in the breast [248]. In contrast, MRI is highly effective in confirming the presence of cancer, though it is less reliable in discriminating among different types of breast cancer because it primarily focuses on imaging instead of the cellular properties of the tissue [249]. These non-invasive diagnostic methods play a crucial role in the early detection of cancer and the continuous assessment of treatment progress, ensuring that care is both prompt and tailored to meet the specific needs of the patient [250, 251].

In breast cancer treatment, diagnostic and treatment techniques are currently available (figure 20(a)) [4]. In breast cancer, particularly TNBC, breast-conserving therapy is normally favored when feasible, as it helps to avoid the need for mastectomy. However, due to risk of tumor recurrence, even after radiation therapy, many patients ultimately want both mastectomy and radiation treatment [250, 252]. Thus, chemotherapy continues to be a cornerstone of systemic therapy for TNBC, with anthracyclines and taxanes being frequently utilized due to their proven efficacy against this aggressive cancer subtype [253, 254]. Nevertheless, the advancement of new technologies is essential to improve the accuracy of drug delivery and reduce the cytotoxic side effects commonly associated with these chemotherapeutic agents [253, 254].

4.3.2. PTT with GQDs. PTT is a promising modality that leverages light-sensitive nanoparticles to specifically target cancer cells. PTT photothermal agents absorb laser light in the NIR range and transform it into heat in a specific area, resulting in cell death [21]. This treatment has the potential for lower toxicity compared to chemotherapy, PDT, or radiation therapy [255]. Photothermal agents include gold nanoparticles, nanocages, silver NPs, carbon nanotubes, reduced graphene, GQDs, polydopamine, polyaniline, cetyl palmitate, and others [222, 256, 257]. GQDs are biocompatible and can efficiently generate heat from NIR irradiation [21].

In addition to PTT, GQDs have been extensively explored in a variety of combination therapy strategies that incorporate PTT as one of the core modalities [258–261]. The rationale behind combining PTT with other therapeutic techniques lies in the ability to capitalize on the unique advantages of each method while mitigating their respective limitations. This integrative approach often leads to therapeutic effects that are either additive, where the total effect equals the sum of individual treatments, or synergistic, where the combined effect exceeds what each therapy could achieve alone. For example,

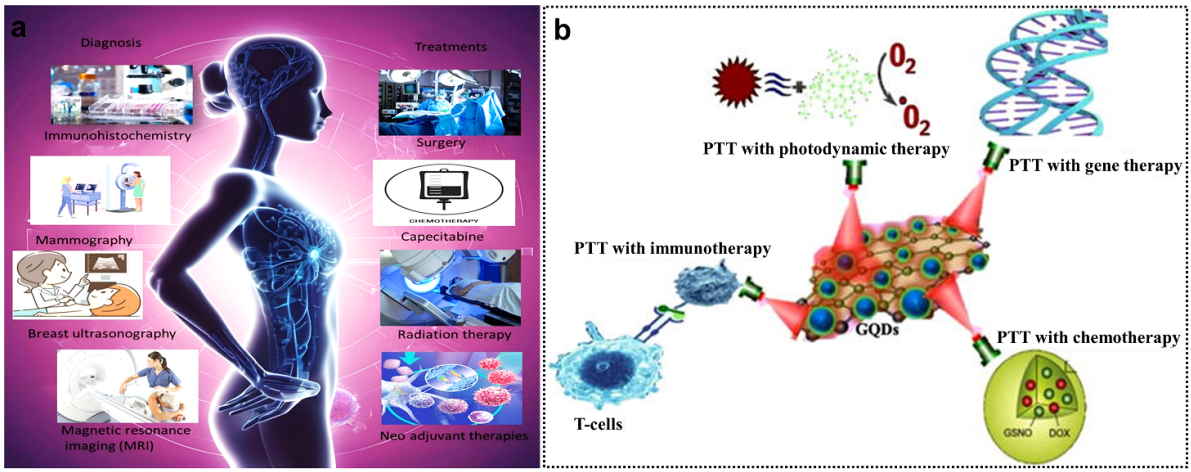

Figure 20. (a) Schematic representation of currently available diagnostic and treatment techniques for breast cancer. Reprinted from [4], Copyright (2025), with permission from Elsevier. (b) Synergistic therapies of GQDs with PPT and gene therapy, chemotherapy, immunotherapy, PDT, etc. Reproduced from [21]. CC BY 4.0.

while PTT can induce localized tumor ablation by converting absorbed light into heat, it may not eliminate all cancer cells—particularly those located in poorly accessible regions or those resistant to heat. By pairing PTT with complementary therapies such as chemotherapy, immunotherapy, PDT, or gene therapy, researchers aim to enhance overall efficacy, improve specificity, and reduce side effects (figure 20(b)). In the following section we discuss some of the important combinational therapies.

4.3.3. PTT and gene therapy with GQDs. Genetic therapy offers an alternative to chemotherapy, targeting signaling activities and inducing cell death in tumor tissue. This treatment approach involves the use of RNA or DNA to either replace a faulty gene or introduce new genes that can fight the disease [262]. A crucial factor for the integration of gene therapy and PTT is the light-induced photothermal impact. The combination of PTT and other nuclear therapeutic agents result in synergistic effects, aiming to destroy the target cell and modulate the expression of disease-related genes. An enhanced photothermal effect facilitates the process of gene therapy by effectively addressing obstacles such as intracellular gene delivery, cellular uptake at different phases, escape from endosomes, and release into the cytosol [263]. Kim *et al* discovered that fluorescent CDs increase the absorption of siRNA by cells without causing harm, thereby suppressing the formation of tumors in breast cells [264]. Luo *et al* also demonstrated the water solubility and biocompatibility of iron-doped CDs, as well as their photothermal efficacy of 63%. These properties improved gene transfection in both laboratory settings and living organisms [265]. In addition, Deng et.al utilized four distinct varieties of GQDs, with A-GQDs introduced to zebrafish resulting in zebrafish embryos exhibiting development inhibition at high concentrations. The remaining three types of GQDs did not induce any adverse effects on development, even at the most concentrated levels [266]. While the potential of next-generation combination treatments is promising, there are significant constraints that need to be addressed. These include the bioavailability of photothermal agents, long-term toxicity, and biocompatibility of gene delivery agents [267].

4.3.4. PTT and chemotherapy with GQDs. Chemotherapy is frequently employed as the main therapy for advanced cancer or as an alternative to surgery for early-stage cancer. It leads to substantial systemic harm and indiscriminate toxicity in both cancerous and healthy cells [268]. There is a strong demand for cancer treatments that are effective in eliminating large solid tumors, disseminated malignant nodules, and tumor reappearance. PTT is a promising approach for treating localized tumors. However, for a tumor mass in close proximity to the treatment boundaries, or removing larger tumors by standard PTT methods is challenging [269]. Combining different techniques improves effectiveness, and so there has been significant research dedicated to studying the combination of PTT and chemotherapy. Various chemotherapeutic drugs, specifically DOX, have demonstrated an augmentation to PTT. In addition, chemo-PTT can stimulate anti-tumor immunity with significant therapeutic benefits in treating both primary and metastatic malignancies [270, 271].

GQDs are emerging as metal-free nanozymes for chemodynamic therapies [38]. Wang *et al* created a GQDs based nanoplatform for PTT enhanced tumor chemotherapy (figure 21(a)) [272]. The delivery vehicle was mesoporous CNPs (MCNs), which possessed exceptional loading capacity. The construction of the nanodrug delivery system (MCN-SS-GQDs) involved attaching the GQDs to MCN pores through disulfide bonds. The GQDs served multiple functions, acting as a PTT agent to enhance the photothermal effect, a switching agent to regulate the controlled release, and a fluorescent

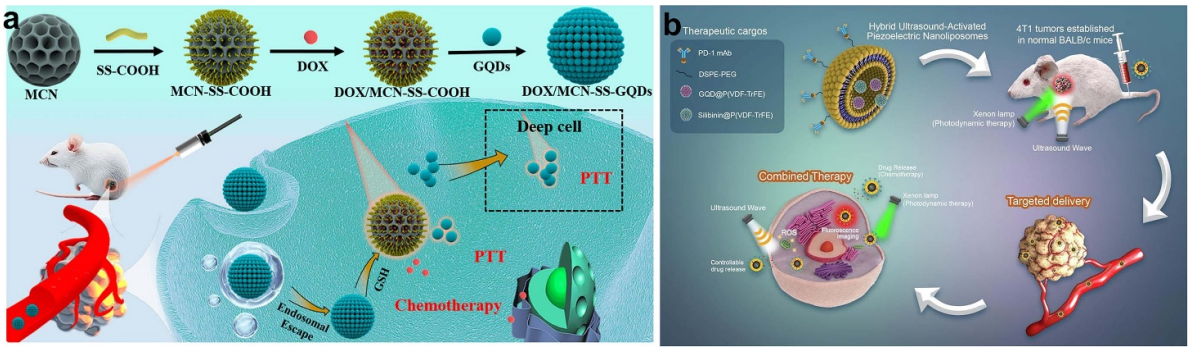

Figure 21. (a) Mechanism of DOX/MCN-SS-GQDs based synergistic PTT and chemotherapy for deep tumor treatment. Reproduced from [272]. CC BY 4.0. (b) Synergistic PTT and chemotherapy with piezoelectric macromolecules (P(VDF–TrFE)) and GQDs. Reprinted from [274], Copyright (2022), with permission from Elsevier.

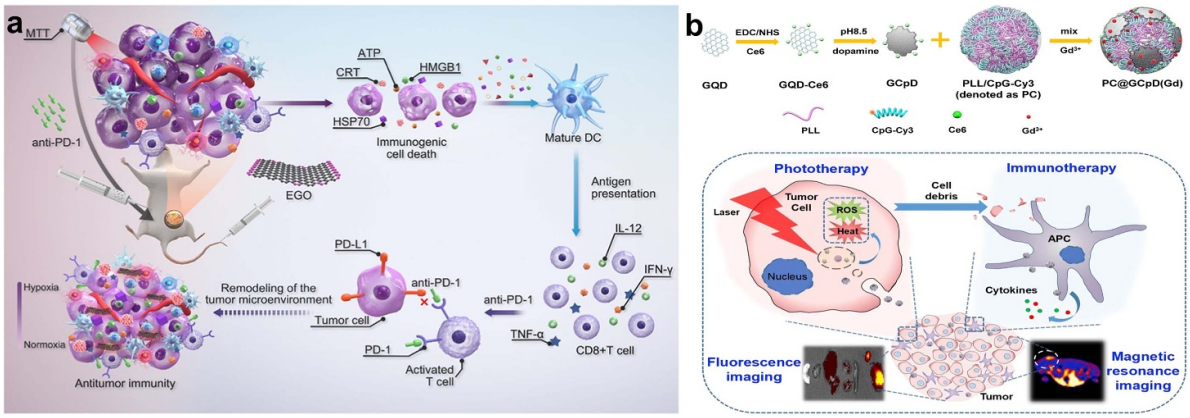

Figure 22. (a) Edge oxidized graphene based thermal immunotherapy for tumor microenvironment reprogramming. Reprinted with permission from [277]. Copyright (2024) American Chemical Society. (b) Mechanism of MRI/FI bimodal photo-immunotherapy facilitated by PC@GCpD(Gd). Reprinted from [280], Copyright (2019), with permission from Elsevier.

agent to monitor the release process. The DOX/MCN-SS-GQDs demonstrated a high drug loading capacity of 29.6%. This composite was stable in the bloodstream and underwent rapid cleavage into DOX/MCN nanoparticles and an ample amount of GQDs upon internalization by cancer cells, particularly in the presence of a high concentration of GSH. The GQDs successfully infiltrated the tumor cells and assisted fluorescence imaging and photothermal ablation. The MCN-SS-GQDs exhibited a remarkable heating effect, achieving a photothermal conversion efficiency of 21.4%. DOX/MCN-SS-GQDs also exhibited a combined chemo-photothermal effects at the cellular level. This drug delivery technology employed a multi-mode therapeutic approach to effectively eliminate tumor cells at varying depths achieving synergistic tumor treatment [272]. Wang *et al* developed a cyclic arginyl-glycyl-aspartic acid (C-RGD) peptide loaded onto GQDs for targeted delivery of DOX. The DOX loading capacity on GQDs could reach 96.6% owing to promising van der Waals interaction (π–π stacking). This synergetic therapy effectively suppressed tumor growth, exhibiting excellent photothermal efficiency and pH-responsive drug release [273].

Fang *et al* synthesized hollow MCNs (HMCNs) combined with GQDs for chemotherapy. These nanoparticles had a uniform size of 120 nm and exhibited drug release controlled by pH and NIR light. The drug loading capacity of HMCN-PEI was determined to be 410 mg per gram of HMCN-PEI, with a high entrapment efficiency of 96.7%. Importantly, they demonstrated minimal toxicity *in vivo*. NIR irradiation enhanced the ability of these nanoparticles to limit tumor growth [275]. Kao and colleagues have similarly presented *in vivo* findings demonstrating the effectiveness of GQDs of a narrower sizes range for cancer therapy [276]. A hybrid composite consisting of GQDs and silibinin covered with piezoelectric poly(vinylidene fluoride–trifluorethylene) (P(VDF–TrFE)) has been developed as an ultrasound-activated nanoliposome for targeted drug delivery (figure 21(b)) [274]. This smart drug delivery formulation released about 80% of the drug over a 240 h period and also achieved generation of hydroxyl radicals and superoxide anions (O^{2-}) [274].

4.3.5. PTT and immunotherapy with GQDs.

Immunotherapy, a treatment method that harnesses the host's immune system to recognize and eradicate cancer cells, is promising for the treatment of particular cancers such as melanoma. Current research is centered on investigating the immune response that occurs after PTT using nanomaterials. Figure 22(a) depicts the process of PTT-induced immunogenic

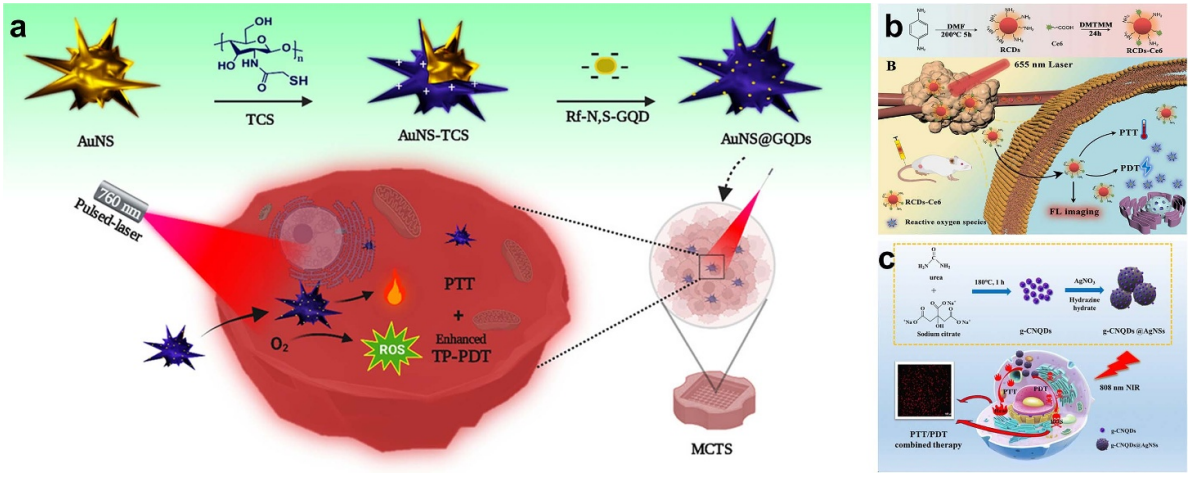

Figure 23. (a) AuNS@GQDs based system for synergistic PTT and TP-PDT treatment. Reproduced from [288]. CC BY 4.0. (b) RCDs-Ce6 drug delivery nanoplatform, fluorescence imaging and realization of PTT/PDT-enhanced synergistic tumor therapy. Reprinted from [289], Copyright (2023), with permission from Elsevier. (c) g-CNQDs@AgNSs based PTT/PDT combination therapy. Reproduced from [290] with permission from the Royal Society of Chemistry.

cell death [277]. In this process, tumor cells are eliminated by nanodrugs delivered to the tumor site either directly or indirectly followed by irradiation. Tumor-associated antigens and cell fragments are thereby released, which in turn activate the body's immune system, resulting in the elimination of any remaining or metastatic cancer cells [278]. Furthermore, immunological memory can aid in preventing the recurrence of cancer. This photothermal immunotherapy utilizes nanomaterials to eradicate tumors and stimulate durable immune responses against cancer [279].

The combination of PTT with immunotherapy has shown promise in improving treatment outcomes for both primary tumors and metastatic cancer cells. Xia *et al* investigated the ability of GQD layers to effectively shield a portion of miR155 from enzymatic breakdown by cross-linking the RNA with GQDs through disulfide linkages. This study established an experimental foundation for the secure transportation of miRNAs across living organisms [281]. Wu *et al* introduced an innovative nanoassembly, PC@GCpD(Gd), composed of polydopamine-stabilized GQD-PS nanocomposites (GCpD), immunostimulatory nanoparticles formed by a polycationic polymer and CpG oligodeoxynucleotide (CpG ODN) (PC), and a Gd^{3+}/Cy3 imaging probe [280]. This system enabled dual magnetic resonance and fluorescence imaging for photo-immunotherapy guidance (figure 22(b)). PC@GCpD(Gd) demonstrated the ability to eliminate tumor cells by amplifying photothermal and photodynamic effects through GCpD. Additionally, it effectively delivered CpG ODN to endosomal Toll-like receptor 9 (TLR9), triggering the sustained release of proinflammatory cytokines and promoting dendritic cell maturation. This immune activation further stimulated the infiltration and activity of T lymphocytes. Under laser irradiation, PC@GCpD(Gd) efficiently suppressed tumor growth in an EMT6 murine mammary cancer model.

4.3.6. PTT and PDT with GQDs. PDT medications generate singlet oxygen by exposure to light. The PSs are designed to efficiently absorb in the NIR region because light at this wavelength can penetrate living tissue more effectively. A combination of PDT with PTT offers two non-invasive modalities for treatment of cancer [35, 282–285]. Wo *et al* [286] developed a multifunctional therapeutic approach by integrating mechanical, magnetic, photodynamic, photothermal, and chemotherapy into a single system. This multimodal platform featured GQDs attached to hollow magnetic nanospheres coated with silica shells (HMNS/SiO_2/GQDs) and loaded with the anticancer drug DOX. The combination of these therapies produced a synergistic effect, leading to cancer cell destruction through four distinct mechanisms [286]. Similarly, Ashkbar *et al* [287] successfully synthesized highly crystalline GQDs from plant leaves using a hydrothermal process and utilized these GQDs for dual PDT and PTT, demonstrating their potential in combined cancer treatments.

Soleimany *et al* created a novel nanohybrid consisting of gold nanostars coated with chitosan bearing thiol groups (AuNS-TCS) for converting light to heat, together with GQDs doped with nitrogen and sulfur, coupled with riboflavin (Rf-N,S-GQD) (figure 23(a)) [288]. When exposed to low-power, single-pulse laser irradiation, the nanohybrid exhibited a synergistic TP-PDT/PTT response. The localized surface plasmon resonance of AuNS aligned with the two-photon absorption wavelength of Rf-N,S-GQD. Singlet oxygen ($^1O_2$) was generated both outside and within the cells. This TP-PDT/PTT combination demonstrated a considerably enhanced phototherapeutic outcome towards both 2D monolayer cells and 3D multicellular tumor spheroids compared to the individual therapies alone.

Other studies on combinational therapy have discovered that the utilization of nanocomposites in conjunction with PDT and PTT could serve as a viable substitute for chemotherapy in

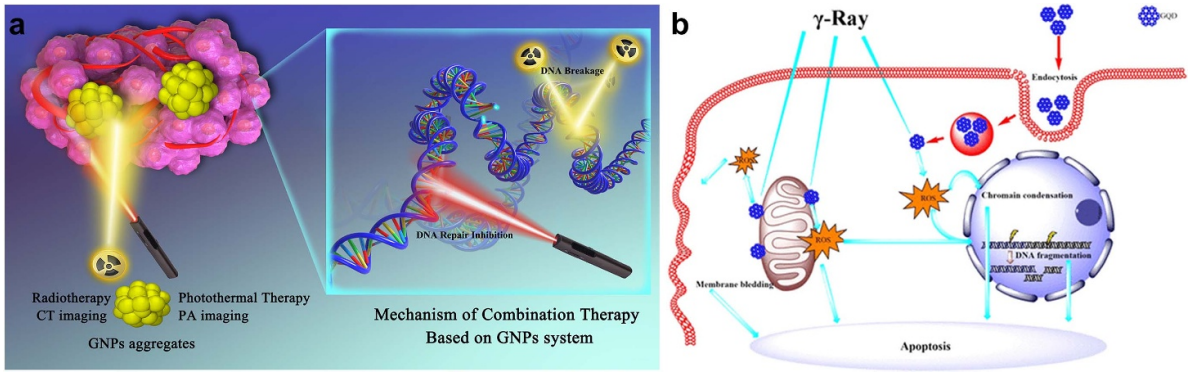

Figure 24. Synergistic PTT and radiotherapy based on GNPs. Reprinted from [293], Copyright (2020), with permission from Elsevier. (b) The mechanism of GQD assisted irradiation-induced cell apoptosis. Reprinted with permission from [294]. Copyright (2018) American Chemical Society.

the treatment of breast tumors [287]. Liu *et al* demonstrated an enhanced PTT and PDT combined effect to effectively eliminate non-small-cell lung cancer cells. This treatment successfully eradicated an *in vivo* tumor xenograft model without any observable adverse effects [291]. However, the limited solubility of most PSs in water and significant phototoxicity hinders their potential use in cancer therapy. To solve this issue, Song *et al* created a nano-platform linking PS Chlorin-e6 (Ce6) onto red-emitting CDs (RCDs-Ce6) (figure 23(b)) [289]. The RCDs have excellent photothermal conversion and can absorb natural sunlight, which helps to minimize the harmful effects of phototoxicity. Moreover, RCDs-Ce6 can simultaneously excite a PTT and PDT response with a single laser. The remarkable fluorescent imaging capacity of RCDs-Ce6 also allows for imaging-guided tumor therapy. *In vivo* investigations demonstrated that RCDs-Ce6 (PTT and PDT) had a pronounced tumor inhibitory impact over a wider degree of tumor distribution.

Similarly He *et al* developed graphite-phase carbon nitride quantum dots (g-CNQDs) in combination with silver nanospheres (AgNSs) to induce a synergistic PTT/PDT response (figure 23(c)) [290]. The g-CNQDs@AgNSs nanocomposite was synthesized by loading g-CNQDs onto the surface of AgNSs via metal amino coordination and *in situ* reduction. In this system, g-CNQDs acted as the PS, while the AgNSs served as the photothermal agent, enabling enhanced therapeutic effects through the combination of PTT and PDT. This nanocomposite exhibited both favorable biocompatibility and impressive photothermal characteristics, efficiently producing ROS when exposed to NIR light. Again, this combined therapy was more effective than either of the individual photothermal or photodynamic therapies.

4.3.7. PTT and radiotherapy with GQDs. Photo-radiotherapy integrates phototherapy and radiation to enhance therapeutic outcomes. The effectiveness of radiotherapy (RT) relies on the availability of oxygen molecules within the tumor region. In the case of solid tumors, the effectiveness of RT is constrained by hypoxia and inadequate blood supply. Soft tumor tissue does not absorb much radiation and so under typical conditions with appropriate levels of radiation, the effectiveness of RT is only moderate.

Employing metallic nanostructures as radiosensitizers, however, enhanced x-ray absorption and improved the efficiency of RT [292]. Zhang *et al* showcased the application of a gold nanoparticle system in RT and PTT (figure 24(a)) that induced DNA damage and repair inhibition with good localization to the tumor site. The radiation efficiency was enhanced, resulting in a decrease in adverse effects [293]. Ruan *et al* have reported GQDs bearing various oxygen-containing functional groups for improved tumor radiation treatment. These researchers observed distinct changes in the cell cycle, including apoptosis, cellular arrest, and inhibition of cell growth. Irradiation induced an overabundance of ROS leading to impaired mitochondrial activity in cancer cells [294]. Mishra *et al* created a nanomaterial (AuPLGA) with potential for PTT to treat tumors resistant to radiation and chemotherapy using a preclinical model [295].

Nano-radiosensitizer can also enhance the efficacy of tumor radiation by improving tumor tissue absorption and the generation of secondary electrons. Jing *et al* synthesized GQDs with a strong oxidative stress response and remarkably high phototoxicity [294]. The combination of GQD and IR significantly increased the arrest of cells in the G2/M stage, suppressing cell proliferation, and boosting apoptosis (figure 24(b)). The primary cause of tumor cell apoptosis was the excessive generation of ROS by the GQDs in conjunction with infrared radiation, which triggered the activation of apoptosis-related regulatory proteins.

4.4. Antiviral therapy

Viral infections are a major health challenge because of the virus's ability to escape conventional therapies by rapid genetic mutation [296]. Immune deficiency syndrome caused by HIV, for example, affects approximately 36.9 million people, worldwide, despite the use of highly active antiretroviral therapy (HAART) to effectively suppress the viral load [297, 298]. However, long-term use of HAART may lead to the development of drug resistance, necessitating changes in medication.

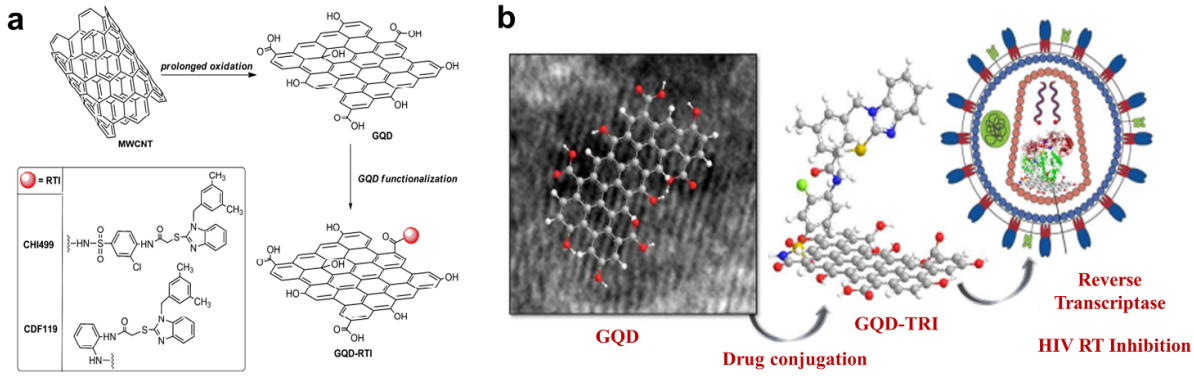

Figure 25. (a) GQD and GQD-RTI conjugates. (b) Conjugation of GQDs with reverse transcriptase inhibitor (RTI) CHI499 and targeting the HIV-1 RTI. Reprinted with permission from [307]. Copyright (2018) American Chemical Society.

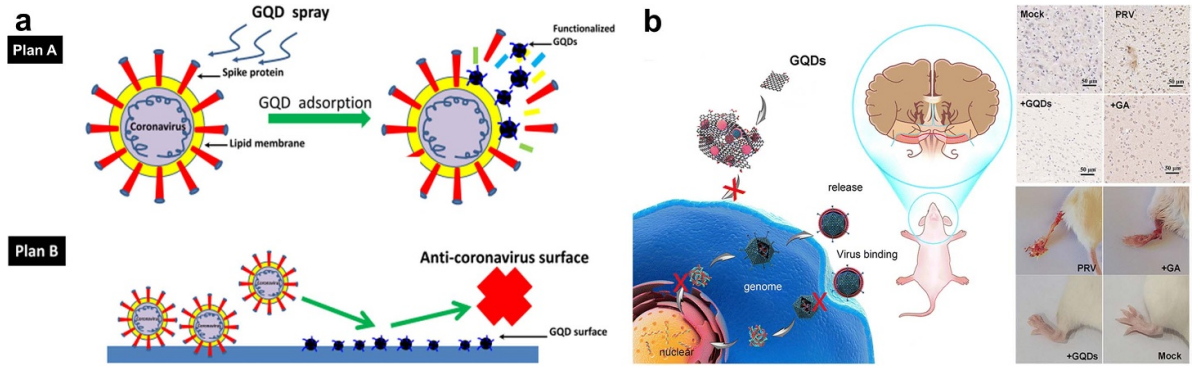

Figure 26. (a) A twofold anti-coronavirus mechanism is activated in the presence of functionalized graphene quantum dots (GQDs). In the first phase (Plan A), the lipid membrane of the virus is disrupted in the liquid phase. In the second phase (Plan B), a protective layer of GQDs forms around the virus, preventing further infection. Reprinted from [309], Copyright (2023), with permission from Elsevier. (b) A schematic illustration of the straightforward one-step synthesis process for GAGQDs and (c) their application in combating PRV infection, highlighting their effectiveness in both *in vitro* and *in vivo* systems. Reproduced from [303] with permission from the Royal Society of Chemistry.

Recently GQDs have emerged as novel antiviral agents for combating various types of viral infections [299–306]. Daniela Jannazzo and colleagues [307] investigated the antiviral activity of GQDs decorated with antiviral agents CHI499 and CDF119 (figure 25(a)). The conjugate GQD-CHI499 exhibited a dual mechanism of action including inhibition of reverse transcriptase activity and inhibiting the virus binding to the cells (figure 25(b)). GQD-CHI499 had an IC50 of 0.09 μg ml^{-1} and EC50 value in cells of 0.066 μg ml^{-1}.

On 30 January 2020, the World Health Organization declared the novel coronavirus pneumonia pandemic a 'public health emergency of international concern' [308]. The novel human coronavirus (SARS-CoV-2)) pandemic highlighted the need for new cure regimens. Recently, researchers [309] have explored the application of functionalized GQDs for combating both coronavirus and enterovirus infections. N-functionalized GQDs were synthesized by a novel solid-phase microwave-assisted (PMMA) protocol. These functionalized GQDs exhibited excellent biocompatibility with H171 and H184 cells after 72 h incubation. The viral inhibition of GQD-coated glass was 99.22% and 99.92% after 8 and 20 h, respectively. The antiviral mechanism of this novel coating involved the interaction between the N-functionalized GQDs and the receptor-binding-domain of the spike protein (figure 26(a)). These functionalized GQDs disrupt the early stages of infection by modifying the viral surface proteins. Furthermore, the functional groups on the GQDs prevent viral entry by promoting the accumulation of ROS. The synthesized GQDs were also used to combat Feline Coronavirus NTU156 (FCoV NTU156) and Enterovirus 71 (EV71), demonstrating exceptional inhibition rates of over 99.9%. In another study, researchers [303] reported the improved *in vivo* antiviral activity against pseudorabies virus (PRV) using gallic acid-based GQDs (GAGQDs). Gallic acid was transformed into GAGQDs using a one-step hydrothermal method (figure 26(b)).

The naturally occurring, low molecular weight polyphenolic GA was chosen as the carbon source due to its anti-inflammatory, antimicrobial, antitumor, and antioxidant properties. Although its structural instability and poor water

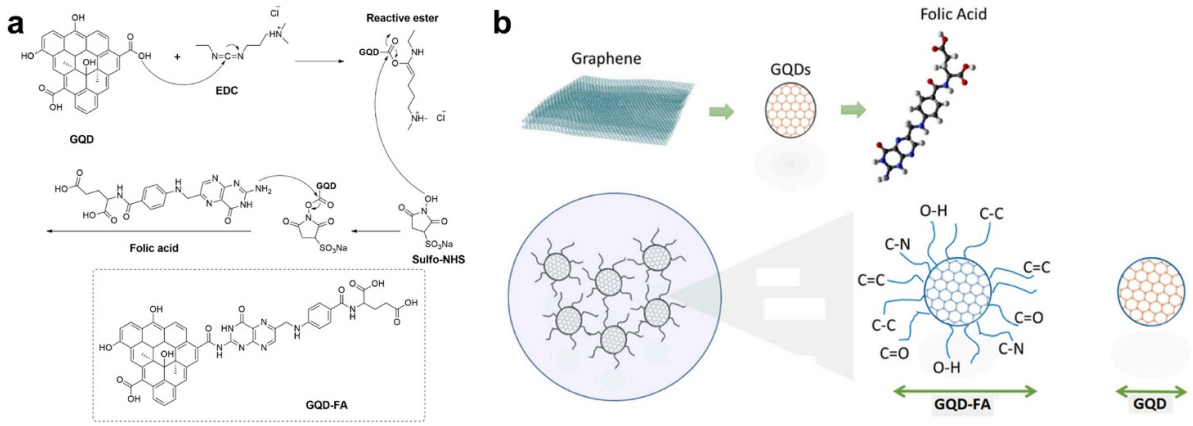

Figure 27. (a) The synthesis of GQD-FA achieved through carbodiimide-mediated functionalization. (b) The typical size of GQD-FA is shown in comparison to unmodified GQDs. Reprinted from [310], Copyright (2022), with permission from Elsevier.

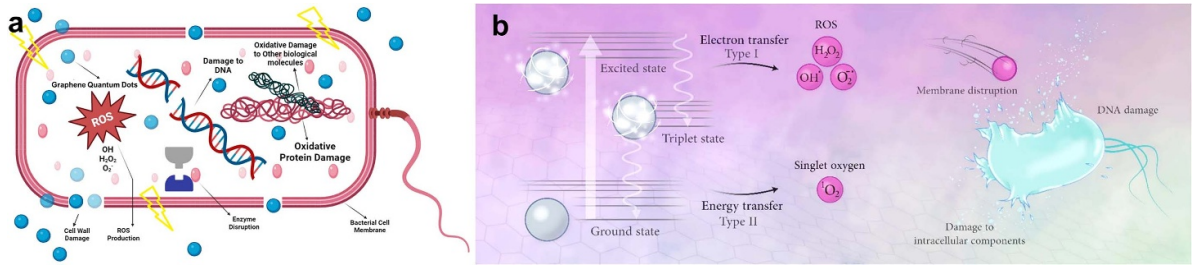

Figure 28. (a) ROS based antibacterial mechanism of GQDs against *E. coli* bacteria. Reproduced from [316]. CC BY 4.0. (b) Schematic representation of the Type I and Type II mechanisms in antibacterial PDT. Reprinted from [5], Copyright (2025), with permission from Elsevier.

solubility pose limitations, GAGQDs derived from GA exhibited significantly improved solubility and enhanced antiviral activity against PRV. Moreover, GAGQDs effectively inhibited the absorption, invasion, and replication stages of PRV proliferation (figure 26(c)).

FA-functionalized GQDs (GQDs-FA) have been assessed for their antiviral activity against Zika virus (ZIKV) infection (figure 27). FA is known to inhibit the folate receptor-α-AMPK signaling pathway, which is critical for ZIKV infection. The GQDs were functionalized with FA by first activating the carboxyl groups on the GQDs using EDC and sulfo-NHS, followed by coupling FA with a 90% yield. GQD-FA demonstrated low cytotoxicity (<1%) in Vero E6 cells, and both GQD and GQD-FA effectively inhibited ZIKV replication *in vitro*. However, the functionalization of GQDs with FA did not enhance their antiviral efficacy against ZIKV replication [310].

4.5. Antibacterial therapy

Bacterial infection is the primary cause of mortality worldwide [311]. Many patients with COVID-19 died from co- and secondary, viral and bacterial infections due to their weakened immune system [312]. Bacteria possess innate antioxidant defense mechanisms to shield themselves from ROS, such as singlet oxygen ($^1O_2$), superoxide anions ($\bullet O_2^-$), hydrogen peroxide (H_2O_2), and hydroxyl radicals ($\bullet$OH), whether these are produced internally or introduced from external sources. However, when ROS levels surpass the capacity of these protective systems, oxidative stress occurs, leading to damage to cellular structures, including membranes, nucleotides, lipids, and proteins (figure 28(a)). This oxidative damage can ultimately result in bacterial cell death [126]. The production of ROS can trigger a series of oxidative reactions that specifically target the bacterial cell membrane. The membrane's lipid bilayer containing a large amount of polyunsaturated fatty acids is principally vulnerable to oxidative damage. This leads to lipid peroxidation, which generates toxic by-products [313]. These by-products compromise the membrane's stability, increasing its fluidity and permeability, and disrupting its role as a selective barrier. As a result, the membrane's integrity is compromised, leading to leakage of crucial intracellular components and, in some cases, cell rupture. The altered membrane permeability results in the loss of essential ions, metabolites, and proteins, which in turn impairs key cellular processes [314, 315].

Beyond damaging the structural integrity of the membrane, ROS can also affect membrane-associated proteins, interfering with their normal functions such as nutrient transport and cellular signaling [315]. Moreover, the oxidative stress generated by ROS can activate bacterial stress response pathways. If the magnitude of damage exceeds the cell's ability

to repair itself, it can lead to cell death, potentially through pathways similar to apoptosis or necrosis. The integrity of the bacterial membrane is vital for cell survival, and its disruption often leads to cell death, underscoring the critical role of ROS in antimicrobial mechanisms [317]. ROS can also interact with key bacterial biomolecules, inducing oxidative modifications to proteins through various pathways [318]. These modifications typically start with ROS reactions that oxidize amino acid residues, particularly those containing sulfur or aromatic groups, such as cysteine, methionine, tyrosine, and tryptophan [319]. Cysteine residues, for instance, are especially vulnerable to oxidation, leading to the formation of disulfide bonds or sulfenic acids. Such oxidative alterations can dramatically affect protein function and stability, potentially causing protein denaturation, loss of function, and even aggregation. Consequently, vital cellular processes, including enzyme activity, cell signaling, and structural integrity, are disrupted.

Similarly, ROS can also inflict substantial damage to bacterial DNA, causing various types of oxidative DNA damage, including single-strand breaks, double-strand breaks, base oxidation, and deoxyribose oxidation, all of which contribute to the degradation of bacterial integrity [320]. Such damage can severely undermine the structural integrity of chromosomes, causing errors in base incorporation during DNA replication and transcription, which complicates bacterial survival and reproduction [321]. These cumulative effects disrupt critical cellular functions, including signaling, metabolism, and DNA integrity, ultimately affecting bacterial viability and highlighting the vital role of ROS in bacterial cell damage.

4.5.1. ROS generation by GQDs. GQDs have gained significant attention for their ability to generate ROS, which contributes to their antimicrobial properties [127]. They can also serve as PSs, capable of absorbing specific wavelengths of light to produce ROS in a controlled way, targeting pathogens with minimal unintended effects. When exposed to light of the appropriate wavelength, GQDs are excited from their ground state (PS) to an excited singlet state (^{1}PS). From this excited state, the electrons may either return to the ground state by emitting fluorescence or transition via intersystem crossing to a more stable triplet state (^{3}PS). The triplet state (^{3}PS) can then interact with surrounding molecules through two competing routes: Type I and Type II reactions, as illustrated in figure 28(b) [5].

In Type I reactions, when GQDs are in their excited triplet state, they can interact with molecular oxygen (O_2) through electron transfer, generating superoxide anions ($_2O_2{}^-$). While these superoxide radicals are relatively benign in biological environments, further electron transfer can lead to the production of more harmful ROS, such as hydroxyl radicals (•OH) and hydrogen peroxide (H_2O_2). These ROS are highly oxidative and can damage essential cellular components like DNA, lipids, carbohydrates, and proteins, ultimately resulting in bacterial cell damage and death. In Type II reactions, the excited GQDs directly interact with triplet-state molecular oxygen ($^3O_2$) via energy transfer, producing singlet oxygen ($^1O_2$). This excited form of oxygen is highly reactive and cytotoxic, and it can cause significant damage to bacterial membranes. These two reaction pathways are central to the mechanism of PDT, a technique originally developed for cancer treatment. PDT offers several advantages, such as high precision, effectiveness, and minimal side effects, making it an attractive therapeutic strategy not only for cancer but also for treating infections induced by biofilms or pathogenic bacteria.

4.5.2. GQDs for treating bacterial infections. GQDs have recently appeared capable of treating bacterial infections and reducing biofilm development [113, 322–326]. Raju *et al* [322] reported the first bottom-up synthesis of crystalline GQDs from indoor dust particles with antibacterial activity and cytotoxicity against human breast cancer cell lines. The dust particles were converted into nanosized, semi-crystalline GQDs that contained oxygen.

These synthesized GQDs exhibited cytotoxic effects in a dose-dependent manner against two human breast cancer cell lines, MDA-MB-231 and MCF-7. Furthermore, they demonstrated significant antibacterial properties against both Gram-positive bacteria (*Bacillus subtilis* and *Staphylococcus aureus*) and Gram-negative bacteria (*Escherichia coli* and *Pseudomonas aeruginosa*) (figure 29).

Safeguarding clean water sources is essential to maintaining aquatic habitats and guaranteeing a sustainable water supply. Bacterial and fungal contamination of water sources is a problem at different points in the water cycle [327]. A recent study examined the production, characterization, and water purification properties of GO quantum dots/silver nanoparticles (GOQD/AgNPs) [328]. The study investigated the antibacterial activity of GOQD in combination with silver nanoparticles against *E. Coli, S. Staphy*, and *S. Aureus*. Higher concentrations of AgNPs in GOQD/AgNP mixes showed larger inhibitory zones against these strains, with *S. Aureus* being the most resistant. Various bacterial species tested for GQD-induced antibacterial activity are summarized in table 2.

In clinical treatment, excessive use of antibiotics can cause drug resistance hindering the treatment of bacterial infections. Su *et al* [113] reported the synthesis of N-heterocycle fused GQDs to develop structurally stable Topoisomerase I (Topo I) inhibitors with broad-spectrum antibacterial and antifungal activities. The authors synthesized N-heterocycle fused GQDs through a one-step protocol using N-containing julolidine as the precursor (figure 30). Having confirmed a strong interaction between GQDs and BSA and liposaccharide (LPS), this study investigated the activity of GQDs against five types of bacteria and one fungus, *viz S. aureus, L. monocytogens*, MRSA, *E. coli, B. subtilis, and C. albicans*. The GQDs caused irreversible damage to cell walls and membranes, as well as inhibited the DNA-binding protein Topo I, leading to DNA damage and bacterial cell death. Additionally,

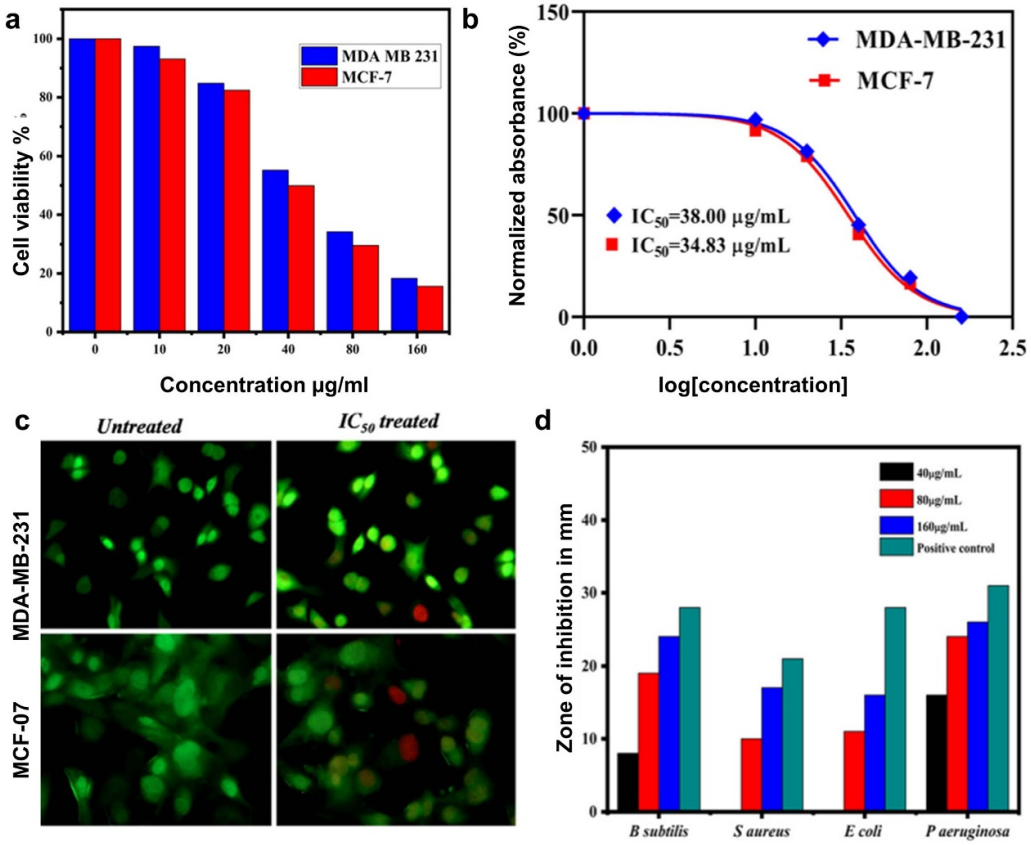

Figure 29. (a) The MTT assay illustrates the inhibition of cell growth in MDA-MB-231 and MCF-7 cells after exposure to various concentrations of GQDs for 24 h. (b) The determination of the IC50 value of GQDs against the MDA-MB-231 and MCF-7 cell lines. (c) Fluorescence microscopy images of GQD-treated MDA-MB-231 and MCF-7 cells stained with AO/EB dual staining (40x magnification, scale bar 100 μm). (d) The antibacterial performance of GQDs. Reproduced from [322] with permission from the Royal Society of Chemistry.

GQDs were effective in preventing biofilm formation and significantly reduced wound infections. In mouse models of skin wounds infected with *MRSA* or *C. albicans*, GQDs promote wound healing.

A recent work describes the creation of GQD/TiO_{2-x} microspheres loaded with nanoantibiotics for use in heterojunction-mediated antibacterial treatments using nanocatalytic therapy and synergetic sonodynamic therapy [323]. This work used 2-ethylimidazole, Pluronic F127, and tetrabutyltitanate as precursors to synthesize TiO_{2-x} microspheres with numerous Ti^{3+} defects utilizing a straightforward reductant co-assembly approach. An oxygen vacancy engineering technique was used to construct the defective TiO_{2-x} microspheres, which had narrow bandgaps (2.0 eV) and Ti^{3+}/Ti^{4+}-mediated multiple-enzyme catalytic activity.

The increased production of ROS observed in the GQD/TiO_{2-x} resulting from the deposition of GQD nanoantibiotics on TiO_{2-x} microspheres was attributed to the accelerated separation of electron–hole pairs, as well as the peroxidase-like catalytic activity mediated by Ti^{3+} and the glutathione depletion mediated by Ti^{4+}. By creating heterojunctions, the multifunctional TiO_{2-x} microspheres enhanced their multiple-enzyme catalytic activities through accelerated carrier transfer and prevented electron–hole pair recombination within the semiconductor. This also improved the sonodynamic and nanocatalytic performance of these microspheres. The *in vitro* antibacterial effects of GQD/TiO_{2-x} were assessed against *S. aureus, E. coli*, and MRSA on treatment with ultrasound using a conventional colony counting technique. The number of MRSA, *E. Coli*, and *S. aureus* colonies in the single ultrasound treatment group did not differ significantly from the control group, indicating that ultrasound irradiation had little impact on bacterial growth. However, TiO_{2-x} plus ultrasound irradiation clearly decreased the number of bacterial colonies, of all three types. All colonies of these bacteria were eradicated in the GQD/TiO_{2-x}.+ ultrasound group, indicating a synergistic effect of sonodynamic and nanocatalytic therapies (figure 31) [323].

Overall, the use of GQDs in biomedical applications depends on tailoring their structure to meet the specific requirements of each application. By precisely adjusting the key characteristics, such as size, surface functional groups, and dopants, GQDs can be fine-tuned to exhibit the desired optical, electronic, and biocompatible properties, making them

Table 2. A summary of bacterial species tested for GQD-induced antibacterial activity.

Bacterial strain	Gram type	Type of GQD	Mechanism	References
Escherichia coli (*E. coli*)	Gram-negative	N-doped GQDs	ROS generation, membrane disruption	[113, 132, 328, 329]
Staphylococcus aureus (*S. aureus*)	Gram-positive	S, N-doped GQDs	ROS generation, cell wall rupture	[132, 328–331]
Methicillin-resistant *S. aureus* (MRSA)	Gram-positive	N-heterocycle modified GQDs	Cell walls damage, upregulating genes	[113, 132]
Salmonella typhi (*S. typhi*)	Gram-negative	GOQD/AgNP	ROS generation, membrane disruption	[328]
Listeria monocytogenes (*L. monocytogenes*)	Gram-positive	N-heterocycle modified GQDs	Cell walls damage, inhibited DNA binding proteins	[113]
Vibrio cholerae	Gram-negative	Hydroxyl-rich GQDs	Membrane electrostatic interaction and cellular metabolism disturbing	[332]
Pseudomonas aeruginosa (*P. aeruginosa*)	Gram-negative	GQDs + photo-dynamic therapy (PDT)	Light-triggered ROS, membrane destabilization	[132]
Bacillus subtilis (*B. subtilis*)	Gram-positive	N-heterocycle modified GQDs, GQDs composites	Physical interaction, cell walls damage, DNA inhibition	[113, 132]
Candida albicans (*C. albicans*)	Gram-positive	N-GQDs	Physical cell walls damage, DNA inhibition	[113, 333]
Ureaplasma urealyticum (*U. urealyticum*)	Gram-positive	Amine–GQDs	Anti-mycoplasma activity	[334]
Staphylococcus saprophyticus (*S. saprophyticus*)	Gram-positive	GQDs	ROS production	[335]
Listeria ivanovii (*L. ivanovii*)	Gram-positive	GQDs	ROS production	[335]

suitable for a broad range of biomedical applications from detection to therapy.

5. Current challenges and proposed solutions

GQDs have demonstrated immense potential as multifunctional nanoplatforms across a variety of biomedical applications, ranging from biosensing to acute disease therapeutics. Despite these promising advancements, several challenges hinder their optimization and clinical translation [336], ranging from material synthesis and functionalization to their interactions within biological systems. These challenges are particularly significant when considering their use in complex biomedical environments, where factors such as sensitivity, selectivity, stability, toxicity and biocompatibility play critical roles [337].

One of the most pressing issues is the absence of standardized synthesis and functionalization protocols, leading to significant batch-to-batch variability. This compromises reproducibility and complicates regulatory validation. Additionally, while promising results have been reported *in vitro* and in small-animal models, the long-term toxicological and immunological behaviors of GQDs remain poorly understood, particularly regarding their biodistribution, metabolism, and excretion in higher organisms. These uncertainties raise concerns about clinical safety and delay approval processes. Another challenge lies in the ambiguous regulatory classification of GQDs—as therapeutic agents, diagnostic tools, or medical devices—which complicates approval pathways across different agencies. Furthermore, the scalability of synthesis under good manufacturing practice (GMP)-compliant conditions remains a major hurdle for industrial implementation.

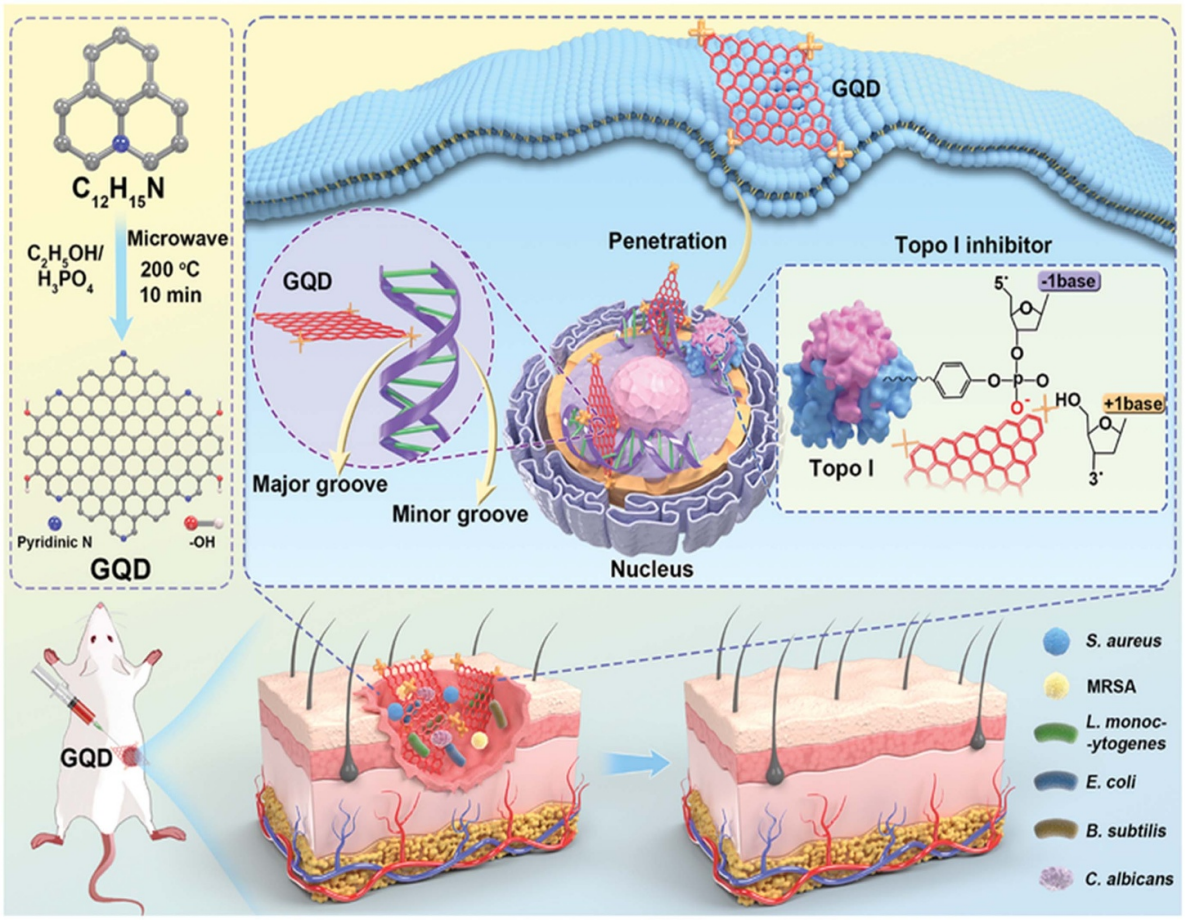

Figure 30. Synthesis of N-heterocycle modified, Topo targeting GQD nanoantibiotics used to treat microbial infections. [113] John Wiley & Sons.© 2023 Wiley-VCH GmbH.

To overcome these barriers, future research should prioritize the development of harmonized, reproducible synthesis methods and comprehensive *in vivo* studies aligned with regulatory toxicology frameworks. Collaborative efforts among researchers, clinicians, industry stakeholders, and regulatory bodies are essential to establish clear translational pathways and unlock the full clinical potential of GQD-based technologies. Table 3 provides an overview of the key challenges and proposed solutions in leveraging GQDs for various biomedical applications.

6. Conclusion and outlook

GQDs have demonstrated exceptional promise as multifunctional nanoplatforms for biomedical applications, owing to tunable PL, excellent aqueous solubility, biocompatibility, and modifiable surface chemistry. Over the past decade, GQDs have been extensively explored for roles in biosensing, imaging, drug delivery, photodynamic and photothermal therapies, and antibacterial strategies. Their unique physicochemical and optical properties position them as next-generation multifunctional platforms, particularly in contexts requiring real-time monitoring, targeted delivery, and combinational therapeutic strategies. This review has summarized recent developments in GQD based materials for fluorescent sensing and biomedical applications.

Despite notable progress, key challenges hinder the practical application of GQDs. Chief among them is the lack of standardized synthesis protocols, which results in inconsistent physicochemical properties and limits reproducibility across studies. Long-term safety concerns—including biocompatibility, biodistribution, and immunological effects—also remain unresolved, hindering clinical confidence. Moreover, while functionalization and heteroatom doping have broadened the application scope of GQDs by enabling tunable reactivity and selectivity, these modifications introduce complexity that complicates predictions of *in vivo* performance. The regulatory landscape further complicates clinical translation, as GQDs often fall outside conventional classification systems. In addition, scalable, GMP-compliant manufacturing processes are still lacking, posing a barrier to commercial integration.

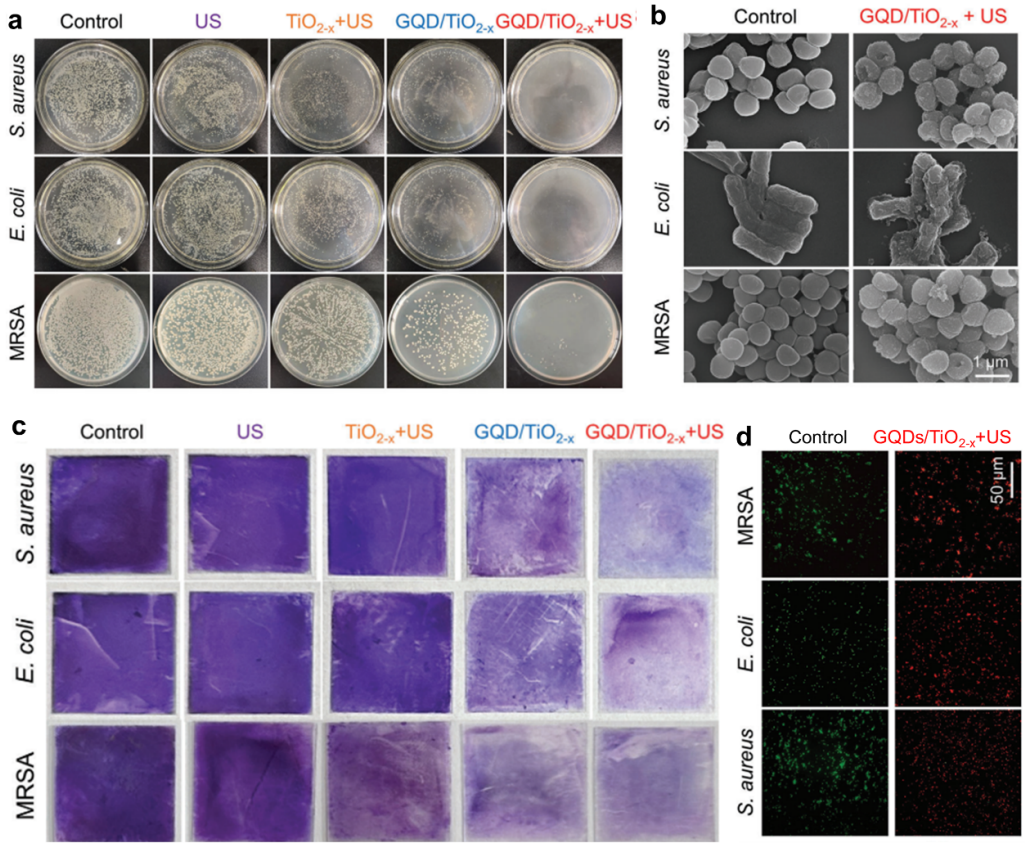

Figure 31. (a) Colonies, (b) SEM images, (c) crystal violet staining of biofilms, and (d) live/dead staining images of *S. aureus, E. coli*, and MRSA after different treatments showing the effectiveness of the GQD/TiO_{2-x} [323]. John Wiley & Sons.© 2024 Wiley-VCH GmbH.

To address these limitations, future research must establish unified synthesis and characterization standards, pursue systematic toxicological evaluations using physiologically relevant models, and foster interdisciplinary collaboration across material science, clinical research, and regulatory frameworks. Emerging tools like artificial intelligence and machine learning may also accelerate the rational design of application-specific GQDs by revealing structure–function relationships. With these strategies, the transformative potential of GQDs in biomedicine can be fully realized. In the following section, we outline promising research directions to guide future developments in this rapidly evolving field.

7. Future perspectives

7.1. Prospective fluorescent sensor developments

Significant progress has been achieved in the development of fluorescence sensors utilizing GQDs, however, there are some challenges that must be addressed before commercialization is possible. GQDs that rely on the coordination or redox reaction of the recognition component, often exhibit limited specificity and weak resistance to interference. In addition, the actual biological applications of fluorescent sensors typically require other functional materials. Despite the ability to modify the fluorescence of GQDs through surface passivation, element doping, and other techniques, a comprehensive understanding of their PL mechanism is currently lacking. The future development of GQD based fluorescent sensors, therefore, lies in understanding the energy transfer between different materials, forecasting changes in fluorescent properties.

Fluorescent sensors utilizing GQDs have shown promise in biomedical imaging and diagnosing and treating diseases. GQDs also demonstrate promise in the fields of electrochemical and magnetic sensing. Fluorescent sensors based on GQDs can be integrated into optical fiber and chip technologies to enable the conversion of photoelectric signals and real-time data analysis for the development of on-site monitoring devices for illness detection and treatment. Additionally, the integration of GQDs with artificial intelligence may reveal fascinating phenomena [341].

7.2. Future biomedical applications

A key area of focus for the development of new GQD-based materials for biomedical applications is selective functionalization to improve the specificity and efficiency of GQDs for targeted drug delivery and imaging applications. Researchers

Table 3. Critical challenges and proposed solutions for GQDs as multifunctional nanoplatforms across a variety of biomedical applications.

Applications	Challenges	Proposed solutions
Biosensing	- Sensitivity and selectivity in complex biological matrices. - PL instability under variable conditions. - Precise surface functionalization.	- Develop hybrid nanostructures to enhance signal transduction. - Use doping or passivation techniques to stabilize fluorescence. - Optimize functionalization strategies for specificity.
Bioimaging	- Low quantum yield for bright fluorescence. - Limited stability in physiological environments. - Restricted tissue penetration *in vivo*.	- Engineer doped or modified GQDs to enhance emission intensity. - Apply surface coatings like PEG for improved biostability. - Shift to NIR-emitting GQDs for deep imaging.
Drug delivery	- Lack of controlled and targeted drug release. - Unknown biodegradability pathways and potential toxic metabolites [338]. - Inefficient cellular targeting [339].	- Integrate pH/temperature-responsive nanocarriers for precise release. - Study long-term biocompatibility and metabolic breakdown. - Use targeting ligands or antibodies for specificity [32].
Cancer Therapeutics	- Insufficient therapeutic efficacy as standalone agents. - Risk of off-target effects and cytotoxicity. - Limited penetration into tumor tissues.	- Combine GQDs with other therapies like chemo/radiotherapy. - Apply biocompatible coatings to reduce cytotoxicity. - Utilize targeting peptides to improve tumor selectivity.
Combinational cancer therapies	- Complexity in achieving synergistic effects across PDT, PTT, and chemotherapy. - Uncontrolled ROS generation. - Tumor microenvironment challenges.	- Design multi-functional systems with controlled drug and energy release. - Optimize ROS levels by co-delivering antioxidants. - Engineer GQDs responsive to tumor-specific conditions.
Antiviral therapy	- Unclear mechanisms of antiviral action. - Potential cytotoxic effects on host cells. - Virus resistance over repeated exposure.	- Investigate GQD interactions with viral components like proteins and DNA/RNA. - Optimize dosages to maximize efficacy with minimal host cytotoxicity. - Use combination antiviral therapies.
Antibacterial therapy	- Limited understanding of antibacterial mechanisms. - Emergence of bacterial resistance. - Balancing biocompatibility with antimicrobial potency.	- Study ROS-based membrane disruption and metabolic interference mechanisms. - Develop combinational antibacterial treatments. - Fine-tune surface functionalization to minimize toxicity.
Cross-cutting challenges	- Scalability and reproducibility. - Limited long-term toxicity data. - Regulatory approval hurdles [340].	- Use green synthesis methods to improve scalability. - Conduct comprehensive *in vivo* toxicity studies. - Collaborate with regulatory bodies to establish standard testing protocols.

are also working to address challenges related to biocompatibility and toxicity. Chiral GQDs and chiral carbons are also emerging as potential candidates to revolutionize the future of biomedical applications [342, 343].

Among the various promising avenues in GQDs for emerging biomedical applications, near-term research should prioritize:

1. Enhancing biocompatibility and targeted delivery mechanisms, as these directly impact clinical safety and efficacy.
2. Innovating multifunctional platforms that integrate diagnosis and therapy (theranostics), which hold significant potential to revolutionize personalized medicine.

Focusing on these areas balances clinical relevance, scalability, and innovation potential, thus accelerating the practical impact of GQDs in biomedicine.

7.3. Future cancer therapeutics

In the past decade, scientists have achieved notable progress in the application of GQDs in new therapeutics. Low cytotoxicity observed in both *in vitro* and *in vivo* experiments, together with good fluorescence exhibited in bioimaging, the efficient conversion of light into heat, and good biocompatibility, have collectively demonstrated the potential of these materials for cancer therapy.

Modifying the surface of GQDs can create novel opportunities for new antitumor agents. The utilization of GQDs and PTT, in conjunction with other combinational therapies has demonstrated significant synergistic benefits. Utilizing GQDs with PTT has the potential for achieving precision and accuracy in tumor treatment. Artificial cell-based anticancer strategies are also emerging research directions for combating cancer [344].

7.4. Future antiviral and antibacterial therapeutics

The possible range of CDs is vast, and they can be relatively quickly screened for antiviral and antibacterial activity. However, while there is a substantial amount of literature available on the synthesis of GQDs, there is a paucity of understanding of the influence of surface, size, shape, and functional groups on antimicrobial activity.

GQDs have demonstrated notable antiviral activity, but their effectiveness is most noteworthy during the initial phases of infection, where the nanoparticle appears to disrupt the contact mechanism between the virus and the cell. Currently, a major hindrance to enhancing antiviral efficacy against a particular virus is the limited understanding of its mode of action. Indeed, the relationship between the antiviral activity of nanoparticles and certain surface functional groups remains inconclusive. There is also a surplus of *in vitro* trials, but a shortage of *in vivo* experiments, which are crucial for accurately evaluating the potential of these systems.

Acknowledgment

A A, J K and S A contributed equally to this work. This work was financially supported by the Applied Basic Research Program of Changzhou (Grant No. CJ20253068), the internal Grant of Jiangsu University of Technology (Grant No. KYY25046) and National Natural Science Foundation of China, Research Fund for International Scientists (Grant No. 52350410475). The authors extend their appreciation to the Deputyship for Research and Innovation, Ministry of Education in Saudi Arabia for funding this research (IFKSU-HCRA-4-1).

ORCID iDs

Aumber Abbas 0000-0002-8663-7824
Tuti Mariana Lim 0000-0002-2319-2813

References

[1] Dananjaya V, Marimuthu S, Yang R, Grace A N and Abeykoon C 2024 Synthesis, properties, applications, 3D printing and machine learning of graphene quantum dots in polymer nanocomposites *Prog. Mater. Sci.* **144** 101282
[2] Ge Z, Graf A M, Keski-Rahkonen J, Slizovskiy S, Polizogopoulos P, Taniguchi T, Watanabe K, Van Haren R, Lederman D and Fal'ko V I 2024 Direct visualization of relativistic quantum scars in graphene quantum dots *Nature* **635** 841–6
[3] Garreis R, Tong C, Terle J, Ruckriegel M J, Gerber J D, Gächter L M, Watanabe K, Taniguchi T, Ihn T and Ensslin K 2024 Long-lived valley states in bilayer graphene quantum dots *Nat. Phys.* **20** 428–34
[4] Dar M S, Rosaiah P, Bhagyalakshmi J, Ahirwar S, Khan A, Tamizhselvi R, Reddy V R M, Palaniappan A and Sahu N K 2025 Graphene quantum dots as nanotherapeutic agents for triple-negative breast cancer: insights from 3D tumor models *Coord. Chem. Rev.* **523** 216247
[5] Zare I, Nasab S Z, Rahi A, Ghaee A, Koohkhezri M, Farani M R, Gholipour H M, Atabaki A H, Hamblin M R and Mostafavi E 2025 Antimicrobial carbon materials-based quantum dots: from synthesis strategies to antibacterial properties for diagnostic and therapeutic applications in wound healing *Coord. Chem. Rev.* **522** 216211
[6] Wang S, Lenzini F, Chen D, Tanner P, Han J, Thiel D, Lobino M and Li Q 2023 Chemically derived graphene quantum dots for high-strain sensing *J. Mater. Sci. Technol.* **141** 110–5
[7] Akbari Nakhjavani S, Mirzajani H, Carrara S and Onbaşlı M C 2024 Advances in biosensor technologies for infectious diseases detection *TrAC Trends Anal. Chem.* **180** 117979
[8] Chen L, Yang S, Li Y, Liu Z, Wang H, Zhang Y, Qi K, Wang G, He P and Ding G 2024 Precursor symmetry triggered modulation of fluorescence quantum yield in graphene quantum dots *Adv. Funct. Mater.* **34** 2401246
[9] Arab K, Jafari A and Shahi F 2024 The role of graphene quantum dots in cutting-edge medical therapies *Polym. Adv. Technol.* **35** e6571
[10] Qian W, Song T, Ye M, Huang X, Li Y and Hao B 2023 Immobilization of GOX on PEG/fluoresence functionalized nanographene oxide to describe fluctuation of glucose level *J. Mater. Sci. Technol.* **164** 111–8

[11] Tang S, Hu H-J, Chang X, Zhang H, Chen Y, Li Y, Li W-X, Hu X, Liao X and Jiang G-B 2025 Group competition mechanism enabled by nitrogen-doped graphene quantum dots for efficient Cd (II) detection and removal *Chem. Eng. J.* **510** 161590
[12] Beygisangchin M, Jakmunee J, Rashid S A, Shafie S and Saetang S 2025 Effect of graphene quantum dot concentration on p-toluenesulfonic acid-doped polyaniline–graphene quantum dot nanocomposites: chemical, optical, and electrical characterization for benzo [def] phenanthrene detection *Opt. Quantum Electron.* **57** 205
[13] Han Y, Hao H, Zeng H, Li H, Niu X, Qi W, Zhang D and Wang K 2024 Harnessing the potential of graphene quantum dots for multifunctional biomedical applications *Chem. Rec.* **24** e202400185
[14] Wang L, Ji Y, Chen Y, Zheng S, Wang F and Li C 2024 Recent research progress of fluorescence biosensors based on carbon dots in early diagnosis of diseases *TrAC Trends Anal. Chem.* **180** 117962
[15] Tade R S, Nangare S N, Patil A G, Pandey A, Deshmukh P K, Patil D R, Agrawal T N, Mutalik S, Patil A M and More M P 2020 Recent advancement in bio-precursor derived graphene quantum dots: synthesis, characterization and toxicological perspective *Nanotechnology* **31** 292001
[16] Danial W H, Mohamed N A S and Majid Z A 2022 Recent advances on the preparation and application of graphene quantum dots for mercury detection: a systematic review *Carbon Lett.* **32** 57–80
[17] Sabzehmeidani M M and Kazemzad M 2022 Quantum dots based sensitive nanosensors for detection of antibiotics in natural products: a review *Sci. Total Environ.* **810** 151997
[18] Yang Y, Cen C, Kan L, Zhao Q, Huang Z and Li S 2024 Organic probes for three-photon fluorescence imaging in NIR-II window: design, applications, and perspectives *Interdiscip. Mater.* **4** 109–37
[19] Chang Y-H, Chiang W-H, Ilhami F B, Tsai C-Y, Huang S-Y and Cheng C-C 2023 Water-soluble graphene quantum dot-based polymer nanoparticles with internal donor/acceptor heterojunctions for efficient and selective detection of cancer cells *J. Colloid Interface Sci.* **637** 389–98
[20] Bai Y, Xu H, Wang H, Fan Y, Li X, Li Y, Fan L, Zhang Y, Qi L and Li Y 2024 Highly efficient loading of procaine on water-soluble carbon dots toward long-acting anesthesia *J. Phys. Chem. A* **128** 1700–10
[21] Dar M S, Tabish T A, Thorat N D, Swati G and Sahu N K 2023 Photothermal therapy using graphene quantum dots *APL Bioeng.* **7** 031502
[22] Tabish T A, Hayat H, Abbas A and Narayan R J 2021 Graphene quantum dot–based electrochemical biosensing for early cancer detection *Curr. Opin. Electrochem.* **30** 100786
[23] Luo Y, Chen J, Abbas A, Li W, Sun Y, Sun Y, Yi J, Lin X, Qiu G and Wen R 2024 Robust giant tunnel electroresistance and negative differential resistance in 2D semiconductor/α-In_2Se_3 ferroelectric tunnel junctions *Adv. Funct. Mater.* **34** 2407253
[24] Kazmi J, Raza S R A, Ahmad W, Masood A, Jalil A, Raub A M, Abbas A, Rafiq M K S and Mohamed M A 2023 Free carrier-mediated ferromagnetism in nonmagnetic ion (Bi–Li) codoped ZnO nanowires *Phys. Chem. Chem. Phys.* **25** 14206–18
[25] Kazmi J, Abbas A, James Young D, Hussain Shah J, Ahmad W, Shoaib Ahmad Shah S, Raza Ali Raza S, Ambri Mohamed M, Govorov A O and Wang Z 2025 ZnO nanowire UV photodetectors: at the intersection of flexibility, biocompatibility, and visible blindness *Mater. Today* **82** 139–80
[26] Abbas A, Zhang Q, Kazmi J, Li Y, Li W, Ahmad W, Zou C and Liang Q 2025 Label-free SERS fingerprinting for chiral discrimination using chiral two-dimensional superlattice *Nano Lett.* **25** 12676–84
[27] Shukla M K, Parihar A, Karthikeyan C, Kumar D and Khan R 2023 Multifunctional GQDs for receptor targeting, drug delivery, and bioimaging in pancreatic cancer *Nanoscale* **15** 14698–716
[28] Mohammed-Ahmed H K, Nakipoglu M, Tezcaner A, Keskin D and Evis Z 2023 Functionalization of graphene oxide quantum dots for anticancer drug delivery *J. Drug Delivery Sci. Technol.* **80** 104199
[29] Kurniawan D, Mathew J, Rahardja M R, Pham H P, Wong P C, Rao N V, Ostrikov K and Chiang W H 2023 Plasma-enabled graphene quantum dot hydrogels as smart anticancer drug nanocarriers *Small* **19** 2206813
[30] Chandra A, Deshpande S, Shinde D B, Pillai V K and Singh N 2014 Mitigating the cytotoxicity of graphene quantum dots and enhancing their applications in bioimaging and drug delivery *ACS Macro Lett.* **3** 1064–8
[31] Mikaeeli Kangarshahi B, Sojdeh S, Daneshgar H, Bagherzadeh M, Naghib S M and Rabiee N 2025 Electroconductive polymer-based biosensors for early cancer detection via liquid biopsy: advances, challenges, and future prospects *TrAC Trends Anal. Chem.* **183** 118062
[32] Xiong Y, Li M and Qing G 2024 Biomolecule-responsive polymers and their bio-applications *Interdiscip. Mater.* **3** 865–96
[33] Su Y, Ye K, Hu J, Zhang Z, Wang Y, Geng B, Pan D and Shen L 2024 Graphene quantum dots eradicate resistant and metastatic cancer cells by enhanced interfacial inhibition *Adv. Healthcare Mater.* **13** 2304648
[34] Lin J, Lin J-H, Yeh T-Y, Zheng J-H, Cho E-C and Lee K-C 2024 Fabrication of hyaluronic acid with graphene quantum dot as a dual drug delivery system for cancer therapy *FlatChem* **44** 100607
[35] Zarepour A, Khosravi A, Ayten N Y, Hatir P Ç, Iravani S and Zarrabi A 2024 Innovative approaches to cancer treatment: graphene quantum dots for photodynamic and photothermal therapies *J. Mater. Chem. B* **12** 4307–34
[36] Zhu X, Zhou Y, Yan S, Qian S, Wang Y, Ju E and Zhang C 2024 Herbal medicine-inspired carbon quantum dots with antibiosis and hemostasis effects for promoting wound healing *ACS Appl. Mater. Interfaces* **16** 8527–37
[37] Balavigneswaran C K and Muthuvijayan V 2024 Carbon quantum dots for medical applications *Nanoparticles in Modern Antimicrobial and Antiviral Applications* (Springer) pp 367–87
[38] Liu H, Deng Z, Zhang Z, Lin W, Zhang M and Wang H 2024 Graphene quantum dots as metal-free nanozymes for chemodynamic therapy of cancer *Matter* **7** 977–90
[39] Rasheed P A, Ankitha M, Pillai V K and Alwarappan S 2024 Graphene quantum dots for biosensing and bioimaging *RSC Adv.* **14** 16001–23
[40] Díaz-García D, Díaz-Sánchez M, Álvarez-Conde J and Gómez-Ruiz S 2024 Emergence of quantum dots as innovative tools for early diagnosis and advanced treatment of breast cancer *ChemMedChem* **19** e202400172
[41] Abbas A, Luo Y, Ahmad W, Mustaqeem M, Kong L, Chen J, Zhou G, Tabish T A, Zhang Q and Liang Q 2024 Recent progress, challenges, and opportunities in 2D materials for flexible displays *Nano Today* **56** 102256
[42] Nisa F U, Tahir M, Khalid S, Amin N, Yin H, Long Y, Tang H, Iiaz K, Khan A U and Naseem M 2025 Revolutionizing micro-scale energy storage by 0D

carbon nanostructures: synthesis, integration, performance optimization mechanisms and sustainable applications *Adv. Funct. Mater.* **35** 2418053
[43] Li G, Liu Z, Gao W and Tang B 2023 Recent advancement in graphene quantum dots based fluorescent sensor: design, construction and bio-medical applications *Coord. Chem. Rev.* **478** 214966
[44] Kalluri A, Dharmadhikari B, Debnath D, Patra P and Kumar C V 2023 Advances in structural modifications and properties of graphene quantum dots for biomedical applications *ACS Omega* **8** 21358–76
[45] Handayani M *et al* 2023 Development of graphene and graphene quantum dots toward biomedical engineering applications: a review *Nanotechnol. Rev.* **12** 20230168
[46] Tade R S and More M P 2025 Emerging application of graphene quantum dots in photodynamic/photothermal and hyperthermia therapies for cancer treatment *Nano Biomed. Eng.* **17** 111–28
[47] Zhao X, Gao W, Zhang H, Qiu X and Luo Y 2020 Graphene quantum dots in biomedical applications: recent advances and future challenges *Handbook of Nanomaterials in Analytical Chemistry* pp 493–505
[48] Yan Y, Gong J, Chen J, Zeng Z, Huang W, Pu K, Liu J and Chen P 2019 Recent advances on graphene quantum dots: from chemistry and physics to applications *Adv. Mater.* **31** 1808283
[49] Abbas A, Rubab S, Rehman A, Irfan S, Sharif H M A, Liang Q and Tabish T A 2023 One-step green synthesis of biomass-derived graphene quantum dots as a highly selective optical sensing probe *Mater. Today Chem.* **30** 101555
[50] Ponomarenko L A, Schedin F, Katsnelson M I, Yang R, Hill E W, Novoselov K S and Geim A K 2008 Chaotic Dirac billiard in graphene quantum dots *Science* **320** 356–8
[51] Abbas A, Abbas S, Tabish T A, Bull S J, Phan A N and Lim T M 2021 Role of precursor microstructure in the development of graphene quantum dots from biomass *J. Environ. Chem. Eng.* **9** 106154
[52] Cançado L G, Monken V P, Campos J L E, Santos J C, Backes C, Chacham H, Neves B R and Jorio A 2024 Science and metrology of defects in graphene using Raman spectroscopy *Carbon* **220** 118801
[53] Santra S, Bose A, Mitra K and Adalder A 2024 Exploring two decades of graphene: the jack of all trades *Appl. Mater. Today* **36** 102066
[54] You W, Zou W, Jiang S, Zhang J, Ge Y, Lu G, Bahnemann D W and Pan J H 2024 Fluorescent carbon quantum dots with controllable physicochemical properties fantastic for emerging applications: a review *Carbon Neutralization* **3** 245–84
[55] Kumar V B, Mirsky S K, Shaked N T and Gazit E 2024 High quantum yield amino acid carbon quantum dots with unparalleled refractive index *ACS Nano* **18** 2421–33
[56] Li W, Wang X, Lin J, Meng X, Wang L, Wang M, Jing Q, Song Y, Vomiero A and Zhao H 2024 Controllable and large-scale synthesis of carbon quantum dots for efficient solid-state optical devices *Nano Energy* **122** 109289
[57] Yang S, Li Y, Chen L, Wang H, Shang L, He P, Dong H, Wang G and Ding G 2023 Fabrication of carbon-based quantum dots via a 'bottom-up' approach: topology, chirality, and free radical processes in 'building blocks' *Small* **19** 2205957
[58] Wang J, Jiang J, Li F, Zou J, Xiang K, Wang H, Li Y and Li X 2023 Emerging carbon-based quantum dots for sustainable photocatalysis *Green Chem.* **25** 32–58
[59] Im M J, Kim J I, Hyeong S K, Moon B J and Bae S 2023 From pristine to heteroatom-doped graphene quantum dots: an essential review and prospects for future research *Small* **19** 2304497
[60] Chung S, Revia R A and Zhang M 2021 Graphene quantum dots and their applications in bioimaging, biosensing, and therapy *Adv. Mater.* **33** 1904362
[61] Đorđević L, Arcudi F, Cacioppo M and Prato M 2022 A multifunctional chemical toolbox to engineer carbon dots for biomedical and energy applications *Nat. Nanotechnol.* **17** 112–30
[62] Zhu S, Song Y, Wang J, Wan H, Zhang Y, Ning Y and Yang B 2017 Photoluminescence mechanism in graphene quantum dots: quantum confinement effect and surface/edge state *Nano Today* **13** 10–14
[63] Ji Z, Dervishi E, Doorn S K and Sykora M 2019 Size-dependent electronic properties of uniform ensembles of strongly confined graphene quantum dots *J. Phys. Chem. Lett.* **10** 953–9
[64] Abbas A, Liang Q, Abbas S, Liaqat M, Rubab S and Tabish T A 2022 Eco-friendly sustainable synthesis of graphene quantum dots from biowaste as a highly selective sensor *Nanomaterials* **12** 3696
[65] Li Y, Chen L, Yang S, Wei G, Ren X, Xu A, Wang H, He P, Dong H and Wang G 2024 Symmetry-triggered tunable phosphorescence lifetime of graphene quantum dots in a solid state *Adv. Mater.* **36** 2313639
[66] Das S and Shukla A 2024 DFT and model hamiltonian study of optoelectronic properties of some low-symmetry graphene quantum dots *J. Phys. Chem. A* **128** 10099–111
[67] Li Y, Yang S, Bao W, Tao Q, Jiang X, Li J, He P, Wang G, Qi K and Dong H 2024 Accelerated proton dissociation in an excited state induces superacidic microenvironments around graphene quantum dots *Nat. Commun.* **15** 6634
[68] Ahmed N, Abbas A, Qamar T H, Hassan S U, Jamali S B and Deng L 2025 Highly efficient, ultralong-lifetime, phosphorescent nitrogen-doped carbon dots via multi-confinement for anticounterfeiting applications *J. Alloys Compd.* **1013** 178586
[69] Ahmed N, Abbas A, Qamar T H, Hassana S U, Jamali S B, Xia P, Gao X and Deng L 2025 Long-lived and stable aqueous room-temperature phosphorescent carbon dot based composites for optical security *J. Appl. Phys.* **58** 215301
[70] Ahmed N, Abbas A, Qamar T H, Ul Hassan S, Jamali S B and Deng L 2025 Carbon dot composites of multicolor dual-mode phosphorescence and thermally enhanced delayed emission *Diam. Relat. Mater.* **153** 111910
[71] Ahmed N, Hussain M, Abbas A, Qamar T H, ul Hassan S, Xia P, Ma L, Gao X and Deng L 2025 Nitrogen and sulfur Co-doped carbon dots with excellent fluorescent thermal stability for anti-counterfeiting and information encryption *Org. Electron.* **139** 107197
[72] Feng J, Xu S, Xia C, Song N, Dong H, Yu L and Dong L 2024 Density functional theory study of the relationship between N-dopants and vacancy defects on graphene quantum dots for oxygen reduction electrocatalysis *ACS Appl. Nano Mater.* **7** 21578–89
[73] Anderson L E, Laitinen A, Zimmerman A, Werkmeister T, Shackleton H, Kruchkov A, Taniguchi T, Watanabe K, Sachdev S and Kim P 2024 Magneto-thermoelectric transport in graphene quantum dot with strong correlations *Phys. Rev. Lett.* **132** 246502
[74] Tang S, Chen D, Yang Y, Wang C, Li X, Wang Y, Gu C and Cao Z 2022 Mechanisms behind multicolor tunable near-infrared triple emission in graphene quantum dots and ratio fluorescent probe for water detection *J. Colloid Interface Sci.* **617** 182–92
[75] Gong P, Sun L, Wang F, Liu X, Yan Z, Wang M, Zhang L, Tian Z, Liu Z and You J 2019 Highly fluorescent N-doped carbon dots with two-photon emission for ultrasensitive

detection of tumor marker and visual monitor anticancer drug loading and delivery *Chem. Eng. J.* **356** 994–1002
[76] Ritter K A and Lyding J W 2009 The influence of edge structure on the electronic properties of graphene quantum dots and nanoribbons *Nat. Mater.* **8** 235–42
[77] Hawrylak P, Potasz P and Devrim Güçlü A 2009 Electronic properties of graphene quantum dots *APS March Meeting Abstracts*
[78] Mandal T, Mishra S R and Singh V 2023 Comprehensive advances in synthesis, fluorescence mechanism and multifunctional applications of red-emitting carbon nanomaterials *Nanoscale Adv.* **5** 5717–65
[79] Li G, Ma Y, Pei M and Lin W 2019 A unique approach to development of a multiratiometric fluorescent composite probe for multichannel bioimaging *Anal. Chem.* **91** 14586–90
[80] Gu S, Hsieh C-T, Tsai Y-Y, Ashraf Gandomi Y, Yeom S, Kihm K D, Fu C-C and Juang R-S 2019 Sulfur and nitrogen co-doped graphene quantum dots as a fluorescent quenching probe for highly sensitive detection toward mercury ions *ACS Appl. Nano Mater.* **2** 790–8
[81] Tian P, Tang L, Teng K S and Lau S P 2018 Graphene quantum dots from chemistry to applications *Mater. Today Chem.* **10** 221–58
[82] Martini L, Chen Z, Mishra N, Barin G B, Fantuzzi P, Ruffieux P, Fasel R, Feng X, Narita A and Coletti C 2019 Structure-dependent electrical properties of graphene nanoribbon devices with graphene electrodes *Carbon* **146** 36–43
[83] Carbonaro C M, Engelbrecht L, Olla C, Cappai A, Maria F C, Melis C, Stagi L, Laaksonen A and Mocci F 2024 Graphene quantum dots and carbon nanodots: modeling of zero-dimensional carbon nanomaterials *Zero-Dimensional Carbon Nanomaterials* (Elsevier) pp 411–82
[84] Zhao X, Wei J, Song T, Wang Z, Yang D, Zhang X, Huo F, Zhang Y and Xiong H-M 2024 Computational insights into carbon dots: evolution of structural models and structure–activity relationships *Chem. Eng. J.* **481** 148779
[85] Guandalini A, Caldarelli G, Macheda F and Mauri F 2025 High-and low-energy many-body effects of graphene in a unified approach *Phys. Rev. B* **111** 075118
[86] Abdelsalam H, Elhaes H and Ibrahim M A 2018 Tuning electronic properties in graphene quantum dots by chemical functionalization: density functional theory calculations *Chem. Phys. Lett.* **695** 138–48
[87] Shen Q, Lin Y, Kawabata Y, Jia Y, Zhang P, Akther N, Guan K, Yoshioka T, Shon H and Matsuyama H 2020 Engineering heterostructured thin-film nanocomposite membrane with functionalized graphene oxide quantum dots (GOQD) for highly efficient reverse osmosis *ACS Appl. Mater. Interfaces* **12** 38662–73
[88] Ye Q, Guo L, Wu D, Yang B, Tao Y, Deng L and Kong Y 2019 Covalent functionalization of bovine serum albumin with graphene quantum dots for stereospecific molecular recognition *Anal. Chem.* **91** 11864–71
[89] Jeong S, Pinals R L, Dharmadhikari B, Song H, Kalluri A, Debnath D, Wu Q, Ham M-H, Patra P and Landry M P 2020 Graphene quantum dot oxidation governs noncovalent biopolymer adsorption *Sci. Rep.* **10** 7074
[90] Zuo W, Tang L, Xiang J, Ji R, Luo L, Rogée L and Ping Lau S 2017 Functionalization of graphene quantum dots by fluorine: preparation, properties, application, and their mechanisms *Appl. Phys. Lett.* **110** 221901
[91] Miao X, Wen S, Su Y, Fu J, Luo X, Wu P, Cai C, Jelinek R, Jiang L-P and Zhu J-J 2019 Graphene quantum dots wrapped gold nanoparticles with integrated enhancement mechanisms as sensitive and homogeneous substrates for surface-enhanced Raman spectroscopy *Anal. Chem.* **91** 7295–303
[92] Massoudi S, Bagheri M, Beygi Khosrowshahi Y and Hosseini M 2023 Antibacterial and cytotoxicity assessment of poly (N-vinyl imidazole)/nitrogen-doped graphene quantum dot nanocomposite hydrogels *Polym. Bull.* **80** 6471–94
[93] Feng B, Dong Y, Shang B, Zhang B, Crans D C and Yang X 2022 Convergent protein phosphatase inhibitor design for PTP1B and TCPTP: exchangeable vanadium coordination complexes on graphene quantum dots *Adv. Funct. Mater.* **32** 2108645
[94] Trpkov D, Vinić M, Dojčilović R and Tošić D 2022 Fast, eco-friendly synthesis of blue luminescent nitrogen-doped graphene quantum dots in glycerol *Opt. Quantum Electron.* **54** 387
[95] Barati F, Avatefi M, Moghadam N B, Asghari S, Ekrami E and Mahmoudifard M 2023 A review of graphene quantum dots and their potential biomedical applications *J. Biomater. Appl.* **37** 1137–58
[96] Tetsuka H, Nagoya A, Fukusumi T and Matsui T 2016 Molecularly designed, nitrogen-functionalized graphene quantum dots for optoelectronic devices *Adv. Mater.* **28** 4632–8
[97] Tabish T A, Scotton C J, Ferguson D C J, Lin L, der Veen A V, Lowry S, Ali M, Jabeen F, Ali M and Winyard P G 2018 Biocompatibility and toxicity of graphene quantum dots for potential application in photodynamic therapy *Nanomedicine* **13** 1923–37
[98] Song Z, Gong J, Soltani R, Fauny J D, Ménard-Moyon C, Chen P and Bianco A 2024 Cellular impact and biodegradability of S-and N-doped graphene quantum dots on human monocytes and macrophages *Adv. Funct. Mater.* **34** 2405856
[99] Hassan Ahmed H E and Soylak M 2024 Exploring the potential of carbon quantum dots (CQDs) as an advanced nanomaterial for effective sensing and extraction of toxic pollutants *TrAC Trends Anal. Chem.* **180** 117939
[100] Xie Y, Wan B, Yang Y, Cui X, Xin Y and Guo L-H 2019 Cytotoxicity and autophagy induction by graphene quantum dots with different functional groups *J. Environ. Sci.* **77** 198–209
[101] Tian X, Xiao B-B, Wu A, Yu L, Zhou J, Wang Y, Wang N, Guan H and Shang Z-F 2016 Hydroxylated-graphene quantum dots induce cells senescence in both p53-dependent and-independent manner *Toxicol. Res.* **5** 1639–48
[102] Mudgal P, Pareek J and Paliwal S 2024 Biodistribution of intravenously transplanted mitochondria conjugated with graphene quantum dots in diabetic rats *J. Fluoresc.* **34** 2725–35
[103] Manjubaashini N, Thangadurai T D, Nataraj D and Thomas S 2024 Biocompatibility and toxicity of graphene quantum dots *Graphene Quantum Dots: The Emerging Luminescent Nanolights* (Springer) pp 265–74
[104] Perini G, Palmieri V, Friggeri G, Augello A, De Spirito M and Papi M 2023 Carboxylated graphene quantum dots-mediated photothermal therapy enhances drug-membrane permeability, ROS production, and the immune system recruitment on 3D glioblastoma models *Cancer Nanotechnol.* **14** 13
[105] Nurunnabi M, Khatun Z, Huh K M, Park S Y, Lee D Y, Cho K J and Lee Y-K 2013 *In vivo* biodistribution and toxicology of carboxylated graphene quantum dots *ACS Nano* **7** 6858–67
[106] Kurapati R, Mukherjee S P, Martín C, Bepete G, Vázquez E, Pénicaud A, Fadeel B and Bianco A 2018 Degradation of single-layer and few-layer graphene by neutrophil myeloperoxidase *Angew. Chem., Int. Ed.* **57** 11722–7
[107] Martins G, Galvan A L S, Valenga M G, Cardozo Martins T A, Bergamini M F and Marcolino-Junior L H

2025 Nitrogen-doped graphene quantum dots (N-GQDs): a promising material for the development of electrochemical immunosensors *ACS Appl. Nano Mater.* **8** 5908–18
[108] Sumit, Gupta S, Sharma S and Kaushal A 2024 Electrochemical determination of type-specific antigens (TSA) associated with orientia tsutsugamushi (Scrub Typhus) by a graphene quantum dot (GQD)-modified screen-printed paper electrode (SPPE) *Anal. Lett.* **58** 1–14
[109] Volarevic V, Paunovic V, Markovic Z, Simovic Markovic B, Misirkic-Marjanovic M, Todorovic-Markovic B, Bojic S, Vucicevic L, Jovanovic S and Arsenijevic N 2014 Large graphene quantum dots alleviate immune-mediated liver damage *ACS Nano* **8** 12098–109
[110] Zhou Y, Sun H, Wang F, Ren J and Qu X 2017 How functional groups influence the ROS generation and cytotoxicity of graphene quantum dots *Chem. Commun.* **53** 10588–91
[111] Ghavamizadeh M, Habibi A, Dastghaib S, Ahmadi M and Mokarram P 2025 Characterization and investigation of the toxicity, genotoxicity, antioxidant, and radical scavenging activity of highly fluorescent nitrogen-doped graphene quantum dots (NGQDs) *Iran. J. Chem. Chem. Eng.* **44** 947–62
[112] Wang D, Zhu L, Chen J-F and Dai L 2015 Can graphene quantum dots cause DNA damage in cells? *Nanoscale* **7** 9894–901
[113] Su Y, Hu J, Wang Y, Li Y, Xiao L, He X, Zhang Z, Cai J, Pan D and Chen Y 2024 N-Heterocycle modified graphene quantum dots as topoisomerase targeted nanoantibiotics for combating microbial infections *Adv. Healthcare Mater.* **13** 2302659
[114] Gao Y and Wang Y 2024 Interplay of graphene–DNA interactions: unveiling sensing potential of graphene materials *Appl. Phys. Rev.* **11** 011306
[115] Hekmat A, Haertlé T, Leblanc R M, Khan H Y, Khan R H and Saboury A A 2024 A review on interaction of nanomaterials of group-XIV (G14) elements of the periodic table with proteins and DNA: applications in biotechnology and pharmacy *BioNanoScience* **14** 1978–2003
[116] Biswas M C, Islam M T, Nandy P K and Hossain M M 2021 Graphene quantum dots (GQDs) for bioimaging and drug delivery applications: a review *ACS Mater. Lett.* **3** 889–911
[117] Hajipour Keyvani A, Mohammadnejad P, Pazoki-Toroudi H, Perez Gilabert I, Chu T, Manshian B B, Soenen S J and Sohrabi B 2025 Advancements in cancer treatment: harnessing the synergistic potential of graphene-based nanomaterials in combination therapy *ACS Appl. Mater. Interfaces* **17** 2756–90
[118] Das N, Srivastava R, Roy S, De A K and Kar R K 2025 Physico-chemical properties and biological evaluation of graphene quantum dots for anticancer drug susceptibility *Colloids Surf. B* **245** 114322
[119] Akmal M H, Kalashgrani M Y, Mousavi S M, Rahmanian V, Sharma N, Gholami A, Althomali R H, Rahman M M and Chiang W-H 2024 Recent advances in synergistic use of GQD-based hydrogels for bioimaging and drug delivery in cancer treatment *J. Mater. Chem. B* **12** 5039–60
[120] Cui G, Wu J, Lin J, Liu W, Chen P, Yu M, Zhou D and Yao G 2021 Graphene-based nanomaterials for breast cancer treatment: promising therapeutic strategies *J. Nanobiotechnol.* **19** 1–30
[121] Yu C, Long Z, Qiu Q, Liu F, Xu Y, Zhang T, Guo R, Zhong W, Huang S and Chen S 2022 Graphene quantum dots-based targeted nanoprobes detecting drug delivery, imaging, and enhanced chemotherapy of nasopharyngeal carcinoma *Bioeng. Transl. Med.* **7** e10270
[122] Hao X, Huang L, Zhao C, Chen S, Lin W, Lin Y, Zhang L, Miao C, Lin X and Chen M 2021 Antibacterial activity of positively charged carbon quantum dots without detectable resistance for wound healing with mixed bacteria infection *Mater. Sci. Eng. C* **123** 111971
[123] Rajendiran K, Zhao Z, Pei D-S and Fu A 2019 Antimicrobial activity and mechanism of functionalized quantum dots *Polymers* **11** 1670
[124] Marković Z M, Budimir Filimonović M D, Milivojević D D, Kovač J and Todorović Marković B M 2024 Antibacterial and antibiofouling activities of carbon polymerized dots/polyurethane and C60/polyurethane composite films *J. Funct. Biomater.* **15** 73
[125] Zhang L, Liu L, Wang J, Niu M, Zhang C, Yu S and Yang Y 2020 Functionalized silver nanoparticles with graphene quantum dots shell layer for effective antibacterial action *J. Nanopart. Res.* **22** 124
[126] Travlou N A, Giannakoudakis D A, Algarra M, Labella A M, Rodríguez-Castellón E and Bandosz T J 2018 S-and N-doped carbon quantum dots: surface chemistry dependent antibacterial activity *Carbon* **135** 104–11
[127] Kováčová M, Špitalská E, Markovic Z and Špitálský Z 2020 Carbon quantum dots as antibacterial photosensitizers and their polymer nanocomposite applications *Part. Part. Syst. Charact.* **37** 1900348
[128] Li Q, Shen X and Xing D 2023 Carbon quantum dots as ROS-generator and-scavenger: a comprehensive review *Dyes Pigments* **208** 110784
[129] Mei L, Gao X, Shi Y, Cheng C, Shi Z, Jiao M, Cao F, Xu Z, Li X and Zhang J 2020 Augmented graphene quantum dot-light irradiation therapy for bacteria-infected wounds *ACS Appl. Mater. Interfaces* **12** 40153–62
[130] Ge J, Lan M, Zhou B, Liu W, Guo L, Wang H, Jia Q, Niu G, Huang X and Zhou H 2014 A graphene quantum dot photodynamic therapy agent with high singlet oxygen generation *Nat. Commun.* **5** 4596
[131] Li P, Liu S, Cao W, Zhang G, Yang X, Gong X and Xing X 2020 Low-toxicity carbon quantum dots derived from gentamicin sulfate to combat antibiotic resistance and eradicate mature biofilms *Chem. Commun.* **56** 2316–9
[132] Wang H, Song Z, Gu J, Li S, Wu Y and Han H 2019 Nitrogen-doped carbon quantum dots for preventing biofilm formation and eradicating drug-resistant bacteria infection *ACS Biomater. Sci. Eng.* **5** 4739–49
[133] Wang Y, Kadiyala U, Qu Z, Elvati P, Altheim C, Kotov N A, Violi A and VanEpps J S 2019 Anti-biofilm activity of graphene quantum dots via self-assembly with bacterial amyloid proteins *ACS Nano* **13** 4278–89
[134] Flemming H-C, Wingender J, Szewzyk U, Steinberg P, Rice S A and Kjelleberg S 2016 Biofilms: an emergent form of bacterial life *Nat. Rev. Microbiol.* **14** 563–75
[135] Pinto R M, Soares F A, Reis S, Nunes C and Van Dijck P 2020 Innovative strategies toward the disassembly of the EPS matrix in bacterial biofilms *Front. Microbiol.* **11** 952
[136] Moreau A, Nguyen D T, Hinbest A J, Zamora A, Weerasekera R, Matej K, Zhou X, Sanchez S, Rodriguez Brenes I and Tai J-S B 2025 Surface remodeling and inversion of cell-matrix interactions underlie community recognition and dispersal in *Vibrio cholerae* biofilms *Nat. Commun.* **16** 327
[137] Abbas S, Abbas A, Zahra T, Kazmi J, Ahmad W, Ahmed N, Lim T M and Cong H 2025 Green and gram-scale synthesis of uniform graphene quantum dots from biomass waste: a highly selective probe for nanomolar Hg^{2+} sensing *Mater. Today Chem.* **47** 102830
[138] Zhu S, Yan X, Sun J, Zhao X-E and Wang X 2019 A novel and sensitive fluorescent assay for artemisinin with

graphene quantum dots based on inner filter effect *Talanta* **200** 163–8
[139] Pramanik R 2025 Nanomaterial-enhanced fluorescence sensors for dopamine neurotransmitters: a photophysical perspective *Anal. Methods* **17** 4251–92
[140] Tang X, Qi Q, Li B, Zhu Z, Lu J and Liu L 2025 Recent advances on fluorescent sensors for detection of pathogenic bacteria *Chemosensors* **13** 182
[141] Ding L, Zhao Z, Li D, Wang X and Chen J 2019 An "off-on" fluorescent sensor for copper ion using graphene quantum dots based on oxidation of l-cysteine *Spectrochim. Acta A* **214** 320–5
[142] Llorent-Martínez E J, Durán G M, Ríos Á and Ruiz-Medina A 2018 Graphene quantum dots–terbium ions as novel sensitive and selective time-resolved luminescent probes *Anal. Bioanal. Chem.* **410** 391–8
[143] Na W, Qu Z, Chen X and Su X 2018 A turn-on fluorescent probe for sensitive detection of sulfide anions and ascorbic acid by using sulfanilic acid and glutathione functionalized graphene quantum dots *Sens. Actuators B* **256** 48–54
[144] Shi H, Chen L and Niu N 2021 An off-on fluorescent probe based on graphene quantum dots intercalated hydrotalcite for determination of ascorbic acid and phytase *Sens. Actuators B* **345** 130353
[145] Zhou C, Liu B, Fang Y, Zhou R, Qian L, Tang S, Ou S and Cheng R 2023 Glucosaminic acid-functionalized graphene quantum dots for sensitive detection of lactose in living cells and real food samples *Sens. Actuators B* **381** 133441
[146] Wang Q, Li L, Wang X, Dong C and Shuang S 2020 Graphene quantum dots wrapped square-plate-like MnO_2 nanocomposite as a fluorescent turn-on sensor for glutathione *Talanta* **219** 121180
[147] Nair R V, Chandran P R, Mohamed A P and Pillai S 2021 Sulphur-doped graphene quantum dot based fluorescent turn-on aptasensor for selective and ultrasensitive detection of omethoate *Anal. Chim. Acta* **1181** 338893
[148] Gu H, Hao L, Ye H, Ma P and Wang Z 2021 Nuclease-assisted target recycling signal amplification strategy for graphene quantum dot-based fluorescent detection of marine biotoxins *Mikrochim. Acta* **188** 118
[149] Fu R, Chen X, Yan X, Li H, Hu T, Wei L, Qu Y and Cheng T 2024 Optical fiber sensors for heavy metal ion sensing *J. Mater. Sci. Technol.* **189** 110–31
[150] Li P, Luo C, Chen X and Huang C 2024 A novel "off-on" ratiometric fluorescent aptasensor for adenosine detection based on FRET between quantum dots and graphene oxide *Spectrochim. Acta A* **305** 123557
[151] Liang J, Yu T, Tan X, Jiang L, He W, Zhan Y, Huang Y, Zhou Z and Li G 2025 High-precision fluorescence platform for point-of-care measurements of low-density lipoprotein based on nitrogen, sulfur-doped graphene quantum dots and ferric tetroxide@ reduced graphene oxide *BioNanoScience* **15** 1–14
[152] Singh H, Kumar D, Deep A, Puri S, Khatri M and Bhardwaj N 2024 Fluorescent nanosensors for detection of microbial toxins in food matrices: a review *J. Food Meas. Charact.* **18** 7669–99
[153] Sittiwanichai S, Archapraditkul C, Japrung D, Shigeta Y, Mori T and Pongprayoon P 2024 Aggregation of apo/glycated human serum albumins and aptamer-saturated graphene quantum dot: a simulation study *Biochemistry* **63** 1697–707
[154] Bai X, Hou X, Ga L and Ai J 2024 Aptamer-carbon quantum dots and silver nanoparticles construct a FRET sensor for sensitive detection of E. coli *Biomed. Anal.* **1** 162–73
[155] Fan Y, Li J, Amin K, Yu H, Yang H, Guo Z and Liu J 2023 Advances in aptamers, and application of mycotoxins detection: a review *Food Res. Int.* **170** 113022
[156] Zahra Q U A, Fang X, Guo H, He L, Abbas A, Luo Z and Qiu B 2025 High-performance selection of small-molecule nucleic acid aptamers and their applications *Anal. Chem.* **97** 12005–12
[157] Serag A, Abdelazim A H, Ramzy S, Alnemari R M, Alzhrani R M, Abduljabbar M H, Althobaiti Y S, Alosaimi M E, Alaqel S I and Almalki A H 2025 A fluorescent sensor based on nitrogen-doped graphene quantum dots and molecularly imprinted polymers for selective and sensitive detection of meropenem in environmental and clinical matrices *Talanta* **296** 128442
[158] Kayani K F 2025 Carbon dots: synthesis, characterization, and applications in the detection of bilirubin–recent advances and challenges *J. Fluoresc.* **35** 1–17
[159] Zhang X, Zhu W, Mei L, Zhang S, Liu J and Wang F 2025 Machine learning-enhanced bacteria detection using a fluorescent sensor array with functionalized graphene quantum dots *ACS Appl. Mater. Interfaces* **17** 3084—96
[160] Gu B, Chen D, Gao B, Liu Z, Wang Z, Wang T, Yang Y, Guo Q and Wang G 2020 Ultrasensitive fluorescent detection of tetracycline based on selective supramolecular interaction of nitrogen chlorine Co–doped graphene quantum dots *ChemistrySelect* **5** 7155–63
[161] Ge S, He J, Ma C, Liu J, Xi F and Dong X 2019 One-step synthesis of boron-doped graphene quantum dots for fluorescent sensors and biosensor *Talanta* **199** 581–9
[162] Xie H, Chen C, Lie J, You R, Qian W, Lin S and Lu Y 2022 Sensitive and selective detection of clenbuterol in meat samples by a graphene quantum dot fluorescent probe based on cationic-etherified starch *Nanomaterials* **12** 691
[163] Li B, Wei J, Jin Y and Bian W 2025 An off–on fluorescent probe based on N, S-GQDs/CoOOH nanocomplexes *in vivo* analysis of ascorbic acid *New J. Chem.* **49** 943–50
[164] Jia Z, Zhang J, Ji Z, Zhang J, Yang X, Shi C, Sun X and Guo Y 2025 2D/0D heterojunction fluorescent probe with schottky barrier based on $Ti_3C_2T_X$ MXene loaded graphene quantum dots for detection of H_2S during food spoilage *Adv. Funct. Mater.* **35** 2412082
[165] Mohandoss S, Priyadharshini A, Velu K S, Napoleon A A, Roy P, Ahmad N, Palanisamy S, You S and Kim S-C 2025 A reversible photoluminescence based on cerium-doped carbon dots for 'on–off–on' dual detection of Fe^{3+} and pyrophosphate ions with live cell application *Inorg. Chem. Commun.* **179** 114824
[166] Boonta W, Talodthaisong C, Sattayaporn S, Chaicham C, Chaicham A, Sahasithiwat S, Kangkaew L and Kulchat S 2020 The synthesis of nitrogen and sulfur co-doped graphene quantum dots for fluorescence detection of cobalt (II) ions in water *Mater. Chem. Front.* **4** 507–16
[167] Ravi P V, Subramaniyam V, Saravanakumar N and Pichumani M 2022 Alkaline N-GQDs fluorescent probe for the ultrasensitive detection of creatinine *Methods Appl. Fluoresc.* **10** 045002
[168] Sheng L, Huangfu B, Xu Q, Tian W, Li Z, Meng A and Tan S 2020 A highly selective and sensitive fluorescent probe for detecting Cr (VI) and cell imaging based on nitrogen-doped graphene quantum dots *J. Alloys Compd.* **820** 153191
[169] Naksen P, Boonruang S, Yuenyong N, Lee H L, Ramachandran P, Anutrasakda W, Amatatongchai M, Pencharee S and Jarujamrus P 2022 Sensitive detection of trace level Cd (II) triggered by chelation enhanced fluorescence (CHEF) 'turn on': nitrogen-doped graphene quantum dots (N-GQDs) as fluorometric paper-based sensor *Talanta* **242** 123305
[170] Yao M, Huang J, Deng Z, Jin W, Yuan Y, Nie J, Wang H, Du F and Zhang Y 2020 Transforming glucose into fluorescent graphene quantum dots via microwave

radiation for sensitive detection of Al^{3+} ions based on aggregation-induced enhanced emission *Analyst* **145** 6981–6
[171] Park S-H, Kwon N, Lee J-H, Yoon J and Shin I 2020 Synthetic ratiometric fluorescent probes for detection of ions *Chem. Soc. Rev.* **49** 143–79
[172] Wen J, Li N, Li D, Zhang M, Lin Y, Liu Z, Lin X and Shui L 2021 Cesium-doped graphene quantum dots as ratiometric fluorescence sensors for blood glucose detection *ACS Appl. Nano Mater.* **4** 8437–46
[173] Tian J, Wei W, Wang J, Ji S, Chen G and Lu J 2018 Fluorescence resonance energy transfer aptasensor between nanoceria and graphene quantum dots for the determination of ochratoxin A *Anal. Chim. Acta* **1000** 265–72
[174] Su D, Li N, Liu Y, Wang M and Su X 2019 Ratiometric fluorescence strategy for p53 gene assay by using nitrogen doped graphene quantum dots and berberine as fluorescence reporters *Anal. Chim. Acta* **1084** 78–84
[175] Luo J, Li S, Pang C, Wang M, Ma X and Zhang C 2022 Highly selective fluorescence probe for imidacloprid measurement based on fluorescence resonance energy transfer *Microchem. J.* **175** 107172
[176] Bhupathi P, Elhassan A-Elgadir T M, Mohammed Ali R H, Sanaan Jabbar H, Gulnoza D, Joshi S, Kadhem Abid M, Ahmed Said E, Alawadi A and Alsaalamy A 2025 Fluorescence resonance energy transfer (FRET)-based sensor for detection of foodborne pathogenic bacteria: a review *Crit. Rev. Anal. Chem.* **55** 233–50
[177] El-Wekil M M, Jardan Y A B, Mostafa A M, Barker J and Ali A B H 2025 A novel fluorescent sensing platform for glutathione based on Förster resonance energy transfer and aggregation-induced emission *Spectrochim. Acta A* **337** 126131
[178] Gao X, Ma Z, Sun M, Liu X, Zhong K, Tang L, Li X and Li J 2022 A highly sensitive ratiometric fluorescent sensor for copper ions and cadmium ions in scallops based on nitrogen doped graphene quantum dots cooperating with gold nanoclusters *Food Chem.* **369** 130964
[179] Qu Z, Yu T and Bi L 2019 A dual-channel ratiometric fluorescent probe for determination of the activity of tyrosinase using nitrogen-doped graphene quantum dots and dopamine-modified CdTe quantum dots *Mikrochim. Acta* **186** 1–9
[180] Su D, Wang M, Liu Q, Chen J and Su X 2019 Dual-emission ratio fluorescence detection of bleomycin based on nitrogen doped graphene quantum dots@ gold nanoclusters assembly *Sens. Actuators B* **290** 163–9
[181] Novoa-De Leon I C, Johny J, Vazquez-Rodriguez S, Avellaneda-Avellaneda D, Shaji S and Sepúlveda-Guzmán S 2025 Nanocarbon hybrid films of reduced graphene oxide and N-doped graphene quantum dots as a metal-free platform for graphene-enhanced raman scattering *ACS Appl. Mater. Interfaces* **17** 17251–9
[182] Cortes F R U, Falomir E, Doñate-Buendía C and Mínguez-Vega G 2025 A review on pulsed laser-based synthesis of carbon and graphene quantum dots in liquids: from fundamentals, chemistry to bio applications and beyond *J. Phys. Chem. C* **129** 10378–414
[183] Luo D, Yu W, Wang X, Tao M, Gao X, Zhang L, Mo Z and Shen J 2025 Oxygen-rich graphene quantum dots enable detection of Pr^3+, Ho^3+, and Er^3+ via spectral overlap engineering *J. Fluoresc.* **35** 1–11
[184] Zahra T, Abbas S, Ou J, Lim T M and Abbas A 2025 Microstructure engineered nanoporous copper for enhanced catalytic degradation of organic pollutants in wastewater *Materials* **18** 2929
[185] Abbas S, Abbas A, Liu Z and Tang C 2020 The two-dimensional boron nitride hierarchical nanostructures: controllable synthesis and superhydrophobicity *Mater. Chem. Phys.* **240** 122145
[186] Khan Z G and Patil P O 2022 Design and synthesis of poly-L-lysine-functionalized graphene quantum dots sensor for specific detection of cysteine and homocysteine *Mater. Chem. Phys.* **276** 125383
[187] Qian L, Zhen Z, Tang S, Zhou C, Ji M, Liu B, Fang Y, Ou S and Cheng R 2022 A coordination-driven fluorescent platform for selective detection of valine in living cells and food samples based on dopamine-functionalized nitrogen doped graphene quantum dots and its construction of molecular logic gate *Sens. Actuators B* **367** 132168
[188] Tian R, Ji P, Wang L, Zhang H and Sun J 2021 TNT sensor based on accumulation layer and effective distance of FRET mechanism with ultra-high sensitivity *Microchem. J.* **160** 105706
[189] Nandi N, Gaurav S, Sarkar P, Kumar S and Sahu K 2021 Hit multiple targets with one arrow: Pb^{2+} and ClO^- detection by edge functionalized graphene quantum dots and their applications in living cells *ACS Appl. Bio Mater.* **4** 7605–14
[190] Li N, Than A, Chen J, Xi F, Liu J and Chen P 2018 Graphene quantum dots based fluorescence turn-on nanoprobe for highly sensitive and selective imaging of hydrogen sulfide in living cells *Biomater. Sci.* **6** 779–84
[191] Tang S, Chen D, Li X, Wang C, Li T, Ma J, Guo G and Guo Q 2022 Promising energy transfer system between fuorine and nitrogen Co-doped graphene quantum dots and Rhodamine B for ratiometric and visual detection of doxycycline in food *Food Chem.* **388** 132936
[192] Wang S, Kang G, Cui F and Zhang Y 2021 Dual-color graphene quantum dots and carbon nanoparticles biosensing platform combined with Exonuclease III-assisted signal amplification for simultaneous detection of multiple DNA targets *Anal. Chim. Acta* **1154** 338346
[193] Masteri-Farahani M, Ghorbani F and Mosleh N 2021 Boric acid modified S and N co-doped graphene quantum dots as simple and inexpensive turn-on fluorescent nanosensor for quantification of glucose *Spectrochim. Acta A* **245** 118892
[194] Zhu S, Bai X, Wang T, Shi Q, Zhu J and Wang B 2021 One-step synthesis of fluorescent graphene quantum dots as an effective fluorescence probe for vanillin detection *RSC Adv.* **11** 9121–9
[195] Kaviani R, Ghaffary S, Jouyban A and Shayanfar A 2020 Developing an analytical method based on graphene quantum dots for quantification of deferiprone in plasma *J. Fluoresc.* **30** 591–600
[196] Zhang H *et al* 2024 Halogen doped graphene quantum dots modulate TDP-43 phase separation and aggregation in the nucleus *Nat. Commun.* **15** 2980
[197] Xiong Z-H, Ya-Nan Z, Xiao-Cong C and Zhao-Hua L 2022 Color-tunable fluorescent nitrogen-doped graphene quantum dots derived from pineapple leaf fiber biomass to detect Hg^{2+} *Chin. J. Anal. Chem.* **50** 69–76
[198] Nair A N, Chava V S, Bose S, Zheng T, Pilla S and Sreenivasan S T 2020 *In situ* doping-enabled metal and nonmetal codoping in graphene quantum dots: synthesis and application for contaminant sensing *ACS Sustain. Chem. Eng.* **8** 16565–76
[199] Nemati F, Zare-Dorabei R, Hosseini M and Ganjali M R 2018 Fluorescence turn-on sensing of thiamine based on Arginine–functionalized graphene quantum dots (Arg-GQDs): central composite design for process optimization *Sens. Actuators B* **255** 2078–85
[200] Zhang C, Feng T, Wang Y, Lei Y, Liu K and Wang T 2025 Top-down fabrication of N-GQDs modified SnO_2 with improved photoelectric characteristics *Part. Part. Syst. Charact.* **42** 2400191

[201] Goel N, Kharangarh P R, Ravindra N M and Dhall S 2025 Enhanced optical properties of graphene quantum dots via strategic doping and codoping *Phys. Status Solidi a* 2500293

[202] Khan Z G, Agrawal T N, Bari S B, Nangare S N and Patil P O 2024 Application of surface nitrogen-doped graphene quantum dots in the sensing of ferric ions and glutathione: spectroscopic investigations and DFT calculations *Spectrochim. Acta A* **306** 123608

[203] Sun W *et al* 2023 Cane molasses derived N-doped graphene quantum dots: dynamic quenching synergistically photoinduced electron transfer for the instant detection of nitrofuran antibiotics *Langmuir* **39** 4394–405

[204] Fu Y, Gao G and Zhi J 2019 Electrochemical synthesis of multicolor fluorescent N-doped graphene quantum dots as a ferric ion sensor and their application in bioimaging *J. Mater. Chem. B* **7** 1494–502

[205] Huang B, He J, Bian S, Zhou C, Li Z, Xi F, Liu J and Dong X 2018 S-doped graphene quantum dots as nanophotocatalyst for visible light degradation *Chin. Chem. Lett.* **29** 1698–701

[206] Anh N T N, Chang P-Y and Doong R-A 2019 Sulfur-doped graphene quantum dot-based paper sensor for highly sensitive and selective detection of 4-nitrophenol in contaminated water and wastewater *RSC Adv.* **9** 26588–97

[207] Liu X, Deng J, Li J, Dong J, Liu H, Zhao J, Luo X, Huo D and Hou C 2023 B-doped graphene quantum dots array as fluorescent sensor platforms for plasticizers detection *Sens. Actuators B* **376** 132989

[208] Ma Y, Chen A, Xie X, Wang X, Wang D, Wang P, Li H, Yang J and Li Y 2019 Doping effect and fluorescence quenching mechanism of N-doped graphene quantum dots in the detection of dopamine *Talanta* **196** 563–71

[209] Qiu G, Han Y, Zhu X, Gong J, Luo T, Zhao C, Liu J, Liu J and Li X 2021 Sensitive detection of sulfide ion based on fluorescent ionic liquid–graphene quantum dots nanocomposite *Front. Chem.* **9** 658045

[210] Wang R, Jiao L, Zhou X, Guo Z, Bian H and Dai H 2021 Highly fluorescent graphene quantum dots from biorefinery waste for tri-channel sensitive detection of Fe^{3+} ions *J. Hazard. Mater.* **412** 125096

[211] Zhang Y, Li K, Ren S, Dang Y, Liu G, Zhang R, Zhang K, Long X and Jia K 2019 Coal-derived graphene quantum dots produced by ultrasonic physical tailoring and their capacity for Cu (II) detection *ACS Sustain. Chem. Eng.* **7** 9793–9

[212] Pongprom A, Chansud N and Bunkoed O 2022 A fluorescence sensor probe based on porous carbon, molecularly imprinted polymer and graphene quantum dots for the detection of trace sulfadimethoxine *J. Photochem. Photobiol. A* **427** 113812

[213] Sharma S, Kumar R and Yadav R M 2023 Polyacrylonitrile/N-doped graphene quantum dots nanocomposite activity as SERS nanosensors for detection of methylene blue *Mater. Today Commun.* **36** 106860

[214] Jampasa S, Khamcharoen W, Wirojsaengthong S, Suea-Ngam A, Traipop S, Ozer T, Unob F, Puthongkham P and Chailapakul O 2024 Recent advances and trends in the applications of nanomaterials in optical sensing platforms *TrAC Trends Anal. Chem.* **180** 117914

[215] Gogoi S, Devi R, Dutta H S, Bordoloi M and Khan R 2019 Ratiometric fluorescence response of a dual light emitting reduced carbon dot/graphene quantum dot nanohybrid towards As (iii) *J. Mater. Chem. C* **7** 10309–17

[216] Li G, Liu Y, Niu J, Pei M and Lin W 2018 A ratiometric fluorescent composite nanomaterial for RNA detection based on graphene quantum dots and molecular probes *J. Mater. Chem. B* **6** 4380–4

[217] Peng D, Zhang L, Liang R-P and Qiu J-D 2018 Rapid detection of mercury ions based on nitrogen-doped graphene quantum dots accelerating formation of manganese porphyrin *ACS Sens.* **3** 1040–7

[218] Sun Z, Jia M, Fu Z, Zhang M, Wang H and Xu Y 2021 High-performance disease diagnosis fluorescent probe based on new type structure YbF_3: er^{3+}@ SiO_2@ GQDs *Chem. Eng. J.* **406** 126755

[219] Liu Y, Xiao Y, Yu M, Cao Y, Li F, Jia P, Guo D, Sun X and Wang L 2020 Ratiometric fluorescent probe based on diazotization-coupling reaction for determination of clenbuterol *J. Agric. Food Chem.* **68** 11578–85

[220] Wang H, Liu J, Chen W, Na J, Huang Y and Li G 2022 A fluorescence aptasensor based on GSH@GQDs and RGO for the detection of Glypican-3 *Spectrochim. Acta A* **270** 120798

[221] Rohaizad N, Mayorga-Martinez C C, Fojtů M, Latiff N M and Pumera M 2021 Two-dimensional materials in biomedical, biosensing and sensing applications *Chem. Soc. Rev.* **50** 619–57

[222] Sharma M, Easha P, Tapasvi G and Reetika R 2020 Nanomaterials in biomedical diagnosis *Nanomaterials in Diagnostic Tools and Devices* (Elsevier) pp 57–83

[223] Li H-J, Sun X, Xue F, Ou N, Sun B-W, Qian D-J, Chen M, Wang D, Yang J and Wang X 2018 Redox induced fluorescence on–off switching based on nitrogen enriched graphene quantum dots for formaldehyde detection and bioimaging *ACS Sustain. Chem. Eng.* **6** 1708–16

[224] Zhang Y, Gao L, Zheng X, Wang Z, Yang C, Tang H, Qu L, Li Y and Zhao Y 2021 Ultraviolet irradiation-responsive dynamic ultralong organic phosphorescence in polymeric systems *Nat. Commun.* **12** 2297

[225] Shang L-L, Song X, Niu C-B, Lv Q-Y, Li C-L, Cui H-F and Zhang S 2021 Red fluorescent nanoprobe based on Ag@ Au nanoparticles and graphene quantum dots for H_2O_2 determination and living cell imaging *Mikrochim. Acta* **188** 291

[226] Lu H-F, Zhang M-M, Wu D, Huang J-L, Zhu L-L, Wang C-M and Zhang Q-L 2018 Colorimetric and fluorescent dual-mode sensing of alkaline phosphatase activity in L-02 cells and its application in living cell imaging based on *in-situ* growth of silver nanoparticles on graphene quantum dots *Sens. Actuators B* **258** 461–9

[227] Liu R, Zhang L, Chen Y, Huang Z, Huang Y and Zhao S 2018 Design of a new near-infrared ratiometric fluorescent nanoprobe for real-time imaging of superoxide anions and hydroxyl radicals in live cells and *in situ* tracing of the inflammation process *in vivo Anal. Chem.* **90** 4452–60

[228] Ma R, Xu M, Liu C, Shi G, Deng J and Zhou T 2020 Stimulus response of GQD-sensitized Tb/GMP ICP nanoparticles with dual-responsive ratiometric fluorescence: toward point-of-use analysis of acetylcholinesterase and organophosphorus pesticide poisoning with acetylcholinesterase as a biomarker *ACS Appl. Mater. Interfaces* **12** 42119–28

[229] Li G, Guo R, Pei M and Lin W 2020 Construction of a novel GQD based ratiometric fluorescent composite probe for viscosity detection *Chem. Commun.* **56** 14649–52

[230] Wong P, Li L, Chea J, Hu W, Poku E, Ebner T, Bowles N, Wong J Y, Yazaki P J and Sligar S 2020 Antibody targeted PET imaging of 64Cu-DOTA-anti-CEA PEGylated lipid nanodiscs in CEA positive tumors *Bioconjugate Chem.* **31** 743–53

[231] Wu C-Y, Lin J-J, Chang W-Y, Hsieh C-Y, Wu C-C, Chen H-S, Hsu H-J, Yang A-S, Hsu M-H and Kuo W-Y 2019 Development of theranostic active-targeting boron-containing gold nanoparticles for boron neutron capture therapy (BNCT) *Colloids Surf. B* **183** 110387

[232] Arjenaki R G, Samieepour G, Ebrahimi S E S, Hamedani M P, Saffari M, Seyedhamzeh M, Kamali A N, Najdian A and Ardestani M S 2024 Development of novel radiolabeled antibody-conjugated graphene quantum dots for targeted *in vivo* breast cancer imaging and biodistribution studies *Arab. J. Chem.* **17** 105518
[233] Enzinger C, Barkhof F, Ciccarelli O, Filippi M, Kappos L, Rocca M A, Ropele S, Rovira À, Schneider T and De Stefano N 2015 Nonconventional MRI and microstructural cerebral changes in multiple sclerosis *Nat. Rev. Neurol.* **11** 676–86
[234] Revia R A and Zhang M 2016 Magnetite nanoparticles for cancer diagnosis, treatment, and treatment monitoring: recent advances *Mater. Today* **19** 157–68
[235] Wang H, Revia R, Mu Q, Lin G, Yen C and Zhang M 2020 Single-layer boron-doped graphene quantum dots for contrast-enhanced *in vivo* T 1-weighted MRI *Nanoscale Horiz.* **5** 573–9
[236] Gómez I J, Křížková P, Dolečková A, Cardo L, Wetzl C, Pizúrová N, Prato M, Medalová J and Zajíčková L 2024 Multifunctional graphene quantum dots: a therapeutic strategy for neurodegenerative diseases by regulating calcium influx, crossing the blood-brain barrier and inhibiting Aβ-protein aggregation *Appl. Mater. Today* **36** 102072
[237] Su Y-L, Yu T-W, Chiang W-H, Chiu H-C, Chang C-H, Chiang C-S and Hu S-H 2017 Hierarchically targeted and penetrated delivery of drugs to tumors by size-changeable graphene quantum dot nanoaircrafts for photolytic therapy *Adv. Funct. Mater.* **27** 1700056
[238] Antoine C, Sahylí Ortega Pijeira M, Ricci-Junior E, Magalhães Rebelo Alencar L and Santos-oliveira R 2022 Graphene quantum dots as bimodal imaging agent for x-ray and computed tomography *Eur. J. Pharm. Biopharm.* **179** 74–78
[239] Rabiee N, Ahmadi S, Soufi G J, Hekmatnia A, Khatami M, Fatahi Y, Iravani S and Varma R S 2022 Quantum dots against SARS-CoV-2: diagnostic and therapeutic potentials *J. Chem. Technol. Biotechnol.* **97** 1640–54
[240] Wu C, Wang C, Han T, Zhou X, Guo S and Zhang J 2013 Insight into the cellular internalization and cytotoxicity of graphene quantum dots *Adv. Healthcare Mater.* **2** 1613–9
[241] Dehvari K, Chiu S-H, Lin J-S, Girma W M, Ling Y-C and Chang J-Y 2020 Heteroatom doped carbon dots with nanoenzyme like properties as theranostic platforms for free radical scavenging, imaging, and chemotherapy *Acta Biomater.* **114** 343–57
[242] Henna T K and Pramod K 2020 Graphene quantum dots redefine nanobiomedicine *Mater. Sci. Eng. C* **110** 110651
[243] Gharepapagh E, Fakhari A, Firuzyar T, Shomali A and Azimi F 2021 Preparation, biodistribution and dosimetry study of Tc-99m labeled N-doped graphene quantum dot nanoparticles as a multimodular radiolabeling agent *New J. Chem.* **45** 3909–19
[244] Teng Y, Yuan S, Shi J and Pong P W T 2022 A multifunctional nanoplatform based on graphene quantum dots-cobalt ferrite for monitoring of drug delivery and fluorescence/magnetic resonance bimodal cellular imaging *Small Sci.* **2** 2200044
[245] Dong J, Zhang Y, Guo P, Xu H, Wang Y and Yang D 2021 GQDs/hMSN nanoplatform: singlet oxygen generation for photodynamic therapy *J. Drug Deliv. Sci. Technol.* **61** 102127
[246] Liang J, Liu J, Jin X, Yao S, Chen B, Huang Q, Hu J, Wan J, Hu Z and Wang B 2020 Versatile nanoplatform loaded with doxorubicin and graphene quantum dots/methylene blue for drug delivery and chemophotothermal/photodynamic synergetic cancer therapy *ACS Appl. Bio Mater.* **3** 7122–32
[247] Uzun Ozsahin D, Ikechukwu Emegano D, Uzun B and Ozsahin I 2022 The systematic review of artificial intelligence applications in breast cancer diagnosis *Diagnostics* **13** 45
[248] Shetty M K 2021 Imaging of the symptomatic breast *Breast & Gynecological Diseases: Role of Imaging in the Management* (Springer) pp 27–79
[249] Yoon J, Han K, Nahm S, Kim M J, Yoon J H, Rho M and Park V Y 2025 Surveillance breast MRI in women with a history of breast cancer: association with occurrence of advanced second breast cancer *Radiology* **314** e240119
[250] Hopkins B and Torres M 2025 Radiotherapy in triple negative breast cancer–current standards and future directions *Curr. Breast Cancer Rep.* **17** 1
[251] Umadevi K, Priyanka L G, Clementina R, Rao E S, Sundeep D and Kumari S 2025 An update and translational perspective in genetics and genomics of breast cancer *Curr. Breast Cancer Rep.* **17** 1–15
[252] Kim J, Fahmy V and Haffty B G 2024 Radiation therapy for triple-negative breast cancer: from molecular insights to clinical perspectives *Expert Rev. Anticancer Ther.* **24** 211–7
[253] Yoder R, Kimler B F, Staley J M, Schwensen K, Wang Y Y, Finke K, O'Dea A, Nye L, Elia M and Crane G 2022 Impact of low versus negative estrogen/progesterone receptor status on clinico-pathologic characteristics and survival outcomes in HER2-negative breast cancer *npj Breast Cancer* **8** 80
[254] Cao L and Niu Y 2020 Triple negative breast cancer: special histological types and emerging therapeutic methods *Cancer Biol. Med.* **17** 293
[255] Chen Y, Fang J, Dai B, Kou J, Lu C and Xu Z 2020 Photothermal effect enhanced photocatalysis realized by photonic crystal and microreactor *Appl. Surf. Sci.* **534** 147640
[256] Guo W, Song X, Liu J, Liu W, Chu X and Lei Z 2024 Quantum dots as a potential multifunctional material for the enhancement of clinical diagnosis strategies and cancer treatments *Nanomaterials* **14** 1088
[257] Fu M, Shen Y, Zhou H, Liu X, Chen W and Ma X 2023 Gallium-based liquid metal micro/nanoparticles for photothermal cancer therapy *J. Mater. Sci. Technol.* **142** 22–33
[258] Kiani M N, Khaliq H, Abubakar M, Rafique M, Jalilov F, Ashraf G A, Ayari-Akkari A and Akremi A 2025 Advancing the potential of nanoparticles for cancer detection and precision therapeutics *Med. Oncol.* **42** 239
[259] Shah I H, Sabir I A, Ashraf M, Rehman A, Ahmad Z, Azam M, Ashraf G A, Ur Rasheed H, Li G and Mouna J 2024 Phyto-fabrication of copper oxide nanoparticles (NPs) utilizing the green approach exhibits antioxidant, antimicrobial, and antifungal activity in Diospyros kaki fruit *Fruit Res.* **4** e022
[260] Saleem M F, Khan N A, Javid M, Ashraf G A, Haleem Y A, Iqbal M F, Bilal M, Wang P and Ma L 2023 Moisture condensation on epitaxial graphene upon cooling *Technologies* **11** 30
[261] Xu S, Chen Y, Jiang Y, Ashraf G A and Guo H 2022 Up-conversion La_4GeO_8: Er^{3+}, Yb^{3+} optical thermometer based on fluorescence intensity ratio technique *J. Lumin.* **251** 119193
[262] Xia W, Tao Z, Zhu B, Zhang W, Liu C, Chen S and Song M 2021 Targeted delivery of drugs and genes using polymer nanocarriers for cancer therapy *Int. J. Mol. Sci.* **22** 9118
[263] Ye L, Chen Y, Mao J, Lei X, Yang Q and Cui C 2021 Dendrimer-modified gold nanorods as a platform for combinational gene therapy and photothermal therapy of tumors *J. Exp. Clin. Cancer Res.* **40** 1–16

[264] Kim S, Choi Y, Park G, Won C, Park Y-J, Lee Y, Kim B-S and Min D-H 2017 Highly efficient gene silencing and bioimaging based on fluorescent carbon dots *in vitro* and *in vivo Nano Res.* **10** 503–19
[265] Luo T, Nie Y, Lu J, Bi Q, Cai Z, Song X, Ai H and Jin R 2021 Iron doped carbon dots based nanohybrids as a tetramodal imaging agent for gene delivery promotion and photothermal-chemodynamic cancer synergistic theranostics *Mater. Des.* **208** 109878
[266] Deng S, Zhang E, Wang Y, Zhao Y, Yang Z, Zheng B, Mu X, Deng X, Shen H and Rong H 2022 *In vivo* toxicity assessment of four types of graphene quantum dots (GQDs) using mRNA sequencing *Toxicol. Lett.* **363** 55–66
[267] Zhang J, Zhao T, Han F, Hu Y and Li Y 2019 Photothermal and gene therapy combined with immunotherapy to gastric cancer by the gold nanoshell-based system *J. Nanobiotechnol.* **17** 1–11
[268] Li Z, Chen Y, Yang Y, Yu Y, Zhang Y, Zhu D, Yu X, Ouyang X, Xie Z and Zhao Y 2019 Recent advances in nanomaterials-based chemo-photothermal combination therapy for improving cancer treatment *Front. Bioeng. Biotechnol.* **7** 293
[269] Chu K F and Dupuy D E 2014 Thermal ablation of tumours: biological mechanisms and advances in therapy *Nat. Rev. Cancer* **14** 199–208
[270] Nam J, Son S, Ochyl L J, Kuai R, Schwendeman A and Moon J J 2018 Chemo-photothermal therapy combination elicits anti-tumor immunity against advanced metastatic cancer *Nat. Commun.* **9** 1074
[271] Wang X, Li C, Qian J, Lv X, Li H, Zou J, Zhang J, Meng X, Liu H and Qian Y 2021 NIR-II responsive hollow magnetite nanoclusters for targeted magnetic resonance imaging-guided photothermal/chemo-therapy and chemodynamic therapy *Small* **17** 2100794
[272] Wang L *et al* 2024 The graphene quantum dots gated nanoplatform for photothermal-enhanced synergetic tumor therapy *Molecules* **29** 615
[273] Wang C, Chen Y, Xu Z, Chen B, Zhang Y, Yi X and Li J 2020 Fabrication and characterization of novel cRGD modified graphene quantum dots for chemo-photothermal combination therapy *Sens. Actuators B* **309** 127732
[274] Ramedani A, Sabzevari O and Simchi A 2022 Hybrid ultrasound-activated nanoparticles based on graphene quantum dots for cancer treatment *Int. J. Pharm.* **629** 122373
[275] Fang J, Liu Y, Chen Y, Ouyang D, Yang G and Yu T 2018 Graphene quantum dots-gated hollow mesoporous carbon nanoplatform for targeting drug delivery and synergistic chemo-photothermal therapy *Int. J. Nanomed.* **13** 5991–6007
[276] Kao F-H, Akhtar N, Chen C-C, Chen H Y, Thakur M K, Chen Y-Y, Chen C-L and Chattopadhyay S 2018 *In vivo* and *in vitro* demonstration of gold nanorod aided photothermal presoftening of B16F10 melanoma for efficient chemotherapy using doxorubicin loaded graphene oxide *ACS Appl. Bio Mater.* **2** 533–43
[277] Zheng J, He Z, Shen L, Chen X, Chen P, Zhang B, Qin H, Xiong Z and Zhang S 2024 Microwave-responsive edge-oxidized graphene for imaging-guided neoadjuvant thermal immunotherapy via promoting immunogenic cell death and redressing hypoxia *ACS Appl. Nano Mater.* **7** 10243–56
[278] Huang L, Li Y, Du Y, Zhang Y, Wang X, Ding Y, Yang X, Meng F, Tu J and Luo L 2019 Mild photothermal therapy potentiates anti-PD-L1 treatment for immunologically cold tumors via an all-in-one and all-in-control strategy *Nat. Commun.* **10** 4871
[279] Chen Q, Xu L, Liang C, Wang C, Peng R and Liu Z 2016 Photothermal therapy with immune-adjuvant nanoparticles together with checkpoint blockade for effective cancer immunotherapy *Nat. Commun.* **7** 13193
[280] Wu C, Guan X, Xu J, Zhang Y, Liu Q, Tian Y, Li S, Qin X, Yang H and Liu Y 2019 Highly efficient cascading synergy of cancer photo-immunotherapy enabled by engineered graphene quantum dots/photosensitizer/CpG oligonucleotides hybrid nanotheranostics *Biomaterials* **205** 106–19
[281] Xia Q, Tang Y, Li W, Liang T, Zhou Y, Liu J and Liu F 2023 Surface-engineered monocyte immunotherapy combined graphene quantum dots effective against solid tumor targets *Int. J. Nanomed.* **18** 2127–40
[282] Zhu S, Wang S, Liu C, Lyu M and Huang Q 2022 Cu-Hemin nanosheets and indocyanine green co-loaded hydrogel for photothermal therapy and amplified photodynamic therapy *Front. Oncol.* **12** 918416
[283] Maharjan P S and Bhattarai H K 2022 Singlet oxygen, photodynamic therapy, and mechanisms of cancer cell death *J. Oncol.* **2022** 1–20
[284] Cai Y, Chai T, Nguyen W, Liu J, Xiao E, Ran X, Ran Y, Du D, Chen W and Chen X 2025 Phototherapy in cancer treatment: strategies and challenges *Signal Transduct. Target. Ther.* **10** 115
[285] Parihar A, Gaur K and Sarbadhikary P 2025 Advanced 2D nanomaterials for phototheranostics of breast cancer: a paradigm shift *Adv. Biol.* **9** 2400441
[286] Wo F, Xu R, Shao Y, Zhang Z, Chu M, Shi D and Liu S 2016 A multimodal system with synergistic effects of magneto-mechanical, photothermal, photodynamic and chemo therapies of cancer in graphene-quantum dot-coated hollow magnetic nanospheres *Theranostics* **6** 485
[287] Ashkbar A, Rezaei F, Attari F and Ashkevarian S 2020 Treatment of breast cancer *in vivo* by dual photodynamic and photothermal approaches with the aid of curcumin photosensitizer and magnetic nanoparticles *Sci. Rep.* **10** 21206
[288] Soleimany A, Khoee S, Dias S and Sarmento B 2023 Exploring low-power single-pulsed laser-triggered two-photon photodynamic/photothermal combination therapy using a gold nanostar/graphene quantum dot nanohybrid *ACS Appl. Mater. Interfaces* **15** 20811–21
[289] Song L, Cheng H, Ren Z, Wang H, Lu J, Zhang J, Zhao Q and Wang S 2023 Red light-emitting carbon dots for reduced phototoxicity and photothermal/photodynamic-enhanced synergistic tumor therapy *Colloids Surf.* **659** 130763
[290] He W, Jin Y, Wang B, Tan J, Yan W, Xiao H, Choi M M F and Bian W 2024 Multifunctional nanocomposites based on graphite-phase carbon nitride quantum dot-silver nanospheres for combined photothermal–photodynamic anti-tumor therapy *New J. Chem.* **48** 3957–65
[291] Liu J, Shi X, Zhang R, Zhang M, He J, Chen J, Wang Z and Wang Q 2021 $CoFe_2O_4$-quantum dots for synergistic photothermal/photodynamic therapy of non-small-cell lung cancer via triggering apoptosis by regulating PI3K/AKT pathway *Nanoscale Res. Lett.* **16** 1–13
[292] Daneshvar F, Salehi F, Karimi M, Vais R D, Mosleh-Shirazi M and Sattarahmady N 2020 Combined x-ray radiotherapy and laser photothermal therapy of melanoma cancer cells using dual-sensitization of platinum nanoparticles *J. Photochem. Photobiol. B* **203** 111737
[293] Zhang Y, Liu J, Yu Y, Chen S, Huang F, Yang C, Chang J, Yang L, Fan S and Liu J 2020 Enhanced radiotherapy using photothermal therapy based on dual-sensitizer of gold nanoparticles with acid-induced aggregation *Nanomed. Nanotechnol. Biol. Med.* **29** 102241

[294] Ruan J, Wang Y, Li F, Jia R, Zhou G, Shao C, Zhu L, Cui M, Yang D-P and Ge S 2018 Graphene quantum dots for radiotherapy *ACS Appl. Mater. Interfaces* **10** 14342–55

[295] Mishra S K, Dhadve A C, Mal A, Reddy B P K, Hole A, Chilakapati M K, Ray P, Srivastava R and De A 2022 Photothermal therapy (PTT) is an effective treatment measure against solid tumors which fails to respond conventional chemo/radiation therapies in clinic *Biomater. Adv.* **143** 213153

[296] Łoczechin A, Séron K, Barras A, Giovanelli E, Belouzard S, Chen Y-T, Metzler-Nolte N, Boukherroub R, Dubuisson J and Szunerits S 2019 Functional carbon quantum dots as medical countermeasures to human coronavirus *ACS Appl. Mater. Interfaces* **11** 42964–74

[297] Kumar R 2018 *Factors Influencing Quality of Life (QOL) Amongst Elderly Caregivers of People Living with HIV/AIDS in Phayao Province, Thailand: A Cross-Sectional Study* (OSF)

[298] Shafer R W and Vuitton D 1999 Highly active antiretroviral therapy (HAART) for the treatment of infection with human immunodeficiency virus type 1 *Biomed. Pharmacother.* **53** 73–86

[299] Moço A C, Gomide J A, Flauzino J M, Brussasco J G, Luz L F, Soares M M, Madurro J M and Brito-Madurro A G 2024 Fentogram electrochemical detection of HIV RNA based on graphene quantum dots and gold nanoparticles *J. Pharm. Biomed. Anal.* **242** 116025

[300] Zor E, Mollarasouli F, Karadurmus L, Ozcelikay G and Ozkan S A 2024 Carbon dots in the detection of pathogenic bacteria and viruses *Crit. Rev. Anal. Chem.* **54** 219–46

[301] Innocenzi P, De Forni D and Lori F 2024 Antiviral activity of carbon dots: strategies and mechanisms of action *Small Struct.* **6** 2400401

[302] Iannazzo D, Giofrè S V, Espro C and Celesti C 2024 Graphene-based materials as nanoplatforms for antiviral therapy and prophylaxis *Expert Opin. Drug Delivery* **21** 751–66

[303] Ye S, Su F, Li J, Yu B, Xu L, Xiong T, Shao K and Yuan X 2024 Enhanced *in vivo* antiviral activity against pseudorabies virus through transforming gallic acid into graphene quantum dots with stimulation of interferon-related immune responses *J. Mater. Chem. B* **12** 122–30

[304] Serrano-Aroca Á, Takayama K, Mishra Y K and de la Fuente-nunez C 2024 Carbon-based nanomaterials for antiviral applications *Adv. Funct. Mater.* **34** 2402023

[305] Bulat T, Zmejkoski D, Marković Z, Satzinger M, Kovač J, Strobl B, Milivojević D and Marković B T 2024 Employing carbon quantum dots to combat cytomegalovirus *Mater. Chem. Phys.* **311** 128495

[306] Anwesha N, Sahu B B, Deshmukh K and Moharana S 2024 Graphene based antibacterial and antiviral functional materials *Antibacterial and Antiviral Functional Materials* vol 2 (ACS Publications) pp 149–84

[307] Iannazzo D, Pistone A, Ferro S, De Luca L, Monforte A M, Romeo R, Buemi M R and Pannecouque C 2018 Graphene quantum dots based systems as HIV inhibitors *Bioconjugate Chem.* **29** 3084–93

[308] Cucinotta D and Vanelli M 2020 WHO declares COVID-19 a pandemic *Acta Bio Med.* **91** 157

[309] Hsieh C-T, Gu S, Gandomi Y A, Fu C-C, Sung P-Y, Juang R-S and Chen C-C 2023 Employing functionalized graphene quantum dots to combat coronavirus and enterovirus *J. Colloid Interface Sci.* **630** 1–10

[310] Pijeira M S O *et al* 2022 Folic acid-functionalized graphene quantum dots: synthesis, characterization, radiolabeling with radium-223 and antiviral effect against Zika virus infection *Eur. J. Pharm. Biopharm.* **180** 91–100

[311] Zheng K, Setyawati M I, Leong D T and Xie J 2017 Antimicrobial gold nanoclusters *ACS Nano*> **11** 6904–10

[312] Langford B J, So M, Raybardhan S, Leung V, Westwood D, MacFadden D R, Soucy J-P R and Daneman N 2020 Bacterial co-infection and secondary infection in patients with COVID-19: a living rapid review and meta-analysis *Clin. Microbiol. Infect.* **26** 1622–9

[313] Chen L, Zhao Y, Shi Q, Du Y, Zeng Q, Liu H, Zhang Z, Zheng H and Wang J J 2024 Preservation effects of photodynamic inactivation-mediated antibacterial film on storage quality of salmon fillets: insights into protein quality *Food Chem.* **444** 138685

[314] Zhang J, Su P, Chen H, Qiao M, Yang B and Zhao X 2023 Impact of reactive oxygen species on cell activity and structural integrity of Gram-positive and Gram-negative bacteria in electrochemical disinfection system *Chem. Eng. J.* **451** 138879

[315] Ali H M, Karam K, Khan T, Wahab S, Ullah S and Sadiq M 2023 Reactive oxygen species induced oxidative damage to DNA, lipids, and proteins of antibiotic-resistant bacteria by plant-based silver nanoparticles *3 Biotech* **13** 414

[316] Esmaeili Y, Toiserkani F, Qazanfarzadeh Z, Ghasemlou M, Naebe M, Barrow C J, Timms W and Jafarzadeh S 2025 Unlocking the potential of green-engineered carbon quantum dots for sustainable packaging biomedical applications and water purification *Adv. Colloid Interface Sci.* **338** 103414

[317] Liu C, Mao X, Meng L and Li J 2022 Stresses make microbe undergo programmed cell death: mechanisms and opportunities *Food Res. Int.* **157** 111273

[318] Zhao Z, Wen S A, Song N, Wang L, Zhou Y, Deng X, Wu C, Zhang G, Chen J and Tian G B 2024 Arginine-enhanced antimicrobial activity of nanozymes against gram-negative bacteria *Adv. Healthcare Mater.* **13** 2301332

[319] Manoharan R R, Prasad A, Pospíšil P and Kzhyshkowska J 2024 ROS signaling in innate immunity via oxidative protein modifications *Front. Immunol.* **15** 1359600

[320] Zhao Y, Ye X, Xiong Z, Ihsan A, Ares I, Martínez M, Lopez-Torres B, Martínez-Larrañaga M-R, Anadón A and Wang X 2023 Cancer metabolism: the role of ROS in DNA damage and induction of apoptosis in cancer cells *Metabolites* **13** 796

[321] Alfei S, Schito G C, Schito A M and Zuccari G 2024 Reactive oxygen species (ROS)-mediated antibacterial oxidative therapies: available methods to generate ROS and a novel option proposal *Int. J. Mol. Sci.* **25** 7182

[322] Raju L, Jacob M S and Rajkumar E 2022 Don't dust off the dust!–a facile synthesis of graphene quantum dots derived from indoor dust towards their cytotoxicity and antibacterial activity *New J. Chem.* **46** 14859–66

[323] Qian Y, Wang J, Geng X, Jia B, Wang L, Li Y-Q, Geng B and Huang W 2024 Graphene quantum dots nanoantibiotic-sensitized TiO_{2-x} heterojunctions for sonodynamic-nanocatalytic therapy of multidrug-resistant bacterial infections *Adv. Healthcare Mater.* **13** 2400659

[324] Rosato R, Santarelli G, Augello A, Perini G, De Spirito M, Sanguinetti M, Papi M and De Maio F 2024 Exploration of the graphene quantum dots-blue light combination: a promising treatment against bacterial infection *Int. J. Mol. Sci.* **25** 8033

[325] Kadyan P, Thillai Arasu P and Kataria S K 2024 Graphene quantum dots: green synthesis, characterization, and antioxidant and antimicrobial potential *Int. J. Biomater.* **2024** 2626006

[326] Cui F, Ning Y, Wang D, Li J, Li X and Li T 2024 Carbon dot-based therapeutics for combating drug-resistant

bacteria and biofilm infections in food preservation *Crit. Rev. Food Sci. Nutrition* **64** 203–19
[327] Kumar R, Singh C K, Misra S, Singh B P, Bhardwaj A K and Chandra K 2024 Water biodiversity: ecosystem services, threats, and conservation *Biodiversity and Bioeconomy* (Elsevier) pp 347–80
[328] Oktay B, Erarslan A, Üstündağ C B and Özerol E A 2024 Preparation and characterization of graphene oxide quantum dots/silver nanoparticles and investigation of their antibacterial effects *Mater. Res. Express* **11** 015603
[329] Wang N, Xu H, Sun S, Guo P, Wang Y, Qian C, Zhong Y and Yang D 2020 Wound therapy via a photo-responsively antibacterial nano-graphene quantum dots conjugate *J. Photochem. Photobiol. B* **210** 111978
[330] Zheng Y-Y, Huang K-T, Lee S-J, Ni J-S and Hsueh Y-H 2024 Nitrogen-doped carbon quantum dots as antimicrobial agents against gram-positive Bacillus subtilis and Staphylococcus aureus under visible white light-emitting diode *Process Biochem.* **146** 225–33
[331] Al-Shawi S G, Andreevna Alekhina N, Aravindhan S, Thangavelu L, Elena A, Viktorovna Kartamysheva N and Rafkatovna Zakieva R 2021 Synthesis of NiO nanoparticles and sulfur, and nitrogen co doped-graphene quantum dots/nio nanocomposites for antibacterial application *J. Nanostruct.* **11** 181–8
[332] Pandiyan S, Arumugam L, Srirengan S P, Pitchan R, Sevugan P, Kannan K, Pitchan G, Hegde T A and Gandhirajan V 2020 Biocompatible carbon quantum dots derived from sugarcane industrial wastes for effective nonlinear optical behavior and antimicrobial activity applications *ACS Omega* **5** 30363–72
[333] Ramachandran P, Khor B-K, Lee C Y, Doong R-A, Oon C E, Thanh N T K and Lee H L 2022 N-doped graphene quantum dots/titanium dioxide nanocomposites: a study of ROS-forming mechanisms, cytotoxicity and photodynamic therapy *Biomedicines* **10** 421
[334] Jiang F *et al* 2013 Eco-friendly synthesis of size-controllable amine-functionalized graphene quantum dots with antimycoplasma properties *Nanoscale* **5** 1137–42
[335] Marković Z M, Jovanović S P, Mašković P Z, Danko M, Mičušík M, Pavlović V B, Milivojević D D, Kleinová A, Špitalský Z and Marković B M T 2018 Photo-induced antibacterial activity of four graphene based nanomaterials on a wide range of bacteria *RSC Adv.* **8** 31337–47
[336] Oliveira L S, Andrade C A S, Oliveira M D L, Zine N, Elaissari A and Errachid A 2025 Recent trends in biosensors for leukemia diagnosis: a critical overview of electrochemical and optical approaches for clinical applicability *TrAC Trends Anal. Chem.* **182** 118063
[337] Santana R M M, Barbosa L S V, Benzi L G, Castro R C, Ribeiro D S M, Korn M G A, Santos J L M and Teixeira L S G 2024 Strategies for enhancing the selectivity of quantum dot-based fluorometric methods *TrAC Trends Anal. Chem.* **180** 117972
[338] Tian Y, Wu W and Li Z A 2025 Emerging chemistry in improving the metabolism or degradability of organic/polymeric conjugated materials for biomedical applications *Interdiscip. Mater.* **4** 52–74
[339] Hao J, Qin C and Wu C 2023 Three-dimensional multicellular biomaterial platforms for biomedical application *Interdiscip. Mater.* **2** 714–34
[340] Wang Q, Hu L, Wang X and Tang R 2024 Expanding from materials to biology inspired by biomineralization *Interdiscip. Mater.* **3** 165–88
[341] Jin X, Cai A, Xu T and Zhang X 2023 Artificial intelligence biosensors for continuous glucose monitoring *Interdiscip. Mater.* **2** 290–307
[342] Zhang Y, Guan J, Luo L, Han X, Wang J, Zheng Y and Xu J 2024 Chiral twisted molecular carbons: synthesis, properties, and applications *Interdiscip. Mater.* **3** 453–79
[343] Chen W, Li B, Gao G and Sun T 2023 Chiral supramolecular nanomaterials: from chirality transfer and amplification to regulation and applications *Interdiscip. Mater.* **2** 689–713
[344] Ren Z-Y *et al* 2024 Atypical artificial cells: novel biomimetic materials for combating cancer *Interdiscip. Mater.* **3** 658–714